STUDIES
ON
EQUATORIAL UNDERCURRENT IN THE INDIAN OCEAN

Thesis Submitted to the University of Cochin
For the Degree
of
DOCTOR OF PHILOSOPHY
IN
PHYSICAL OCEANOGRAPHY

By
P. M. MURALEEDHARAN, M. Sc.

SCHOOL OF MARINE SCIENCES,
UNIVERSITY OF COCHIN
COCHIN - 682016

SEPTEMBER 1984

" to my beloved parents "

C E R T I F I C A T E

This is to certify that this Thesis is an authentic record of research work carried out by Sri P.M.Muraleedharan, M.Sc. under my supervision and guidance in the School of Marine Sciences for the Ph.D. Degree of the University of Cochin and no part of it has previously formed the basis for the award of any other degree in any University.

Dr. G.S. SHARMA
(Supervising Teacher)
Professor of Physical Oceanography
School of Marine Sciences
University of Cochin

Cochin - 682 016,
September, 1984.

ACKNOWLEDGEMENT

I am highly indebted and wish to record my deep sense of gratitude to Dr.G.S.Sharma, Professor of Physical Oceanography, School of Marine Sciences, University of Cochin, for suggesting the problem, the valuable guidance, the constant encouragements and critical scrutiny of the manuscript.

My thanks are due to the authorities of the University of Cochin for providing the necessary facilities. I gratefully acknowledge University Grants Commission, New Delhi for awarding a Junior Research Fellowship during the tenure of which the present study was carried out. I am also grateful to National Institute of Oceanography, Goa and its Regional Centre at Cochin for furnishing some oceanographic data.

I am thankful to Sri K.V.Chandran, University of Cochin, for typing the thesis.

Last but the least, I wish to thank my friends who helped me during the different phases of the study and its completion.

CONTENTS

PREFACE

For many reasons, progress in understanding equatorial circulation in the Indian Ocean has been slow. The equatorial regions are vast and remote. The swift currents and high vertical shears enhanced the curiosity of the explorers. The validity of the geostrophic approximation close to the equator was a topic of argument for a long time since the discovery of the Equatorial Undercurrent in the Pacific Ocean by Cromwell et al. (1954).

Since the atmospheric and oceanic processes are so intimately coupled to one another, the surface oceanic conditions mainly depends on the surface wind pattern. As far as the Equatorial Undercurrent is concerned, its formation, existence and termination depend on the surface wind structure.

Indian Ocean is the only one of the three major oceans that is land locked in its northern boundary while the rest are open towards poles. This peculiar situation of the Indian Ocean gives rise to a unique interplay of oceanic and continental climate called the monsoons in its northern region. The effect of monsoon is even felt in the subsurface layers that influences the structure of the Undercurrent in the Indian Ocean. Hence it is proposed

to study the structure of the Undercurrent in the Indian Ocean and its seasonal variation using the available hydrographic data.

The thesis has been divided into six chapters with further sub divisions.

Chapter one consists of two sections. Section one presents the general introduction while section two describes the materials and methods of the present investigation.

Transequatorial distribution of hydrographic properties are presented in chapter two.

Chapter three deals with the bivariate distribution of zonal flux at different longitude in different months.

The general features of the Equatorial Undercurrent in the Indian Ocean and its comparison with that of the other oceans are coming under chapter four.

Major characteristics of the Equatorial Jet are discussed in the fifth chapter.

The last chapter presents summary of the investigation and conclusion arrived at.

Abbreviations

^{o}C	:	Degree centigrade
cm	:	Centimeter
Fig.	:	Figure
ml/l	:	Milli litre per litre
km	:	Kilometer
m	:	Meter
s^{-1}	:	Per second
%	:	Percentage
%o	:	Parts per mille
cl/t	:	Centi litre per ton
mi/day	:	Miles per day

CHAPTER - I

CHAPTER - 1

SECTION 1 - INTRODUCTION

Oceanographic studies, which gained tremendous momentum after the Second World War, cover the entire expanse of the world oceans. However, the tropical zone has received special attention during this period. The tropical zone ($23^{o}30'S$ - $23^{o}30'N$) constitutes 42.5% of the total area of the world oceans. Processes, originating in the tropical zone have a great influence on general atmospheric and ocean circulations which in turn govern the climate and weather conditions over the whole of the earth. Equatorial current system, occupying the tropical zone, constitutes four main currents viz: South Equatorial Current, North Equatorial Current, Equatorial Countercurrent, and Equatorial Undercurrent, besides the recently discovered South and North Equatorial countercurrents (Reid, 1959).

Europeans knew of the occurrence of the trade winds and equatorial currents in the early 16th century. Equatorial Countercurrent was discovered only around the beginning of the 19th century. The earliest information on the Equatorial Countercurrent in the eastern Pacific

was given by Kruzenshtern after his voyage on the Nadezhda, 1803-1806 (Khanaichenko, 1974). It was also reported by Kotzebu during a voyage on the Predpriyatie, 1823-1826, and by Litke after his cruise on the Senyarin, 1826-1829 (Khanaichenko, 1974). On the basis of observations during his voyage on the Vityaz in 1866-1889, Makarov (1894) stated that the equatorial current encompassed the water layer extending to a depth of 200 m but the Equatorial Countercurrent was much shallower. Krummel (1877) for the first time argued that the Countercurrent in the Atlantic Ocean was a compensating current flowing between the two westerly currents namely North Equatorial and South Equatorial Currents. Defant (1936), in his extensive study, argued that the Countercurrent was a current of high saline water in the subsurface layer, contradicting the then existing belief that the Countercurrent was exclusively a surface phenomenon.

Attempts to explain the nature of the Equatorial Countercurrent and to arrive at a theoretical model were made by Krummel (1877,1911), Ekman (1905,1923), Defant (1935,1941), Schott (1939), Montgomery and Palmen (1940), Sverdrup (1940,1947), Torade (1941) and Shtokman (1946, 1948). However, a subsurface countercurrent flowing due east along the equator and considerably stronger than

the surface Equatorial Countercurrent was discovered in 1952 by the oceanographers Cromwell, Montgomery and Stroup (1954). Iselin (1959) and Neumann (1960) were of the opinion that a similar current exists in the Atlantic Ocean but doubted the existence of such currents in the Indian Ocean which exhibits monsoon circulation quite different from the other major oceans. But Yoshida (1959,1961) from Yamanaka's (1958) section hinted the existence of the Equatorial Undercurrent in the Indian Ocean.

Oceanographic surveys in the equatorial regions during recent years have established the existence of this current in all the major oceans. Buchanan suspected a similar current at the central Atlantic as early as 1886 (Buchanan, 1886,1888). His measurements from the ship Bucaneer, showed the existence of this current at $13^{o}W$ near the equator with speeds more than 1 knot towards the southeast at a depth of 55 m while the surface waters moved slowly towards the west (Neumann, 1960; Montgomery and Stroup, 1962; Montgomery, 1962). Puls (1895), who was unaware of these measurements, noted that when the trades die out for a period of time, the surface flow at the equator is eastward. He postulated that an eastward subsurface current might be present at all times,

but it is not clear whether he was referring to the latitudes of the Countercurrent as Stroup and Montgomery (1963) believes or whether he was referring to the equator as Metcalf (1963) suspects. The whole attention was diverted to this branch of the current system when Cromwell, Montgomery and Stroup discovered the Undercurrent in the Pacific in August 1952 and suggested the name Equatorial Undercurrent (Cromwell et al., 1954).

There was a bit confusion at that moment among the scientists regarding the appropriate name for the current. Shortly after Cromwell's death, Knauss and King (1958) proposed the name "Cromwell Current" for the Pacific Equatorial Undercurrent. The Equatorial Undercurrent in the Atlantic Ocean, measured for the first time using a direct reading current meter on board the R/V Mikhail Lomonosov, has frequently been referred to as the Lomonosov Current. Wooster (1960) has noted that the name Equatorial Undercurrent is more consistant than either of the other names. However, Rual (1969) and Rotchi and Wauthy (1969) protest that to call the current a 'Sous-Courant' in French is to commit a solecism. A Russian scientist, Burkov (1966) suggested another name 'Deep Equatorial Countercurrent' for a reversal of the surface westward flow at subsurface depth. An intense eastward jet in the

vicinity of the thermocline at the equator is referred to as an Equatorial Undercurrent (Philander, 1973).

The Equatorial Undercurrent is a narrow subsurface eastward flow whose driving force is the pressure gradient developed by the cumulation of water at the western region by the continuous and steady easterly trade winds. The effect of meridional wind component destroy the symmetry of the Undercurrent about the equator (Robinson, 1966). During the periods of calm, i.e., when the restoring force is released, the flow at the equator is frequently eastward (Puls, 1895; Voigt, 1961; Istoshina and Kalashnikov, 1965; Masuzawa, 1967; Philander, 1973). The energy balance shown by Wyrtki and Bennett (1963) demonstrates that in the western part of the current the potential energy developed by the piling up of water is chiefly converted into kinetic energy while in the eastern part the energy dissipates due to friction. Along the entire length of the Undercurrent about half of the potential energy is converted into kinetic energy and half dissipated by friction (Wyrtki and Bennett, 1963). The eastward Undercurrent has a width of approximately 3^{o} and can attain speeds upto 170 cm s^{-1}. The westward current below the eastward Undercurrent is

named as Intermediate Equatorial Current by Hisard and Rual (1970). This name derives from the location of this current in the intermediate water of the Pacific (Reid, 1965). Speeds of about 40 cm s^{-1} have been recorded in the westward Intermediate Equatorial Current.

In the eastern parts of the Pacific and Atlantic oceans where there is, usually, no deep homogeneous surface layer at the equator, the Equatorial Undercurrent is very sensitive to changes of local wind conditions. During weak surface easterlies the Undercurrent is symmetric about the equator, has its down stream flow in geostrophic balance, and is marked by deep penetration of warm water of high oxygen concentration (Knauss, 1960; Philander, 1973; Hasong and Zaneveld, 1974). The isotherms and isopleths of oxygen concentration ridge at the equator so that there is, usually, a narrow belt of cold water of low oxygen content at the surface (Knauss, 1966). If the winds should die out for a period of time, the surface flow is eastward rather than westward, a phenomenon referred to as the surfacing of the Undercurrent (Knauss, 1960; Jones, 1969; Taft et al., 1973) and have been explained, theoretically, by Roden (1962). An increase in the intensity of the easterlies cause the isotherms to ridge in a more pronounced manner and to trough in a less pronounced manner. In effect, the westward current gains strength and produces upwelling

while the eastward subsurface current weakens (Knauss, 1960,1966; Jones, 1969). When the trades are very intense their northward component appears to cause an assymmetric Undercurrent (its core moves upwind), and then the Undercurrent has no longer its zonal velocity component in geostrophic balance. Once the core of the Undercurrent is moved to either of the hemispheres and when the restoring force is released the core oscillates north and south due to the combined action of its large inertia and the changing coriolis force in the two hemispheres (Titov, 1977). This wavelike oscillation is called the meandering of the Undercurrent. Standing or eastward travelling meanders are possible only if the Equatorial Undercurrent is unstable (Duing, 1974; Philander, 1979). Federov (1965) dealt analytically with the problem of possible free oscillations of the Equatorial Undercurrent and arrived at the result that the period of such oscillations could be of the order of magnitude of three days.

The importance of horizontal currents for the development of internal boundary waves were first recognised by Helmholtz (1868,1890). Investigations in this field have been, mainly, concerned with the stability or instability of currents with continuously varying stream profiles (Goldstein, 1931; Haurwitz, 1931; Taylor, 1931; Synge, 1933; Eliassen et al., 1953; Drazin, 1958; Case,

1960; Dikii, 1960; Menkes, 1960; Miles, 1961). The interrelationship between the horizontal current and internal waves is described by Wunch (1977), and Philander and Pacanowski (1980,1981). Theoretically, free internal waves exist only between the inertial and vaisala frequencies (Eckart, 1960). The stability of the mean current depends largely upon the Richardson Number. Internal waves are possible, only, if the Richardson Number exceeds 1/4 (Drazin, 1958; Miles, 1961; Long, 1972). Any depth at which the velocity of the mean current equals the phase velocity of the internal waves, there the internal waves vanish (Krauss, 1966). The relationship between the internal waves and turbulence has been studied by different authors (Long, 1972; Garett and Munk, 1972; Kitaigorodsky et al., 1973; Munk and Garett, 1973; Paoyih-ho, 1973; Morozov, 1974 and Schott and Zantopp, 1980.

Analogous to the surface homogeneous layer, a secondary homogeneous layer of water at the equator where the vertical gradient of temperature and salinity are relatively small was discussed by Seitz (1967) and proposed the name thermostad. Montgomery and Stroup (1962) have named this feature 'Equatorial 13^{o}C water' or simply '13 C water'. This'13 C water' within the depth interval of 150-200 m, appears to be closely associated with the

Equatorial Undercurrent, having somewhat the same meridional extent and flowing eastward beneath the core of the highest eastward current. More detailed study about this watermass was carried out by Stroup (1969) and Jones (1973). Taft and Jones (1973) found a secondary maximum of the Equatorial Undercurrent to be located at the base of this layer of low vertical stability. In some regions, the Undercurrent splits and form southern and northern branches (Burkov and Ovchinnikov, 1960; Wooster, 1961; Reid, 1964; Khanaichenko et al., 1965; Khanaichenko, 1966,1969,1974; Voituriez, 1981).

1.1.1. Theoretical studies

A perplexing number of theories have been proposed to explain the Equatorial Undercurrent. Many of these neglect density gradients. In such models, westward surface winds cause the sea surface to slope upward from east to west. The resultant eastward pressure gradient is sufficient to drive a subsurface eastward current below the westward surface flow. In this model the parameters, on which the flow depends, are the radius of the earth R, the angular velocity of the earth Ω, the coefficient of vertical and horizontal eddy viscosity γ_v and γ_h and the intensity of the wind stress τ_o. If the fluid is stratified, a typical apparent temperature difference ΔT,

the coefficients of thermal diffusivity K_v and K_H, the coefficient of thermal expansion α and the gravitational acceleration 'g' also enter the problem.

Detailed theoretical analysis of Undercurrent and related atmospheric and oceanic phenomena have been carried out by different authors (Fofonoff and Montgomery, 1955; Yoshida, 1955,1959; Arthur, 1960; Charney, 1960; Robinson, 1960,1966; Stommel, 1960; Veronis, 1960; Hidaka, 1962,1980; Wyrtki and Bennett, 1963; Ichiye, 1964; Matsuno, 1966; Kozlov, 1967; Leishman, 1967; Bryan and Cox, 1968; Krivelevitch, 1968,1969; Charney and Spiege, 1971; Colin and Rotschi, 1971; Gill, 1971,1972; Philander, 1971,1972, 1973,1981; Stone, 1971; Mc Kee, 1973; Williams and Gibson, 1974; Korotayev et al., 1977; Cane, 1979; Mc Creary, 1980; Mc Phaden, 1981; Mallik, 1982; Pozdynin, 1982).

The equator is dynamically a unique region because the vertical component of the earth's rotation vanishes there. This singularity creates a problem when calculating the currents at the equator. The existing geostrophic relation in calculating the current does not hold good at or very near the equator. The various calculations of currents at the equator have been made by starting with the dynamic equation in some approximate form (Weenink and Groen, 1952; Jerlov, 1953; Yoshida et al., 1953; Yoshida,

1955; Wyrtki, 1956; Hidaka and Nagata, 1958; Arthur, 1960; Charney, 1960; Veronis, 1960; Gill, 1971). In most cases, a surface boundary condition (wind stress) has been introduced, and a bottom boundary condition (zero stress at some depth) has been assumed.

As a basis for a review of the different methods, a set of dynamical equations for steady state conditions is introduced.

$$u\frac{\partial u}{\partial x}+v\frac{\partial u}{\partial y}+w\frac{\partial u}{\partial z} = fv-2\Omega w\cos\phi-\frac{1}{\rho}\frac{\partial P}{\partial x}+\frac{1}{\rho}\frac{\partial \tau_x}{\partial z}+\frac{A_H}{\rho}\left[\frac{\partial^2 u}{\partial x^2}+\frac{\partial^2 u}{\partial y^2}\right] \quad -- 1$$

$$u\frac{\partial v}{\partial x}+v\frac{\partial v}{\partial y}+w\frac{\partial v}{\partial z} = -fu-\frac{1}{\rho}\frac{\partial P}{\partial y}+\frac{1}{\rho}\frac{\partial \tau_y}{\partial z}+A_H\left[\frac{\partial^2 v}{\partial x^2}+\frac{\partial^2 v}{\partial y^2}\right] \quad ---------- 2$$

$$u\frac{\partial w}{\partial x}+v\frac{\partial w}{\partial y}+w\frac{\partial w}{\partial z} = -2\Omega u\cos\phi-g-\frac{1}{\rho}\frac{\partial P}{\partial z} \quad ---------- 3$$

$$\frac{\partial}{\partial x}(\rho u)+\frac{\partial}{\partial y}(\rho v)+\frac{\partial}{\partial z}(\rho w) = 0 \quad ---------- 4$$

The rectangular co-ordinate system has its origin at the sea surface, with x axis directed eastward, y northward, z upward, and u,v and w represent the corresponding velocity components. The coriolis parameter is $f = 2\Omega\sin\phi$, where Ω is the angular velocity of the earth and ϕ is the latitude. The pressure is p, the density ρ, the acceleration due to gravity g, and the x - and y - components of shearing

stresses accross the horizontal plane are τ_x and τ_y respectively. Equations (1) and (2) represent the horizontal components of equation of relative motion with the coefficient of lateral eddy viscosity, A_H, taken as uniform. Pressure is determined from observation of density by application of the hydrostatic equation (3). An assumption of a steady density field gives the equation of continuity in form (4). A detailed analysis of velocity calculation at the equator is made from these equations in simplified form.

Sverdrup (1947) and Reid (1948) introduced the net mass transport from surface to great depths as a variable in place of velocity. The distribution of density is not taken into account in this model. Arthur (1960) assumed that two important terms in the x component of equation of motion at the equator are the pressure gradient and the frictional stress accross the horizontal plane. Jerlov (1953) and others have differentiated the geostrophic formula for zonal motion to remove the indeterminacy at the equator. Arthur (1960) accepts the validity of his approximation because, acceleration and friction terms appear to be neglegible, but its usefulness is limited by the difficulty in obtaining sufficiently accurate estimates of $\frac{\partial^2 P}{\partial y^2}$ which is due to the meridional curvature of the

pressure field. Very recently, Hayes (1982) used the differentiated form of geostrophic equation to calculate the zonal velocity in the upper 500 m at the equator by estimating the meridional curvature of the pressure field between $1^{o}N$ and $1^{o}S$.

Yoshida et al., (1953) gave an over emphasize to lateral friction terms in the equation of motion and landed in uncertainty. Wyrtki (1956) used, essentially, the same method to calculate mass transport of the surface layer. Gill (1971) introduced lateral friction for reachin solutions to the geostrophic breakdown at the equator. Mc Kee (1973) confirms Gill's solution for the linear case and extends it to include nonlinear effects. Hidaka and Nagata (1958) could calculate u and v from (1) and (2) assuming the wind stress and pressure gradients from observations with acceleration neglected. The result shows an Undercurrent, but the method cannot be considered valid because of the magnitude of field of acceleration. Fofonoff and Montgomery (1955) finds the Undercurrent to be consistent with conservation of absolute vorticity in an equatorward flow of a layer of constant thickness. The acceleration term $v\frac{\partial u}{\partial y}$ is found to be important, but the treatment considers the condition near but not right on the equator.

Charney (1960) and Stommel (1960) developed their models by assuming equatorial motion produced by a uniform eastwind flowing over a homogeneous ocean of constant depth. In his paper Charney shows how the inertial terms can be included in the simple homogeneous model, and in a paper after that Veronis (1960) shows how the thermal field can also be included. Main features of the Equatorial Undercurrent are discussed by Ichiye (1964) in his model of wind driven circulation in a homogeneous ocean. Robinson (1966) calculated the first order correction due to nonlinearities and found that, irrespective of the direction of zonal wind, the correction term always corresponds to eastward flow. The importance of nonlinear terms at the equator is emphasised by different authors (Knauss, 1966; Krivelevich, 1969; Mc Kee, 1973; Shapiro, 1974).

Circulation pattern for various types of wind stresse have been described by Philander (1971). Calculations of Charney and Spiegal (1971) give the meridional structure of the flow. One of the Charney and Spiegal's most interesting results anticipated by Robinson (1966), is the upwind displacement of the core of the Undercurrent when the winds have a meridional component. This is in response to the meridional pressure gradient set up by the wind (Gill, 1972)

Philander and Pacanowski (1981) describes in detail about the proportional strengthening of Equatorial Undercurrent with the period of surface easterlies. In the case of westward winds a different nonlinear mechanism intensifies the eastward Equatorial Undercurrent and weakens the westward surface flow (Philander and Pacanowski, 1980). Also the same mechanism intensifies the eastward equatorial surface jet and weakens the westward undercurrent as observed by the authors.

1.1.2. Pacific ocean

For a systematic review of the Equatorial Undercurrent in the Pacific ocean, it is necessary to divide the equatorial Pacific ocean into three parts viz; the western Pacific (from 130°E to 175°E), the central Pacific (from 175°E to 125°W) and the eastern Pacific (from 125°W to 80°W). This system of splitting the area gives a clear picture of the structure of velocity and continuity of the Equatorial Undercurrent in its way to the east. A lot of works has been contributed, which concerned with the surface as well as deep waters of the equatorial Pacific, by various authors (Yoshida et al., 1953; Knauss, 1960,1963,1966; Wyrtki and Bennett, 1963; Piton, 1969; Hidaka, 1972; Kosnyrev and Felsenbaum, 1973; Wyrtki, 1974,1975; Williams and Gibson,

1974; Masaaki and Wyrtki, 1981; Wyrtki et al., 1981).

(a) Western Pacific (130°E - 175°E)

This region differs from the rest of the Pacific in having monsoons; the southeast trades cross the equator during the summer (July and August) in winter (around February) the winds are, usually, north easterlies north of the equator but can have an eastward component at the equator. The variable eastward equatorial flow, west of 137°E, can be viewed as the Undercurrent in its formative stage. The source of this eastward flow is the Mindanao Current and the New Guinea Coastal Current (Bogdanov and Popov, 1960; Masuzawa, 1969; Akamatsu and Sawara, 1969). Tracing the high oxyty water in the western Pacific, Rougerie (1969) concluded that a part of the Undercurrent may originate in the Coral Sea. Observations of Chekotillo (1970) and Ivanov et al., (1976) suggest that the Equatorial Undercurrent originates at or around 135°E. In the initial stage, northern and southern branches of the eastward flow combine to form the Undercurrent (Burkov, 1960; Burkov and Ovchinnikov, 1960; Wyrtki and Kendall, 1967; Jarrige, 1968; Kendall, 1969).

Most of the authors indicate that the surface waters near the coast of New Guinea, some times, move eastward, whereas the subsurface flow is usually westwards (Yamanaka et al., 1965; Masuzawa et al., 1970; Akamatsu and Sawara, 1969). It is apparent from the figure drawn by Kort et al. (1966) that the zonal flow in between 132°E and 152°E is the most complicated. The subsurface westward flowing Intermediate Equatorial Current, observed by Rual (1969), Hisard and Rual (1970), Hisard et al. (1970) and Magnier et al. (1973), is poor in oxygen and rich in phosphate (Rotschi and Wauthy, 1969).

The structure of the currents, above the permanent eastward current in the thermocline, changes quite dramatically, when the wind direction changes from east to west. The double celled structure of the Undercurrent is observed when the wind blows from east and its disappearance with the reversal of the wind shows its interrelationship (Hisard et al., 1970). This double celled structure was first observed by Noel and Merle (1969) and further evidence of such bicellular structure was discussed by Yoshida et al. (1959), Colin et al. (1971), Magnier et al. (1973) and Ivanov et al. (1976). Montgomery (1962) assembled all available western Pacific stations within 70 miles of the equator and found that 95% of them indicated an eastward flow at 150 m and 85% indicated an eastward current at 200 m.

In March 1967 at 170°E when the winds were easterlies, Hisard et al. (1970) observed convergence at 3°N and 3°S and divergence close to the equator. At the bottom of the mixed layer (at the level of the core of the Undercurrent), equatorial flow was measured at 1°N and 1°S. Chekotillo (1970) calculated the velocity of ascending flow between 136°E and 140°E as 10^{-1} cm s^{-1} and concluded that intense upwelling takes place in the western part of the ocean.

The north south oscillation of the core of the Undercurrent is observed in the western Pacific by Colin et al. (1971), Ivanov et al. (1976) and Bubnov and Yegorikhin (1982).

Hisard et al. (1969), on comparing five sections made between March and August 1967 across the equator at 170°E, found that the Undercurrent is the most intense and has a maximum transport in July (55×10^6 m^3 s^{-1}) and a minimum in April (15×10^6 m^3 s^{-1}).

(b) Central Pacific (175°E - 125°W)

Two independent subsurface eastward currents seperated by a layer of strong stability are possible in the presence of a westward wind (Philander, 1973).

An eastward wind on the other hand, could lead to eastward surface flow and, at the base of the homogeneous layer to westward subsurface flow. Such profiles have been observed in the western Pacific and should also be possible in the western part of central Pacific, since a homogeneous surface layer is present as far east as 140°W. Istoshina and Kalashnikov (1965) observed such a profile at 180° meridian in December 1962 and January 1963. Colin et al. (1971) noticed a westward surface flow driven by westward winds and, below that, eastward flow with a bicellular structure, occurred in the west but not east of 150°W in February 1969. Similar phenomenon was noticed by Taft et al. (1974) at 150°W in April with an eastward surface current. Taft and Jones (1973) found the secondary maximum to be located at the base of the layer of low vertical stability, which is called thermostad after Seitz (1967). The thermostad was formed by the shear induced dynamic instability below the velocity core of the Cromwell Current (Halpern, 1980).

East of 140°W, where there is no deep homogeneous surface layer and where the wind does not reverse direction seasonally, the Undercurrent has never been observed to have more than a single cell in the vicinity of the thermocline.

The presence of the deep westward intermediate equatorial current below the Undercurrent has been established by different authors (Knauss, 1960,1966; Istoshin and Kuklin, 1962; Taft et al., 1973; Leetmaa and Spain, 1981; Bubnov et al., 1982). This current is the main source of the nutrient rich waters by which the enrichment of the Cromwell Current is taking place at the level of 13°C Equatorial Water as Jones (1973) pointed out. Tsuchiya (1981) traced this water mass and found it to be originated from the surface and thermocline layers of Tasman Sea and Northeast of Newzealand.

The most striking feature of the subsurface temperature field is the equatorial spreading of thermocline (Wooster and Jennings, 1955; Wooster and Cromwell, 1958; Knauss, 1960; Montgomery, 1962; Montgomery and Stroup, 1962). Direct measurements of Knauss (1960) and Montgomery and Stroup (1962) show that the core of the Undercurrent lies within the thermocline. Halpern's (1980a) observation at 152°W was in good agreement with the above result, though he (1980b) observed the core of the Undercurrent at 166°E near the bottom of the thermocline. According to Forrester (1964), the core of the Undercurrent is associated with 20°C isotherm, with both the isotherm and current core shoaling eastward. Between 140°W and 150°W, the spreading is found to be less pronounced during January and February and

concludes that the Undercurrent may weaken during these months than during the rest of the year (Forrester, 1964).

Comparing the observations of Knauss (1960,1966) and Jones (1969); Philander (1973) concludes that the intense westward winds intensify the surface westward flows and the core of the Undercurrent becomes weaker and shallower. The assymetric Undercurrent is the result of meridional component of the wind, and the upwind shift of the core of the Undercurrent is due to the meridional pressure gradient (Gill, 1972). Such an assymetric Undercurrent is found further to the east, where the winds have a strong northward component (Bjerknes, 1961). But Colin et al. (1971) found the core of the Undercurrent south of the equator at 154°W when the winds were from the east-north-east.

East of 140°W both the transport and the maximum eastward velocity decreases down stream. The transport at 140°W, 115.5°W and 93.5°W are found to be 22 x 10^6 m^3 s^{-1}, 19 x 10^6 m^3 s^{-1} and 8 x 10^6 m^3 s^{-1} respectively (Knauss 1966; Taft and Jones, 1973). Associated with diminishing transport there is a decrease in the width of the Undercurrent (Knauss, 1966; Christensen, 1971). Measurements of Wyrtki et al. (1981) reveal that the water transport of the Equatorial Undercurrent in the central Pacific varied from 25 x 10^6 m^3 s^{-1} in January

to 51 x 10^6 m^3 s^{-1} in July. These values are comparable with the transport observed by Knox and Halpern (1982) at 152°W.

Le Masson and Piton (1968) have compared the various computations of isobaric surfaces in the Pacific. It appears that the sea surface slopes down towards the east along the equator with an inclination of 5 x 10^{-8}. This slope corresponds to an eastward pressure gradient of 5 x 10^{-5} dynes per gram at the surface. The slope of the sea surface appears to reverse in the vicinity of the Gilbert Islands (Austin, 1958; Le Masson and Piton, 1968).

(c) Eastern Pacific (125°W to 80°W)

Velocity measurements just west of the Galapagos Island indicate the flow with a strong northward component. The depth of the thermocline decreases from 125 m near 180° to approximately 50 m east of 120°W (Halpern, 1980). The core of the Cromwell Current was within the central region of the thermocline at 110°W, whereas in the central equatorial Pacific the core was near the bottom of the thermocline (Halpern, 1980). The measurements of Knauss (1962) along 118°W, 96°W, 93.5°W and 87°W indicate that the Cromwell Current becomes both thinner and symmetrical with respect to the equator as it approaches the islands. It sinks and moves around the islands to the north of the equator. The

subsurface eastward flow along 87°W (east of Galapagos) with a maximum of 25 cm s^{-1} north of the equator, led Knauss (1966) to postulate that the Undercurrent flows around the northern rather than southern side of the Galapagos Islands. This is consistent with the observation of Hasong and Zaneveld (1973). But Taft and Jones (1973) and Leetmaa (1982) observed the bulk of the eastward flow to the west of the Galapagos lies asymmetrically south of the equator. Taft and Jones (1973) were of the opinion that this asymmetry may be due to the southerly component of the wind at the equator in the eastern Pacific. Christensen's (1971) measurements are in accordance with Knauss's (1966) suggestion that there may be no loss of transport as the Undercurrent flows around the islands. Christensen (1971) estimates the transport at both 92°W and 89°W (west and east of Galapagos Islands) to be 3×10^6 m^3 s^{-1} each while Knauss's (1966) value at 87°W is 4×10^6 m^3 s^{-1}. West of the islands, the transport of the Undercurrent decreases to half of the value during its course from 110°W to 95°W (Taft and Jones, 1973; Leetmaa, 1982).

In the west and east of the islands an equatorial front is developed which is clearly defined at the sea surface by a large horizontal gradient of temperature, salinity, σ_t and nitrate (Hasong and Zaneveld, 1974). They suggest that

this equatorial front is associated with the equatorial upwelling. A similar front was observed by Wooster (1969) in between Peru and Galapagos. The distribution of water characteristics shows that the extension of the Cromwell Current to the eastern side of the islands derives primarily from water flowing around the northern side of the islands (Hasong and Zaneveld, 1973). Stevenson and Taft (1971) have reviewed the analysis of temperature, salinity and oxygen data for the equatorial region east of the Galapagos and came to the conclusion that there is a close association between the Undercurrent and high salinity core, the location of which frequently coincides with the southern edge of the equatorial front. The salinity core can be traced eastward across the Pacific to the Galapagos (Knauss, 1966; Tsuchiya, 1968). It is probably, deflected southward around the islands. This would imply that the Undercurrent has a southern branch (White, 1969). White (1971,1973) observed an unusual meandering pattern of Pacific Equatorial Undercurrent downstream from the Galapagos and called it as an oceanic wake.

The presence of first baroclinic mode Kelvin wave in the eastern equatorial Pacific was confirmed by Ripa and

Hayes (1981). Meyers (1979) by the annual and semi-annual sea level and thermocline oscillations, suggests the presence of Kelvin wave in this region. Kindle (1979) verified this hypothesis in a numerical simulation.

The effect of islands on equatorially trapped waves induced by the sudden onset of zonal wind are investigated by Yoon (1981) by solving the shallow water equations, numerically. Recently, numerical calculations (Philander and Pacanowski, 1980; Semtner and Holland, 1980) for equatorial oceans have neglected islands. Results of Yoon (1981) suggest that as far as Kelvin Waves are concerned, these numerical models will give reasonable results except near islands, whereas for Rossby Waves, islands might have to be included in the numerical models.

The other important works concerned with the eastern equatorial Pacific are Wyrtki (1967), Tsuchiya (1975), Hayes and Milburn (1980) and Leetmaa (1982).

1.1.3. Atlantic Ocean

The equatorial circulation in the Atlantic ocean has some similarity with the Pacific equatorial current system. The westward flowing South Equatorial Current covers the

whole equatorial region and even reaches upto 2^{o} to $3^{o}N$, and the southern boundary of the North Equatorial Current lies around $7^{o}N$. The Equatorial Countercurrent is embedded between the North Equatorial Current and the South Equatorial Current (Sverdrup et al., 1942). The western boundary currents, especially in the tropical region, play a vital role in the feeding mechanism of Atlantic Equatorial Undercurrent (Metcalf and Stalcup, 1967; Khanaichenko, 1974). Khanaichenko et al. (1965) and Khanaichenko and Khlystov (1966) are of the opinion that the Lomonosov Current is fed mainly by waters from the northern anticyclonic gyre. But Ponomarenko (1965) strongly supported the view of Metcalf and Stalcup (1967) that the Lomonosov Current is fed from the southern anticyclonic gyre. Measurements taken off north eastern Brazil, since 1963, have caused a revision of ideas about the circulation pattern in that area (Cochrane, 1963,1965, 1966; Williams, 1966; Metcalf and Stalcup, 1967; Metcalf, 1968; Ingham and Elder, 1970). The southern part of the coastal current referred to as the North Brazilian Coastal Current by Metcalf and Stalcup (1967) curves back on itself and becomes the Equatorial Undercurrent. According to Cochrane (1963,1965), the Undercurrent at the equator begins near 38^{o} or $39^{o}W$ at the confluence of two currents, one from each hemisphere.

The structure of the Undercurrent is found to be variable over a period of days, even as far east as 33°W (Ingham and Elder, 1970). From about 30°W to within 80 nautical miles (150 km) of the African Coast, the Equatorial Undercurrent is a permanent feature of the equatorial circulation. Its most outstanding feature is a subsurface core of water of very high salinity (Metcalf et al., 1962a,1962b; Neumann and Williams, 1965; Rinkel et al., 1966; Mazeika, 1968; Neumann, 1969; Voigt et al. 1969; Khanaichenko, 1972,1974; Voituriez and Herbland, 1979). Philander (1973) is of the opinion that the Undercurrent derives this core from the North Brazilian Coastal Current and there is no evidence of advection of high salinity water into the Undercurrent, east of 35°W. The depth of the high salinity core decreases towards east, which is the consequence of the negative slope of the sea surface (Defant, 1941; Neumann, 1965; Katz et al., 1977). Note, however, that the core oscillates in both vertical and horizontal planes. Vertical oscillations of the core of maximum speed at a fixed location have been noted by Rinkel (1963) at 17°W. Evidence for lateral oscillations and lateral current displacements to the north and south of the equator have been reported by Metcalf et al. (1962),

Rinkel (1963), Neumann and Williams (1965), Stalcup and Metcalf (1966) and Sturm and Voigt (1966). There is evidence that the current splits into two cores flowing just a little north and south Neumann and Williams, 1965; Sturm and Voigt, 1966; Khanaichenko, 1974). Though, the region of maximum salinity is closely associated with the region of highest eastward velocity, the two maxima need not coincide (Philander, 1973). Sturm and Voigt (1966) and Voigt et al. (1969) found, the maximum current to be below the salinity maximum. Rinkel (1966,1969) found it to be above the salinity maximum.

The Undercurrent is, usually, sandwitched between westward subsurface flow and westward surface flow except when the winds die out for a period of time, when the Undercurrent surfaces (Voigt, 1961; Stalcup and Parker, 1965; Sturm and Voigt, 1966; Metcalf and Stalcup, 1967; Katz and Silvia, 1982). The observations of Puls (1895), Krummel (1911) and Schumacher (1940) mentioned similar surface eastward flow at the equator even before the discovery of the Undercurrent in the Pacific ocean.

The Equatorial Undercurrent in the Atlantic, as elsewhere, is characterized by an equatorial spreading of

isotherms and oxygen isopleths (Metcalf et al., 1962; Reid, 1964; Neumann and Williams, 1965). A layer of low vertical stability, similar to the one in the Pacific, called thermostad (Seitz, 1967), is clearly discernible below the core of the Undercurrent. The eastward velocity is seen to have a secondary maximum just below the thermostad (Bubnov et al., 1976). The occasional reversal of winds over Atlantic and the possibility of deep mixed surface layer are positive factors, as pointed out by Philander (1973), for the development of multicore system of Undercurrent. Brosin and Nehring (1968) observed such a phenomenon at 30°W and find hints of an Undercurrent with two or more maxima in the measurements of Kolesnikov et al. (1966). The eastward increase of vertical transfer of momentum destroys the bicellular structure of the Undercurrent when it travels from west to east (Philander, 1973).

Measurements of the Equatorial Undercurrent in the western Atlantic by the use of submarines (Crease and Pogson, 1964) show its structure and its maximum eastward speed to be quite variable. Brosin and Negring (1968) measured a maximum subsurface eastward velocity of 57 cm s^{-1} at 29°30'W in September 1966. Measurements with current metres and parachute drogues show the maximum eastward speed

in the western Atlantic comes around 80 cm s^{-1} at the depth ranging 60-100 m (Voit and Strekalov, 1964; Stalcup and Parker, 1965; Neumann and Williams, 1965; Stalcup and Metcalf, 1966). Kolesnikov et al. (1966) found the maximum current at 30°W to vary between 80 and 107 cm s^{-1}, depending on the season. Ponomarenko (1963) measured a maximum eastward speed of 116 cm s^{-1}. According to Metcalf et al. (1962), the Undercurrent can attain a speed of 130 cm s^{-1}, and the depth of the layer of eastward flow can be as much as 350 metres, but Stalcup and Metcalf (1966) caution that their values may be too high because they are based on shear measurements.

Estimates of the transport of the Undercurrent also vary considerably. Those who report a typical maximum eastward speed of 80 cm s^{-1} estimated its transport to be approximately 14 x 10^6 m^3 s^{-1}. However, Khanaichenko et al. (1965) calculated a transport of 37.4 x 10^6 m^3 s^{-1} at 18°W, which is one of the highest values. Katz et al. (1981) has got an average transport of 21 x 10^6 m^3 s^{-1} with a maximum of 44 x 10^6 m^3 s^{-1} in March. Between late May and August the value is 25% below the average. The structure of western Atlantic Equatorial Undercurrent is further studied by Pochapsky (1962) and Lass and Hagen (1980).

Between 20°W and 10°W the Undercurrent is always present irrespective of the season (Metcalf et al., 1962a, 1962b; Neumann and Williams, 1965; Mazeika, 1968). Parachute drogue measurements at 8°W and 4°W show that the Undercurrent was much more intense in the spring of 1964 (approximately 73 cm s^{-1}) at 8°W (Rinkel et al., 1966) than in the autumn of 1964 (44 cm s^{-1}) at 8°W (Gerard et al., 1965). Salinities in excess of 36.2‰ were traced upto 2°E during spring (Williams, 1966), but in the autumn the same isohaline closed off near 25°W (Neumann, 1969). Kolesnikov et al. (1966) and Sturm and Voigt (1966) have observed a southward displacement of the core of the Undercurrent between the spring and the fall.

The eastward wind over the eastern Atlantic causes a reversal of sign of the zonal slope of the sea surface. Fuglister (1960) have observed a positive slope of sea surface east of 7°W. According to Rinkel et al. (1960), the reversal of slope of the sea surface is taking place in between 5°E and 6°E in the spring of 1964. This reversal of the sea surface slope retards the Undercurrent. The measurements of Sturm and Voigt (1966) and Kolesnikov et al. (1971) indicate the retardation. The transport of the Undercurrent also decreases from west to east in the Atlantic (Kolesnikov et al., 1971).

Many of the authors noted a southward displacement of the core of the Undercurrent when it reaches its termination point (Gerard et al., 1965; Sturm and Voigt, 1966; Kolesnikov et al., 1971). Rinkel et al. (1966) noted the disappearance of the high salinity core which is closely associated with the core of the Undercurrent, from a zonal section along the equator near 6°E, after which it veered in a southeastward direction, terminating near 7°E, 1°30'S. The observations of Neumann (1969) and Hisard and Morliere (1973) support this phenomenon. There is also an indication that another branch of high salinity water spreads northeast from the equator.

1.1.4. Indian Ocean

The most extensive observations at the equator in the Indian ocean were made during the Lusiad Expedition from June 28 to September 24, 1962 and from February 16 to May 15, 1963. Preliminary reports were published by Knauss and Taft (1963,1964) and Taft (1967). A detailed report incorporating all the results of the Lusiad Expedition appeared as a bulletin of the Scripp's Institution of Oceanography (Taft and Knauss, 1967). Observations of the Equatorial Undercurrent by the R.R.S. Discovery in the western Indian ocean in March-June 1964 were made by Swallow (1964,1967). Kort (1977) and Eriksen (1979) have covered

the whole width of the Equatorial Indian ocean during the northeast monsoon season, whereas Leetmaa and Stommel (1980) have given more importance to yearly variation of Undercurrent at a particular longitude ($55^{o}30'E$) towards the end of the northeast monsoon and beginning of the southwest monsoon.

The sea surface temperature in the tropical Indian ocean always increases from west to east, so that the upper isotherm slope downward from west to east. This implies a westward pressure force at the surface. The lower isotherms were observed to slope upward to the east in March and April 1963 (Taft and Knauss, 1967). Similar structure of the thermocline is observed in the equatorial region during the northeast monsoon season (Eriksen, 1979). The reversal of sign of the slope of the isobaric surfaces occurred at 50 db in the western part of the Indian ocean and at 75 db in the east (Taft and Knauss, 1967). There was, consequently, an eastward pressure force at the depth of the equatorial thermocline in March and April 1963.

After the onset of the southwest monsoon, the upward slope of the sea surface increase towards the east. By July 1963 it had reached a value of 5.2×10^{-8} and -1.7×10^{-8} in the March-April section (positive slope indicates a westward force). Eriksen (1979) measured a

slope of 9.2×10^{-8} over the eastern region at 50 db from December-January section. The negative slope (eastward force) of 1.7×10^{-8} during March-April is very much less compared with the slope of the Pacific and Atlantic.

In February 1961, towards the end of the northeast monsoon, Ivanov (1964) measured an eastward current of 63 cm s^{-1} at a depth of 150 m at 0^{o}, $93^{o}E$. Taft and Knauss (1967) observed the maximum eastward speed of 15 cm s^{-1} at 0^{o}, $85^{o}E$ in late February 1963 and 65 cm s^{-1} in early April 1963. So in 1963 the Undercurrent formed much later. From these inferences, Philander (1973) suggests that not more than 45 days is necessary for the Undercurrent to establish. The Undercurrent in spring of 1963 was at shallower depth in the west (85 m at $61^{o}E$) than in the east (110 m at $92^{o}E$) and was observed to be stable over a period of atleast three weeks (Taft and Knauss, 1967). They found a maximum eastward transport of 11×10^{6} m^{3} s^{-1} at $92^{o}E$ during April where the highest velocity of 81 cm s^{-1} was observed. At $61^{o}E$ the transport was less by a factor of 2. Taft and Knauss's (1967) results show that the velocity of the Undercurrent increases from west to east while Kort (1977) observed a decrease of eastward velocity from west to east. Swallow (1964,1967) measured an eastward flow of 100 ± 20 cm s^{-1} at a

depth of 75 m at 0^{o}, 58^{o}E in March 1964. He got a transport of 14 x 10^{6} m^{3} s^{-1} in the western Indian ocean. At $55^{o}30'$E a mean eastward velocity of 80 cm s^{-1} is observed at a depth of 75-100 m by Leetmaa and Stommel (1980) during March of 1975 and 1976. Neyman et al.'s (1978) measurements at 50^{o}E is in good agreement with the above results. Further east (at 73^{o}E) Knox (1974) measured a velocity of 75 cm s^{-1} in the vicinity of the Maldive Islands during February-March 1972.

The conditions over the Pacific and Atlantic are such that with persistant easterlies there is an Undercurrent driven by the eastward pressure gradient. It is suggested that the Undercurrent that has been observed in the Indian ocean in the early spring is, similarly, driven by an eastward pressure force. The predominant westerly wind over Indian ocean causes eastward surface flow and consequently, downwelling at the equator. The eastward momentum put in by the wind at the surface is advected downward giving subsurface eastward flow (Cane, 1980).

From the beginning of May onwards, as the southwesterlies increase in intensity, the westward surface flow disappeares and the subsurface core of the eastward flow became weaker and asymmetric about the equator. The northward component of the winds appeared to cause an

upwind displacement of the core of the Undercurrent (Charney and Spiegel, 1971). During the early June, Swallow (1964,1967) observed an Undercurrent of 85 cm s^{-1} at $1^{o}S$, $58^{o}E$, with a transport of 17 x 10^{6} m^{3} s^{-1}. In late August the Undercurrent core was at $2^{o}S$, $55^{o}E$ and with speeds upto 65 cm s^{-1} and a transport of 5 x 10^{6} m^{3} s^{-1} (Bruce, 1973).

The Undercurrent is seemed to be weakened after the onset of the southwest monsoon in the early part of the summers of 1963 and 1964 (Taft and Knauss, 1967). Measurements at $53^{o}E$ and $62^{o}E$ in July and August 1962 and at $79^{o}E$ in July 1962, showed the Undercurrent, as well as the features, usually, associated with it; spreading of thermocline, high salinity core etc. to be absent. The flow at $89^{o}E$ in September 1962 was similar to that observed at $79^{o}E$ but the Undercurrent was more variable than it usually is in the spring. Sharma (1968) inferred its presence in the Indian ocean as early as November. Muraleedharan et al. (1980), from the hydrographic characteristics, deduced its presence from January to June.

At the surface of the Indian Ocean along the equator a narrow, jet like current known as Equatorial Jet flows eastward at high speed during both transition periods between the two monsoons (Wyrtki, 1973). Wyrtki points out

two reasons for the narrowness of the jet. The convergent nature of the Ekman transport at the equator and conservation of vorticity forces an eastward flow to concentrate along the equator. It has a width of 500 km flowing symmetrically about the equator. It originates in the central Indian ocean by the uplifting of the thermocline and sinks at its eastern terminus (Wyrtki, 1973). O'Brien and Hurlburt (1974) developed a nonlinear numerical model and a simple analytical theory to explain the basic features of the Equatorial Jet. Knox (1976) observed a westward flow at the surface immediately after the disappearance of surface westerlies which may be due to the relaxation of water piled up at the eastern boundary (Anonymous, 1952). A similar effect is found in a time dependent numerical model of O'Brien and Hurlburt (1974). Cresswell _et al_. (1981), by using a satellite tracked drifting buoy, could trace the Equatorial Jet over 3000 km eastward never more than 2^{o} off the equator between 6 November and 24 December 1980. The equatorial troughing of the surface thermocline and ridging of the bottom thermocline is associated with the Equatorial Jet (Muraleedharan _et al_.,1980). Current measurements over nearly two years at Gan in the Maldive Islands show the appearance of the Jet in the thermocline as well as at the surface with speeds exceeding 100 cm s^{-1} (Knox, 1976). Erikson (1979) could trace the saline Arabian Sea water

from 60°E to 90°E during the northeast monsoon and concluded that the plausible explanation for high saline water in the east is due to the transport of water by the Jet.

In view of the diversified views expressed by various workers, the author is tempted to work in detail the mass transport during the transition periods and discuss the plausible explanation for its establishment in the Indian ocean.

1.1.5. Equatorial Upwelling

Upwelling is a process by which the subsurface water in the sea moves towards the surface. Conversely, a downward displacement of water is called downwelling or sinking. Defant (1936) identified two regions of divergence in the equatorial zone, one at the equator due to winds and the other at the northern boundary of the Equatorial Counter Current. It is noted that the equatorial upwelling regions are of very high productivity (Dietrich, 1957). Now it is generally accepted that the upwelling at the equator is closely associated with the Equatorial Undercurrent (Yoshida 1954,1967; Hidaka, 1966; Ichiye, 1966; Murthy and Taylor, 1969; Hasong and Zaneveld, 1974; Voituriez and Hisard, 1975; Berret, 1976; Hisard et al., 1977; Hisard and Merle, 1978; Voituriez and Herbland, 1979).

In the Pacific, equatorial upwelling is discussed by Cromwell (1953); Austin (1958); Wooster and Cromwell (1958) and Wyrtki (1981). The results of Austin and Rinkel (1958) suggest that the most intense upwelling occurs in the eastern and central Pacific and there is no evidence of upwelling in the western Pacific. But the increased concentration of phosphate in the upper 60 m in the western Pacific, according to Rotschi and Jarrige (1968), is the result of reinforced upwelling by the intensification of the east component of the trade wind at the equator. Observations of Donguy and Henin (1980) from 1955 to 1978 proved that the equatorial upwelling is associated with the presence of the Inter Tropical Convergence Zone (I.T.C.Z). Strong cloudiness is the indication of the presence of I.T.C.Z. Strong cloudiness is located at the northern boundary of the equatorial upwelling during its peak stage (Flohn, 1972). During the seasonal absence of upwelling, the position of the I.T.C.Z. is southern most and the cloudy zone is south of the equator. Henin and Donguy (197o) suggested that the sea surface temperature minimum and the equatorial ridging of isotherms observed in the central Pacific are the indications of upwelling. The intensity of upwelling is minimum during November to March and maximum during June to September. During anomalous conditions as observed by Wyrtki et al. (1977), the mixed layer depth in the

central Pacific deepens and the surface temperature increases, probably because of the absence of the equatorial upwelling. Wyrtki (1981) indicates the velocity of upwelling to be of the order of 1 meter per day in the equatorial Pacific, which is much less than the value obtained by Halpern (1980) from surface current divergence. The vertical velocity of 3 meter per day was observed by Wyrtki and Eldin (1982) in the central Pacific. They noted the effect of equatorial waves on upwelling. Such waves are generated in response to a variable wind stress, or in response to a wind patch and have maximum vertical speeds within the thermocline.

In the Atlantic, strong equatorial upwelling is expected since the Undercurrent is well developed (Neuman, 1960; Knauss 1963). The surface warm water present in the eastern equatorial Atlantic from October to May and its disappearance between June and September when the trade winds intensify steadily indicates the presence of upwelling (Philander, 1979). The vertical nutrient flux associated with the Equatorial Undercurrent at 30°W has been studied by Kaiser and Postel (1979). The influence of internal waves on upwelling is evident from the observation of Moore et al. (1978). In the wake of the Kelvin wave, that propagate into the eastern Atlantic, oceanic conditions are more favourable for upwelling.

The wind system and circulation pattern in the Indian ocean differ markedly from those of the other major oceans. But upwelling is evident when the Equatorial Undercurrent is established (Taft and Knauss, 1967). Works of Swallow (1964) and Sharma (1968) also show the evidence of equatorial upwelling. Taft (1971) on the basis of his observations in the central Indian ocean concludes that the equatorial upwelling is absent in the Indian ocean during either monsoon phase. This appears to be due to the presence of eastward wind stress at the equator in the Indian ocean rather than westward stress. Ryther et al. (1966) is of the opinion that the western side of the Equatorial Indian ocean (45°E to 75°E) is found to be more productive compared to the eastern portion.

SECTION - II - MATERIALS AND METHODS

An important thermal feature associated with the Equatorial Undercurrent has been described by Wooster and Jennings (1955) and Wooster and Cromwell (1958). The upper isothermal surfaces ridge at the equator, while in the lower part of the thermocline they trough. The thermal structure is of the form to agree with geostrophic equilibrium within the Undercurrent has been recognised by Yoshida (1959), Knauss (1960), Tsuchiya (1961) and Montgomery and Stroup (1962). The trough in the isothermal

surfaces represents an upward increase of the eastward component of geostrophic current. The geostrophic current is maximum at the depth where the isothermal surfaces become level. Above this depth, the ridge in isothermal surfaces represents an upward decrease of the eastward component of geostrophic current.

Wooster and Cromwell (1958) noted that the equatorial troughing of isothermal surfaces in the lower part of the thermocline is even exceeded by the troughing of equiscalar surfaces of both oxygen and phosphate, so that certain isothermal (isanosteric) surfaces show an oxygen maximum and phosphate minimum along the equator. Salinity exhibits strong lateral contrasts within the Undercurrent. Metcalf et al. (1962) first drew attention to the significances of the high salinity core developed within the thermocline in the Atlantic ocean. According to Montgomery (1962), the evidence of the Equatorial Undercurrent can be found from the distributions of water properties viz., temperature or specific volume anomaly, salinity and oxyty or phosphate. Based on the hydrographic features; the presence of the Equatorial Undercurrent in the Indian Ocean is inferred and a detailed study is carried out in its longitudinal and seasonal variation.

Oceanographic data collected along the transequatorial sections by different research vessels in different years are

utilised for the study. The details of the oceanographic data used in the present study are given in table 1. In each month transequatorial sections are selected such that atleast one section is located in each region of the western, central and eastern Equatorial Indian ocean, so as to study the longitudinal variation of the Undercurrent. Due to paucity of the data in the western Indian ocean during September, October and December, no definite conclusions could be drawn about the Equatorial Undercurren in this part of the Indian ocean.

To facilitate an easy comparison of the distributi of hydrographic properties each set of diagrams is superimposed and represented with different types of notation. The isotherms are drawn at an interval of 1^{c} while the isohalines and oxypleths are drawn at interv of 0.1‰ and 0.5 ml/l respectively. The observations taken so far, reveal that the Equatorial Undercurren confined to a maximum depth of 300 m and so the ver distributions of temperature, salinity and oxyty a equator from 5^{o}N to 5^{o}S have been analysed upto 300 m.

1.2.2. Computation of geostrophic currer

The general formula for computi from the slope of the isobaric surf

utilised for the study. The details of the oceanographic data used in the present study are given in table 1. In each month transequatorial sections are selected such that atleast one section is located in each region of the western, central and eastern Equatorial Indian ocean, so as to study the longitudinal variation of the Undercurrent. Due to paucity of the data in the western Indian ocean during September, October and December, no definite conclusions could be drawn about the Equatorial Undercurrent in this part of the Indian ocean.

To facilitate an easy comparison of the distribution of hydrographic properties each set of diagrams is superimposed and represented with different types of notation. The isotherms are drawn at an interval of $1^{o}C$ while the isohalines and oxypleths are drawn at intervals of 0.1‰ and 0.5 ml/l respectively. The observations, taken so far, reveal that the Equatorial Undercurrent is confined to a maximum depth of 300 m and so the vertical distributions of temperature, salinity and oxyty across the equator from $5^{o}N$ to $5^{o}S$ have been analysed upto a depth of 300 m.

1.2.2. Computation of geostrophic current and zonal flux

The general formula for computing ocean
from the slope of the isobaric surfaces wa

utilised for the study. The details of the oceanographic data used in the present study are given in table 1. In each month transequatorial sections are selected such that atleast one section is located in each region of the western, central and eastern Equatorial Indian ocean, so as to study the longitudinal variation of the Undercurrent. Due to paucity of the data in the western Indian ocean during September, October and December, no definite conclusions could be drawn about the Equatorial Undercurrent in this part of the Indian ocean.

To facilitate an easy comparison of the distribution of hydrographic properties each set of diagrams is superimposed and represented with different types of notation. The isotherms are drawn at an interval of $1^{o}C$ while the isohalines and oxypleths are drawn at intervals of 0.1‰ and 0.5 ml/l respectively. The observations, taken so far, reveal that the Equatorial Undercurrent is confined to a maximum depth of 300 m and so the vertical distributions of temperature, salinity and oxyty across the equator from $5^{o}N$ to $5^{o}S$ have been analysed upto a depth of 300 m.

1.2.2. Computation of geostrophic current and zonal flux

The general formula for computing ocean currents from the slope of the isobaric surfaces was derived by

Table 1

Sl. No.	Ship's name	No. of Stns.	Cruise No./ N.O.D.C. Cruise No./Expdn.	Period	Longitud in degre and minu tes
1	2	3	4	5	6
1	Adademik - Korelov	8	Not known	4-6th Feb. 1973	65°
2	"	10	Not known	10-13th Mar. 1973	65°
3	Akademik - Shirshov	17	7	20-27th May 1971	65°
4	"	10	7	26-30th Jun. 1971	65°
5	Akademik - Vernadskii	10	10	20-27th Feb. 1975	54°.3
6	"	10	11	7-9th Jul. 1975	54°30
7	Anton Brunn	5	Lusiad V, Cr.2	14-17th Jul. 1963	80°
8	Argo	17	Lusiad V	17-26th Feb. 1963	85°
9	Argo	17	"	19-25th Apr. 1963	92°
10	"	16	Lusiad II	31st Jul. - 11th Aug. 1962	53°
11	"	17	"	14-21st Aug. 1962	62°
12	"	17	"	29th Aug. - 5th Sep. 1962	79°
13	Atlantis II	14	15	21-25th Apr. 1965	49°-5
14	Discovery	19	74-030	16-24th Mar. 1964	57°.5
15	"	10	Not known	11-15th Apr. 1961	78°
16	Koyo-Maru	13	14	22nd Nov. - 6th Dec. 1962	94°
17	Kagoshima-Maru	9	63.3	26th Nov. - 4th Dec. 1963	86°
18	Meteor	10	06-007	29th Jan. - 2nd Feb. 1965	58°

1	2	3	4	5	6
19	Norcel	6	35-009	2-6th Mar. 1959	90°
20	"	5	35-842	11-15th Nov. 1955	54°-58°
21	OB	6	1	2-6th Jun. 1956	55°
22	Pioneer	17	OPR-442	26-31st May 1964	84°
23	"	17	OPR-442	1-5th Jun. 1964	88°
24	Shoyo-Maru	13	Not known	8-12th Nov. 1976	64°
25	Vithyas	8	31	22-25th Jan. 1960	76°
26	"	7	31	7-12th Jan. 1960	86°.30'
27	"	15	35	2-12th Sep. 1962	91°.30'
28	"	13	35	29th Sep. - 7th Oct. 1962	77°
29	"	10	35	22-28th Oct. 1962	84°
30	"	8	31	10-15th Dec. 1960	71°
31	Voeikov.A.I.	11	90-0433	23-26th May 1973	55°

Mohn in 1885. Because of the indiscrimination of Mohn's theory and also due to the invention of Ekman Theory (Ekman, 1939), Mohn's formula received less attention. Meanwhile, on the basis of Bjerkne's Circulation Theorem (Bjerknes, 1900), Sandstrom and Helland-Hansen (1903) obtained formula to compute current velocities at different horizons from the distribution of water density. This method became known later as the dynamic method for computing ocean currents. It is based on the assumption that in a steady state the horizontal pressure gradient and the coriolis force are in equilibrium in the sea below the mixed layer. The coriolis force vanishes at the equator and increases, nonlinearly, towards the higher latitudes. So, the dynamic method does not hold good at and near the equator. However, some observations indicate the validity of the geostrophy beyond the limits of $0^{o}30'$ from the equator in the oceans.

Knauss (1960) reported first that the Equatorial Undercurrent was in geostrophic balance. During the period of observation, the current was symmetrical about the equator. Later in 1966, such symmetry is not observed and so he concluded that the Equatorial Undercurrent was not in geostrophic balance (Knauss, 1966). His argument was supported by Taft and Jones (1973). Some other investigators have found evidence of geostrophic balance in the Equatorial

Undercurrent (Montgomery and Stroup, 1962; Metcalf, Voorhis and Stalcup, 1962; Reid, 1964; Taft, Hickey, Wunch and Baken, 1974; Lukas, 1981; Lukas and Firing, 1984; Hayes, 1982). Wyrtki (1982) finds large differences between geostrophic transport and measured transport of the Equatorial Undercurrent. Lukas and Firing (1984) remarked that all the studies mentioned above have used quasisynoptic sections for the determination of geostrophic balance in the Equatorial Undercurrent. In the present study an attempt is made to compute the zonal flux of the Equatorial Undercurrent, assuming that the Equatorial Undercurrent is in geostrophic balance, beyond 30' from equator.

Since the real ocean is always baroclinic where the isobaric surfaces do not coincide with isosteric surfaces, horizontal density gradients develop. The horizontal density gradient produces circulation which tends to adjust the mass distribution closer to that of static equilibrium, a tendency of establishing barotrophic mass field. In a baroclinic ocean the isosteres intersect the isobars at an angle and so horizontal displacement of water takes place from the high pressure to the low pressure regions along the isosteric surfaces. Therefore, instead of depthwise, steric levelwise computation of the currents is more accurate and reliable.

The first attempt to compute the geostrophic volume flux from acceleration potential at each steric level was made by Montgomery and Stroup (1962). By dividing the flux into each bivariate classes, defined by thermosteric anomaly and salinity, they successfully estimated the zonal geostrophic transport in the Pacific ocean. Masuzawa (1964), after certain modification, used the same method for estimating the zonal geostrophic flux in the Pacific ocean along various longitudes. In order to obtain a similar representation, rather a simple method is used in his work. He distributed the flux into each bivariate class defined by potential temperature and salinity. Later Cochrane et al. (1979) used the same technique to estimate the zonal transport of the Subthermocline Countercurrent in the Equatorial Atlantic ocean.

Apart from the two methods of graphical computation from a vertical section of specific volume anomaly, the method, introduced by Montgomery and Stroup (1962), gives the function $\phi_a + p\delta$ at chosen isanosteric surfaces. The symbol ϕ_a stands for anomaly of geopotential, relative to the reference surface, P for sea pressure, and δ for specifi volume anomaly. The function $\phi_a + p\delta$ has been called acceleration potential (Montgomery and Spilhaus, 1941). This function is simpler to calculate than ϕ_a alone.

Furthermore, this method leads directly to the estimation of geostrophic currents at the chosen isanosteric surfaces.

The anomaly of geopotential is defined by an integral along a vertical line,

$$\phi_a = \int_p^{p_o} \delta \, dp$$

where P_o is the reference pressure. Changing the variable of integration gives the acceleration potential.

$$\phi_a + p\delta = p_o \delta_o + \int_{\delta_o}^{\delta} p \, d\delta$$

where δ_o is the specific volume anomaly at the reference pressure. Since the pressure terms in the anomaly of specific volume in the upper 300 m are negligible, it is now replaced by thermosteric anomaly (δ_T), and ϕ_a and $\phi_a + p\delta$ are modified correspondingly.

The numerical integration has been carried out at each whole degree of latitude to yield the acceleration potential at chosen standard isanosteres and at the sea surface (where p = 0 and $\phi_a + p\delta$ reduces to ϕ_a)

Now the geostrophic velocity takes the form

$$V = \frac{\phi_A - \phi_B}{2\Omega L \sin\theta}$$

where ϕ_A and ϕ_B are the acceleration potentials at stations A and B respectively, L is the distance betwee the stations, Ω is the angular velocity and θ is the me latitude.

The velocity at different isanosteres such as δ_T = 120, 130,140,150,160,170,180,190,200,220,240..... cl/t upto the surface are computed in between two stations and plotted. To compute the geostrophic volume flux throu each vertical meridional quadrangle formed by two successi whole degrees of latitude and two successive standard isanosteres, the vertical profile of velocity is superimpo by the vertical section of thermosteric anomaly. By knowing the mean length and thickness of each quadrangle a the velocity of the water flowing through it, the flux can calculated.

Tait (1955), Timofeev (1956) and Montgomery and Stroup (1962) have chosen the unit of flux to be km^3 $hour^-$ but in the present investigation the unit selected is 10^6 m^3 s^{-1}.

The method of representation is novel that it displays the flux on a temperature-salinity diagram. Characteristic classes are chosen that are defined by thermosteric anomaly and salinity. The second step theref

is to aportion the flux through each quadrangle defined by standard isanosteres and whole degrees of latitude into classes bounded by each 0.2‰ salinity. This was done by superimposing the vertical salinity section with the vertical distribution of zonal flux. Eastward (positive) and westward (negative) fluxes are separately displayed for each characteristic class with intervals of 40 cl/t in thermosteric anomaly and 0.2‰ salinity. The total flux between any two consecutive intervals of thermosteric anomaly is shown at the top and that of salinity on the right hand side of the diagrams.

In the present study, zonal flux has been calculate across eleven selected sections. Of these, four sections occupy in the western Indian ocean during February, March, May and July, one in the central Indian ocean during March and six in the eastern Indian ocean during April, May, June, September, October and November.

1.2.3. Limitations

Normally in Oceanography, although the data collected over a longer period is used to interpret it as a synoptic condition because the acceleration in the oceans is supposed to be neglegible. However, in the

Indian Ocean because of the changes in the oceanic circulations semiannually, it is desirable to have a distinction of one season from the other. As far as possible to meet this demand the author tried to select the sections that run over a short period. Therefore, with regards to the transequatorial sections they are almost synoptic. But the data used for various sections do not pertain to the same year. They are collected on board various research vessels that belong to different countries and the methods of collection are likely to be different also. Under such circumstances an exact comparison of one with the other is not very reasonable. Because of such circumstances, it was not possible on certain occasions to give a definite conclusion. For example, while the Equatorial Undercurrent in the central region could not be traced in January, there is an indication of the Undercurrent in December in the central region with the associated features of spreading of thermocline. This is, possibly, because of the comparison of two different years data. Sometimes, the availability of the oceanographic data spaced at a longer intervals, also gives rise to an indefinite conclusion.

With regards to the zonal flux estimation, it is not very correct to compute the same at and near the

equator as it leads to uncertainty, the coriolis parameter which comes in the denominator, being zero. To avoid this problem for computation of the zonal flux,. the current was computed between no two stations across the equator. It is always seen that the zonal flux is computed between two stations that lie only in one hemisphere. Care is also taken that the computation of average geostrophic current between two stations falls beyond $0^{o}30'$ from the equator.

CHAPTER - II

CHAPTER - II

TRANSEQUATORIAL SECTION OF HYDROGRAPHIC PROPERTIES

Among the hydrographic properties - temperature, salinity and oxygen, used to infer the presence of Equatorial Undercurrent, temperature gives a better indication of the direction of the zonal currents. The vertical displacement of water can be identified through the thickness of the thermocline. Salinity is the next reliable property to trace the Equatorial Undercurrent in the Indian ocean. Eventhough oxygen distribution is less reliable than temperature and salinity, it has been frequently used to confirm the presence or absence of the Undercurrent.

Owing to paucity of relevant data, transequatorial sections of temperature, salinity and oxyty could not be presented for all the months in all the three zones namely western, central and eastern. Moreover, oxyty data are not available for March and August in the eastern Indian ocean and for November in the western Indian ocean.

2.1. JANUARY

The section along $58^{o}E$ is confined to $3^{o}S$ to $2^{o}N$ only. As a result, a detailed discussion about the distribution of properties is not possible. Nevertheless,

some important features are well depicted. The isotherms show a vertically diverging tendency from about $0^{o}30'S$ to $1^{o}N$, from where again they converge (Fig. 1). Therefore, the spreading of the thermocline is predominant between the equator and $1^{o}N$. The thickness of the thermocline is the lowest around $1^{o}S$ and it shows an increasing tendency towards the south. The increase of the thickness is mainly because of the troughing of the isotherms in the subsurface depths. The depth of the mixed layer is almost constant southward from $1^{o}S$. The thermal structure indicates a westerly flow at the equator at the surface.

If the thermal structure is discussed independent of the salinity structure, it shows an apparent sloping of the sea surface downward to the south. But clubbed with the salinity structure, the pycnocline does show the sloping down on either side of the equator as the low and high salinity waters are respectively placed in the southern and northern hemispheres. Therefore, the presence of the Equatorial Undercurrent can be inferred to be confined to the equator, although it seems to be at about $1^{o}N$ based on the spreading of the thermocline. This inference can be corroborated with the presence of a highly oxygenated water at the equator in the subsurface level. The shifting of the high salinity core, slightly, northward

may be the effect of the high saline water present in the western side of the Equatorial Indian ocean, particularly, in the northern hemisphere. This may be further confirmed from the presence of a high salinity tongue protruding southward upto about 100 m depth.

The section along 76°E runs between 5°N and 5°S. The top of the thermocline appears to slope upward on either side of the equator, but in the subsurface layers the isotherms run almost parallel without much variation in the depth of the lower part of the thermocline (Fig. 2). It is interesting to note that the salinity decreases north and southward from 3°N and 3°S respectively. The low salinity water in the northern most part of the section may be the influx from the Bay of Bengal. The low salinity water in the southern most part of the section may be from the Pacific ocean flowing along the South Equatorial Current (Sharma et al., 1982). The intrusion of high salinity water from the northern hemisphere at subsurface depth to wards the equatorial region is indicated by a tongue structure. Perhaps, it is because of this intrusion of high salinity water from the north that the salinity between 3°N and 2°S is relatively higher in the upper layers. From the thermal structure, it is obvious that the zonal flow is easterly both at the upper layers and subsurface depths.

In the surface layer, from the thermal structure alone it can be inferred that the easterly flow is not strong but the strong meridional salinity gradients on either side of the equator definitely produces stronger flow. Along the equator, in the depth range of 75-125 m the horizontal gradients are strong in the thermal structure as well as in the salinity. Obviously, the subsurface easterly flow is likely to be stronger than the surface easterlies. Although the thermal structure does not indicate a conspicuous Equatorial Undercurrent, the high salinity core indicates the present of Equatorial Undercurrent. The conspicuous nature of the Undercurrent might have been masked because of the easterly flow in the upper layers. Had the flow in the surface been westerly the presence of the Undercurrent would have been more conspicuous. The distribution of oxygen with higher values in the equatorial region extending into subsurface depths is an indication of the strong easterly flow in the normal depth range of the Equatorial Undercurrent.

The vertical distribution of hydrographic properties along $86^{o}30'E$ is presented in Fig. 3 and this distribution pertains to the conditions in the eastern region of the Indian ocean under study. The transequatorial salinity gradients in this section are more conspicuous compared to

the previous one, mainly because of very low salinity waters of the Bay of Bengal in the north and the Pacific ocean water in the south with higher salinity water at the equator in the eastern part of the Indian ocean. Obviously, they give rise to a strong easterly flow at the equator. The temperature structure below 50 m depth shows the sloping of the thermocline upward on either side of the equator, indicating the presence of an easterly flow. The incursion of high salinity water from the north as well as south in the depth range of 50-125 m along this section is indicated by protruded high salinity tongues. The value of the salinity in the high salinity tongue of the northern hemisphere is higher than that of the southern hemisphere. In the equatorial region the presence of the Undercurrent is clearly demonstrated by the high salinity core but the normal features associated with an Undercurrent are not well depicted because, the surface flow also is easterly. Oxygen distribution confirms the presence of a strong easterly flow in the subsurface depths.

Summing up the results for the month of January, it can be realised that the surface flow along the equator is westerly in the western region while it is easterly in the central and the eastern regions. The subsurface flow all along the width of the Indian ocean at the equator is easterly. That may be the reason why the normal hydrographic

characteristics of an Equatorial Undercurrent are well depicted in the western region while they are not very conspicuous in the other two regions. While the incursion of the high salinity water from the north is noticed in the subsurface depths in all the three sections, the high salinity water from the southern hemisphere is prominent only in the eastern section.

2.2. FEBRUARY

The distribution of hydrographic properties along $54^{o}30'E$ is confined between $2^{o}N$ and S. Eventhough the section is of limited extent, still it indicates some of the important features associated with the Equatorial Undercurrent namely ridging of the thermocline in the upper layers, troughing in the subsurface layers, high salinity core around the equator and penetration of high oxyty water to the deeper layers. While the salinity increases from N to S, the colder water prevail around the equator with the temperature less than $26^{o}C$. Therefore, it is not possible to identify the definite direction of the surface flow. However, the presence of the Equatorial Undercurrent is obviously present with all its associated characteristics as specified above.

Thermal structure along $65^{o}E$ shows the spreading of the thermocline at the equator showing the presence of westerly flow at the surface and easterly flow at subsurface

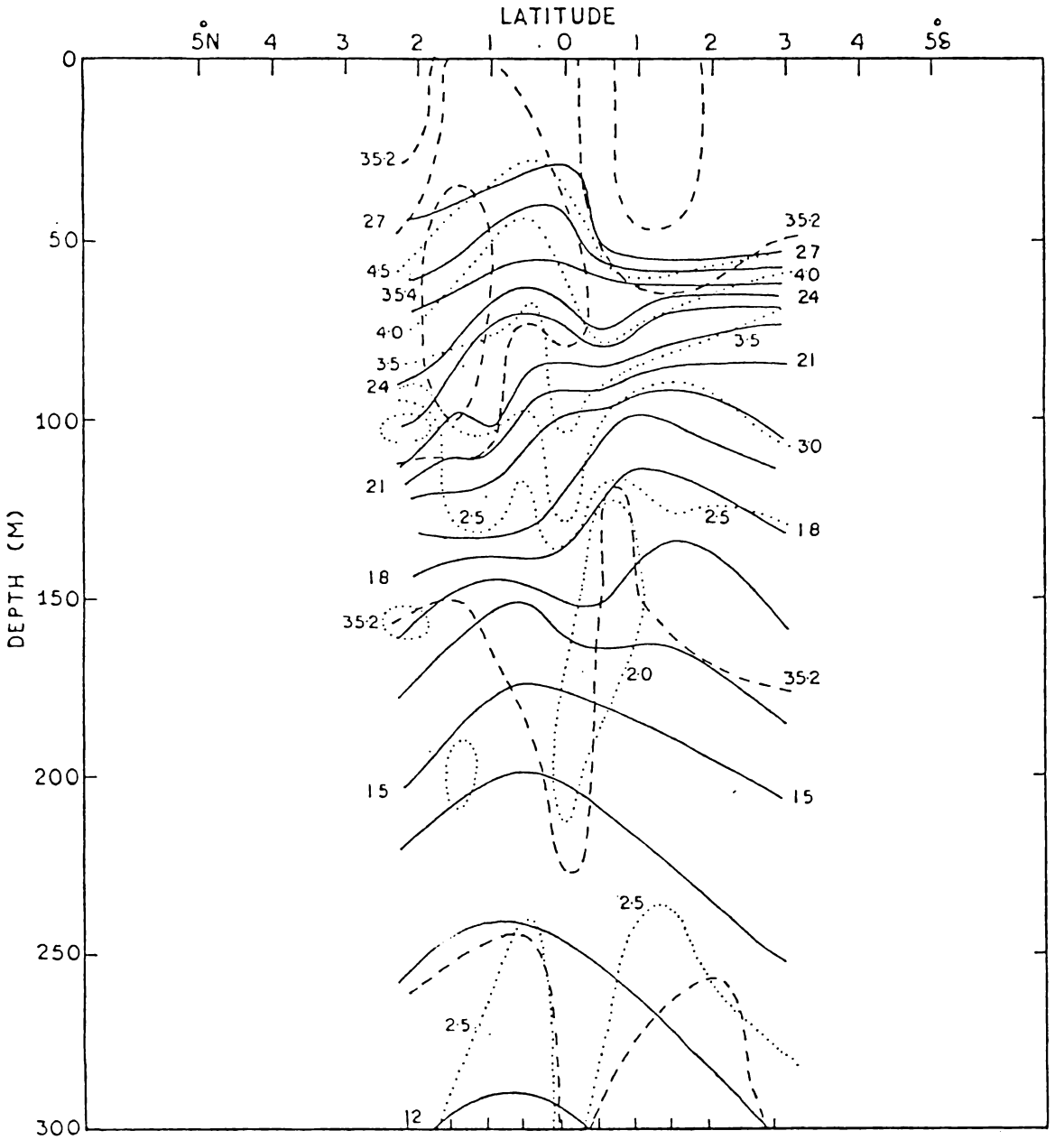

Fig. 1. Vertical section of temperature (solid lines - ^{o}C), Salinity (dashed lines - parts per mille) and dissolved oxygen (dotted lines - ml/l) at 58°E (January - February, 1965).

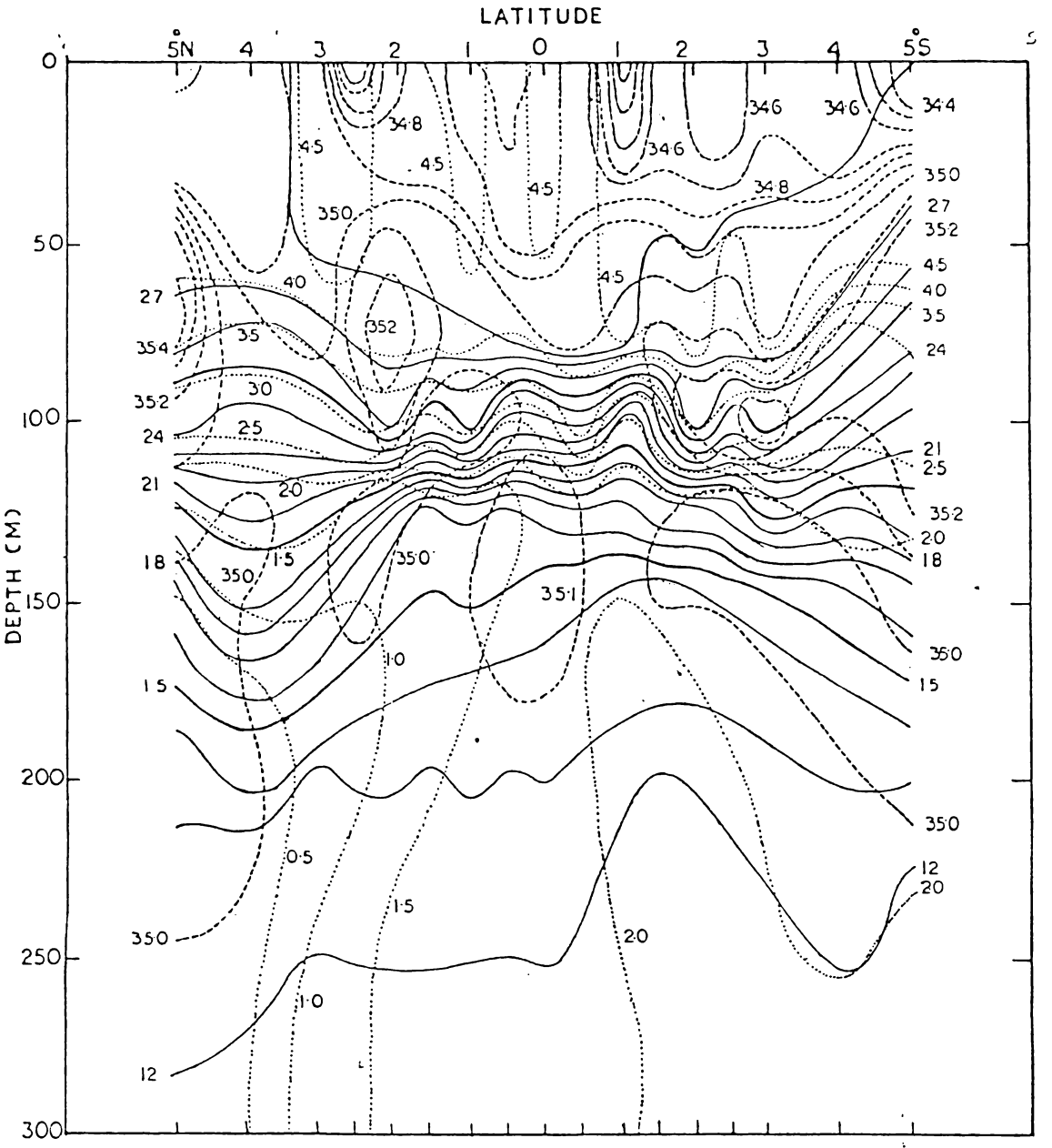

Fig. 2. Vertical section of temperature (solid lines - ^{o}C), Salinity (dashed lines - parts per mille) and dissolved oxygen (dotted lines - ml/l) at 76°E (January, 1960).

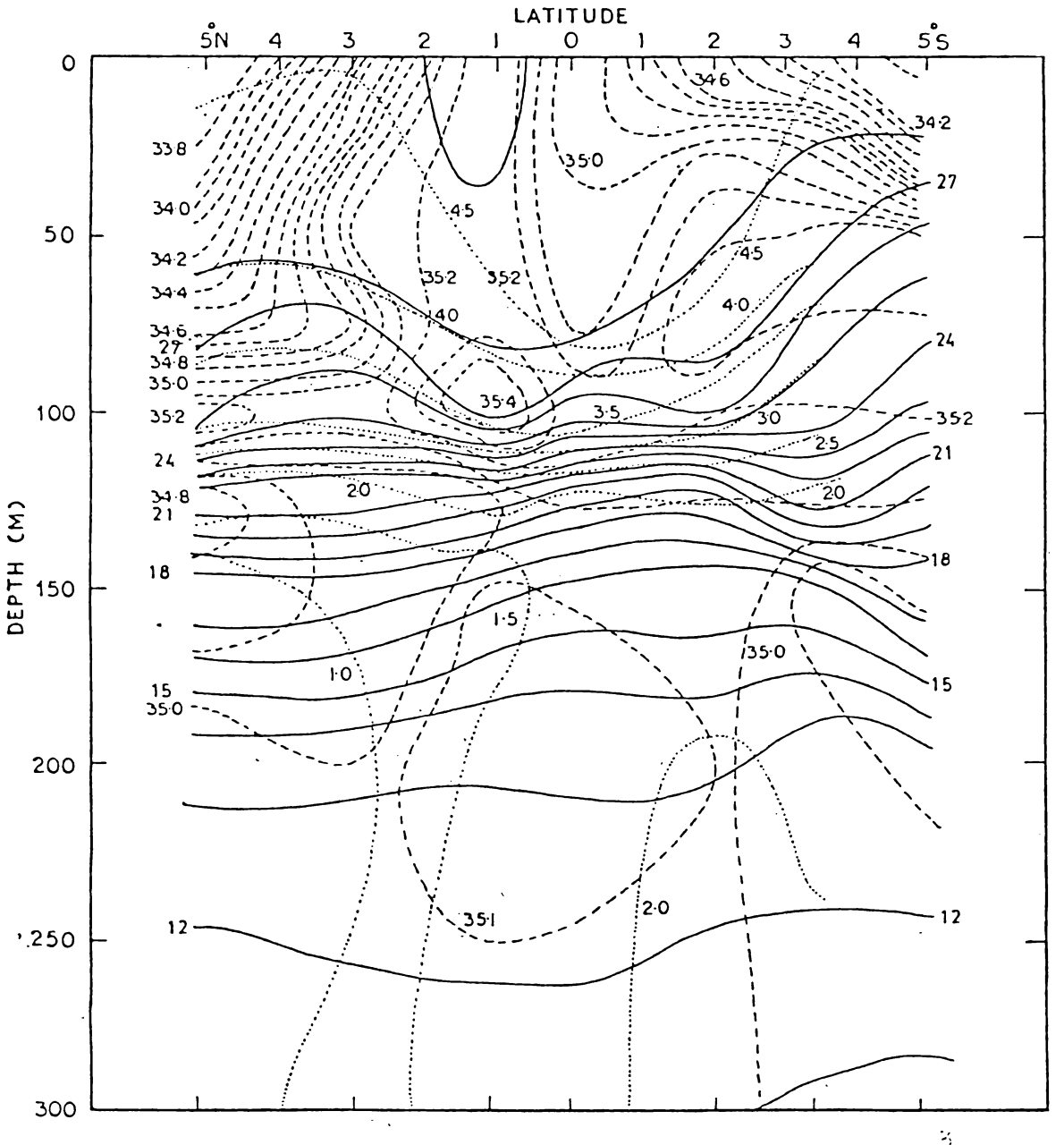

Fig. 3. Vertical section of temperature (solid lines - ^{o}C), Salinity (dashed lines - parts per mille) and dissolved oxygen (dotted lines - ml/l) at 86°30'E (January, 1960).

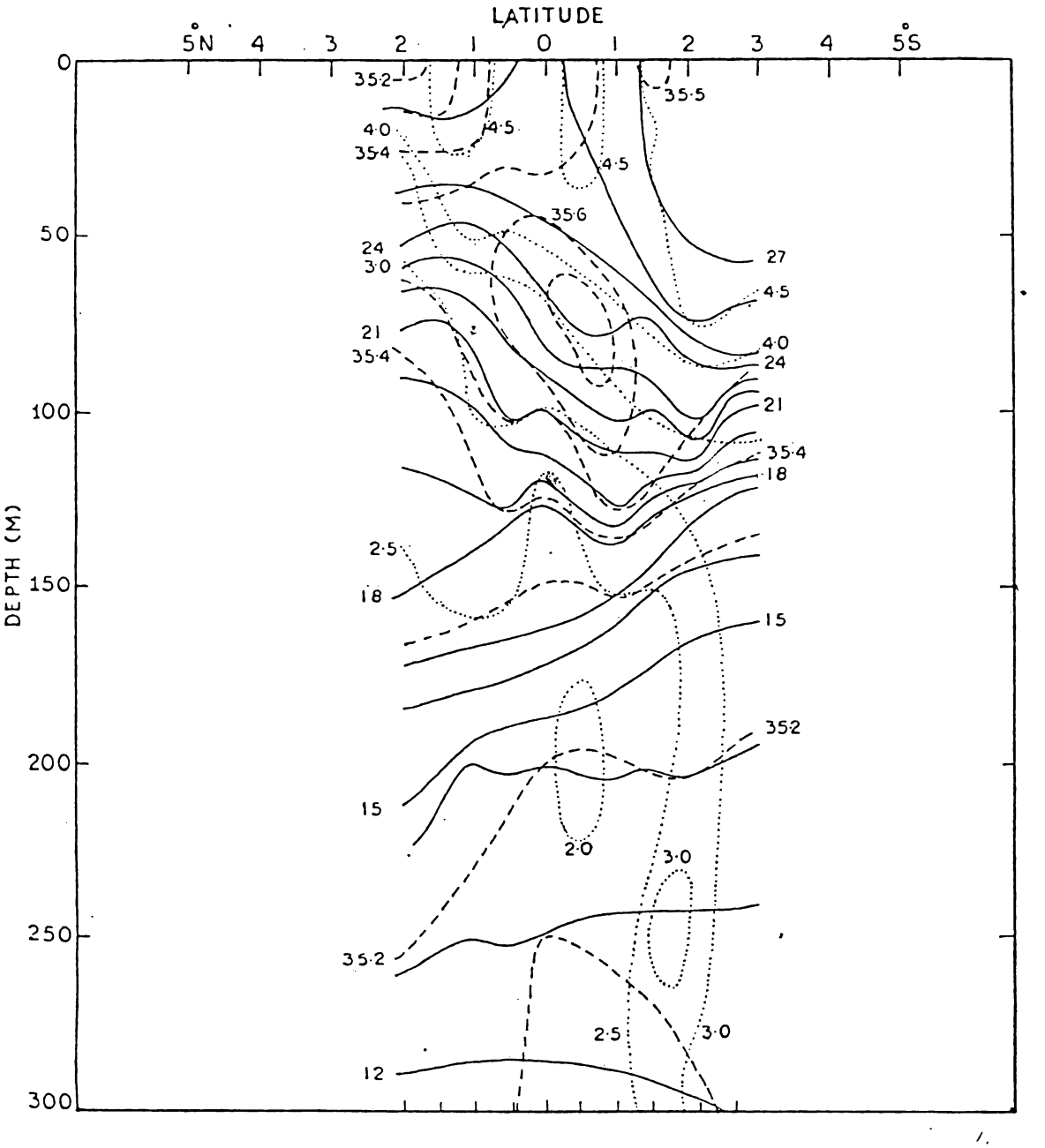

Fig. 4. Vertical section of temperature (solid lines - ^{o}C), Salinity (dashed lines - parts per mille) and dissolved oxygen (dotted lines - ml/l) at 54°30'E (February, 1975).

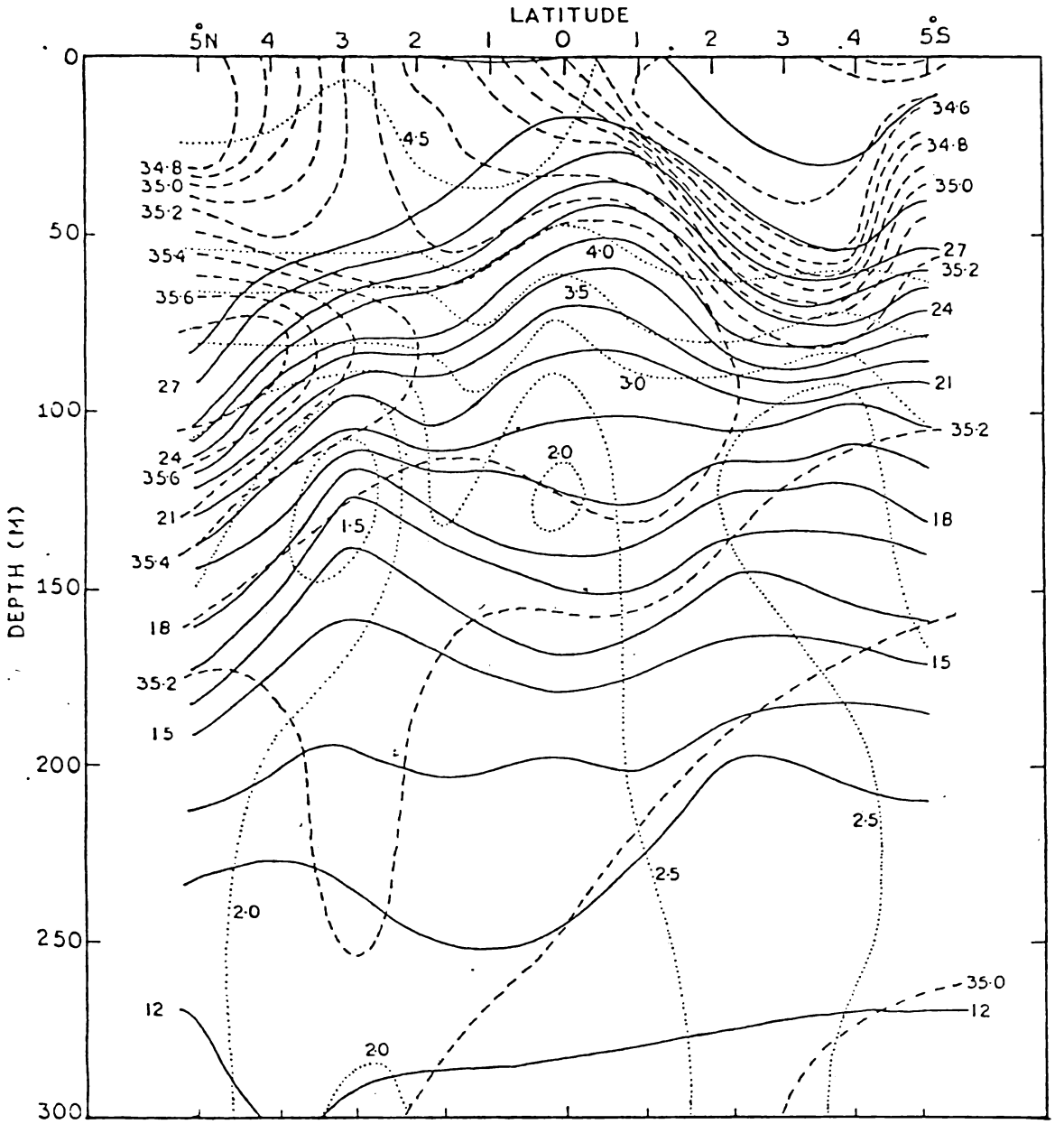

Fig. 5. Vertical section of temperature (solid lines - ^{o}C), Salinity (dashed lines - parts per mille) and dissolved oxygen (dotted lines - ml/l) at 65^{o}E (February, 1973).

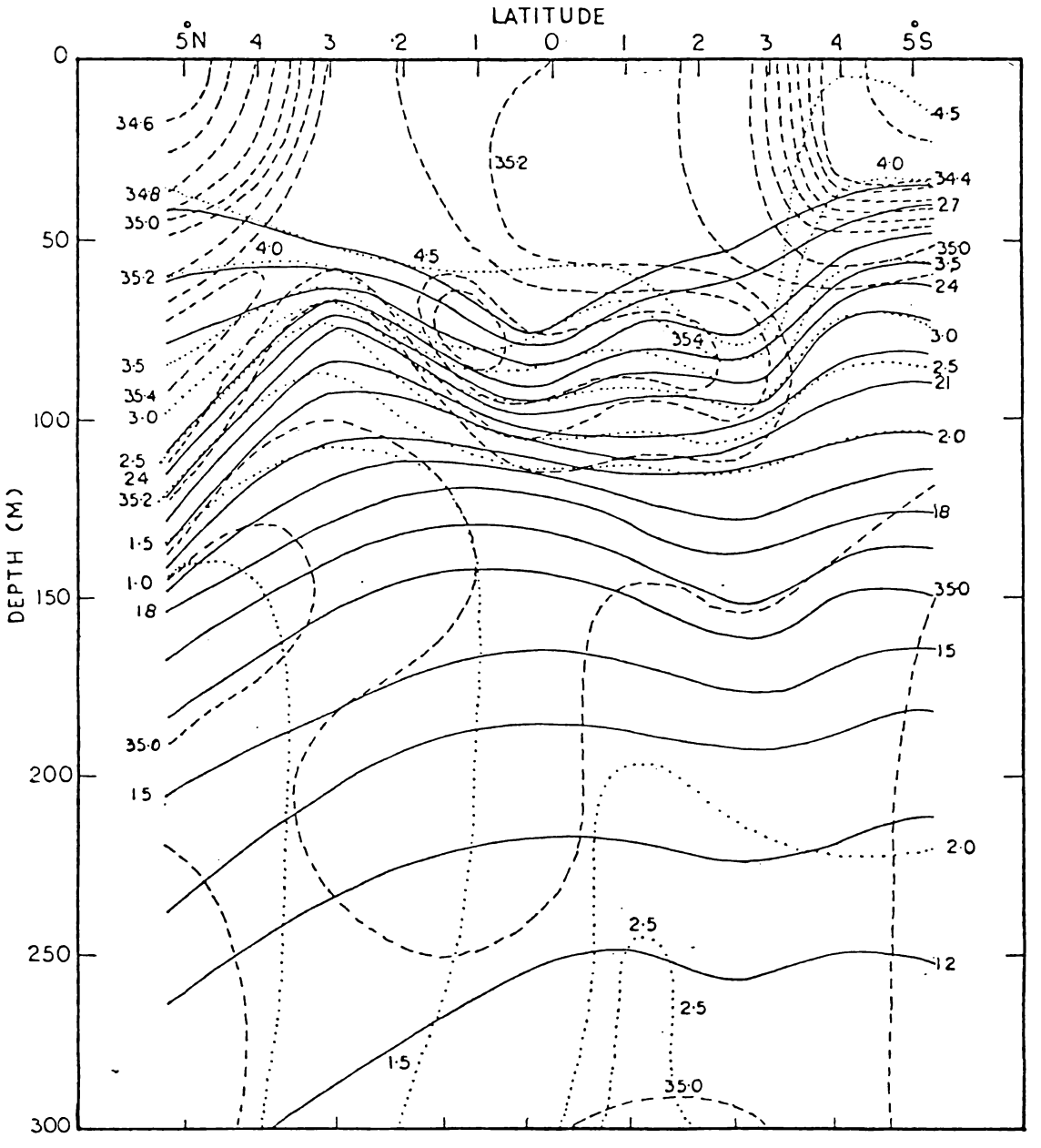

Fig. 6. Vertical section of temperature (solid lines - ^{o}C), Salinity (dashed lines - parts per mille) and dissolved oxygen (dotted lines - ml/l) at 85°E (February, 1963).

depths (Fig. 5). The surface salinity decreases on either side from 3°N. Ofcourse, the salinity is relatively higher in the northern region compared to the southern. The high salinity tongue extends towards the equator from the north in the depth range of 75-125 m. There is no similar subsurface high salinity tongue from the southern hemisphere. Perhaps, it may be because of this feature that there is no high salinity core associated with the Undercurrent below the equator. Nevertheless, the high salinity water in the depth range of 75-125 m below the equator is a definite indication of the Equatorial Undercurrent. It is interesting to note that the oxyty is lower in the southern hemisphere in the upper layer compared to that in the northern hemisphere and in the subsurface depth the conditions are reversed.

The distribution pattern of hydrographic properties along 85°E is a deviation from the normal pattern observed in the other sections. Isolated alternate high and low salinity cells are noticed in the upper layers (Fig. 6). The thermocline contracts near the equator and spreads on either side. Associated with the contraction of the thermocline, the high salinity cells are located on either side of the equator in the depth range of 50-120 m. The horizontal gradients of temperature and salinity indicate easterly flow in the upper 100 m and westerly flow below. However, it may be noted that the atmospheric and oceanic

conditions in the year 1963 when this section was covered was a deviation from the normal condition (Taft and Knauss, 1967; Uda and Nakamura, 1973). Therefore, it is not reasonable to rely much on this section to draw any definite conclusion.

In February it appears that the Equatorial Undercurrent which is conspicuously shown in the western region only, during January is extended to the central region. It also appears that the strength of the Equatorial Undercurrent is increased from January to February.

2.3. MARCH

The spreading of the thermocline at the equator along 58°E is very much pronounced and it is associated with a strong high salinity core (Fig. 7). Both from the salinity and thermal structures, the surface flow is westerly and it is expected to be relatively strong because of intense horizontal gradients. It is also further obvious that the easterly flow is strengthened as indicated by the horizontal gradients below 50 m. The indication of the Undercurrent is further supported by the oxygen distribution, having higher values extending to subsurface depths below the equator.

The section along 65°E depicts the ideal situation of the development of an Equatorial Undercurrent with the associated features of spreading of thermocline, high salinity core, and high oxyty water mixing downwards (Fig. 8). It is also further conspicuous that the subsurface flow of easterly is very strong. The high salinity core below the equator appears to be the extension of the high salinity tongue protruding from north around 100 m depth.

Along 90°E the thermal structure shows spreading of the thermocline but its features are not so pronounced as they are along 58°E and 65°E. In the spreading of the thermocline at the equator the troughing of the isotherms in the subsurface depth dominate over the ridging in the upper layers (Fig. 9). Therefore, it can be inferred that the build up of the easterly flow in the upper layers may be less than that in the layers below. The high salinity water associated with the core of the Undercurrent is an extension of the high salinity tongue from the southern hemisphere. The isolated high salinity core below 4°N is not normally expected to be prevailing as the water from the Bay of Bengal should be associated with a low salinity tongue. Therefore, it is not immediately clear how such a high salinity core is present as an isolated one. Unfortunately, the oxygen data is not available to support the presence of the Undercurrent.

The hydrographic features of the sections during March confirm the strengthening of the Equatorial Undercurrent from west to east and also indicate that the surface flow is westerly even in the eastern region.

2.4. APRIL

The distribution of temperature along the transequatorial section between 49°E and 53°E shows a wavy nature of isotherm, ofcourse, with the spreading of thermocline around the equator (Fig. 10). The wavy nature of the isotherm is mainly confined to the upper layers which, perhaps, might have been influenced by the internal waves generated at the boundary of the discontinuity layer. The surface salinity in the north is much higher compared to that of the south. The spreading of the thermocline and the high salinity core, slightly north of the equator, indicate the presence of an easterly flow. The high salinity core is the extension of the high salinity tongue of the northern hemisphere. Although there is an indication of the Equatorial Undercurrent, its features related to the hydrographic properties are not very assertive, probably, because the Equatorial Undercurrent may only begin to develop in this region. Below 150 m, the bottom of the thermocline slopes continuously down from 5°S to 5°N. Such a condition implies that the flow below 150 m is in opposite direction in both the hemispheres. The oxypleths also show a wavy

nature confirming the influence of the internal waves. It is further possible that the influence of the internal waves might have partly masked the conspicuous features associated with the Undercurrent.

The isotherms in the upper levels along 78°E also show wavy nature. However, the spreading of the thermocline at the equator is prominent. The salinity increases on either side of the equator. The flow pattern at the surface is likely to be controlled by horizontal salinity gradient alone as there is no variation of surface temperature between 5°N and 5°S (Fig. 11). The high salinity core at 100 m depth along the equator is pronounced and it is connected with the high salinity tongue from the south. Another high salinity core seperated from the main one at the equator, is noticed at about 3°N. The separation of these two appears to be due to sinking of the low salinity water at about 2°N as a result of convergence.

The salinity distribution in the surface layers along 92°E shows strong meridional gradients. The surface values of salinity appear to be abnormally low in the southern sector of the section. At about 4°S the salinity is even less than 33.8‰ for which a plausible explanation is not clearly known except to suspect that there might have

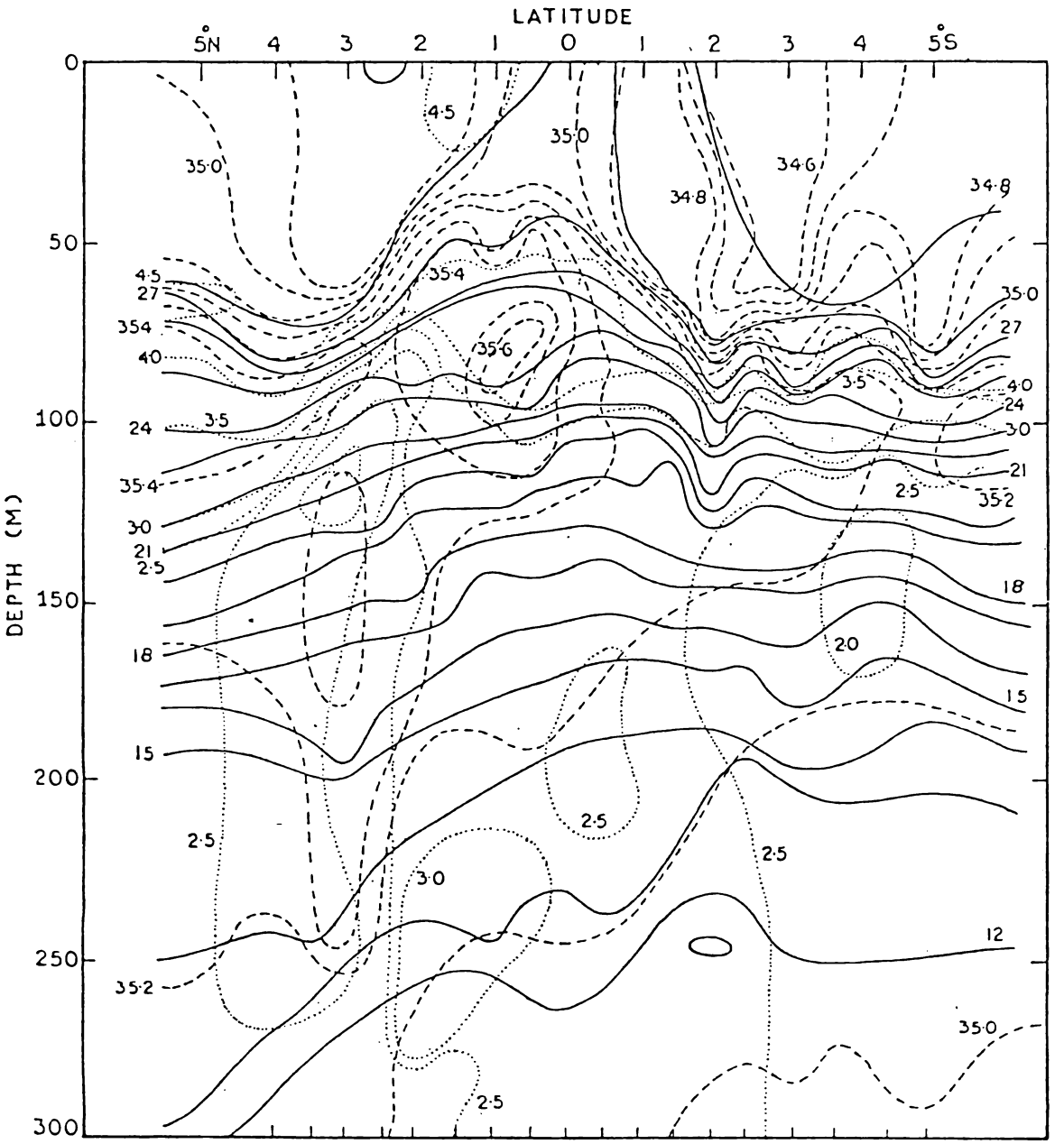

Fig. 7. Vertical section of temperature (solid lines - ^{o}C), Salinity (dashed lines - parts per mille) and dissolved oxygen (dotted lines - ml/l) at 57°59'E (March, 1964).

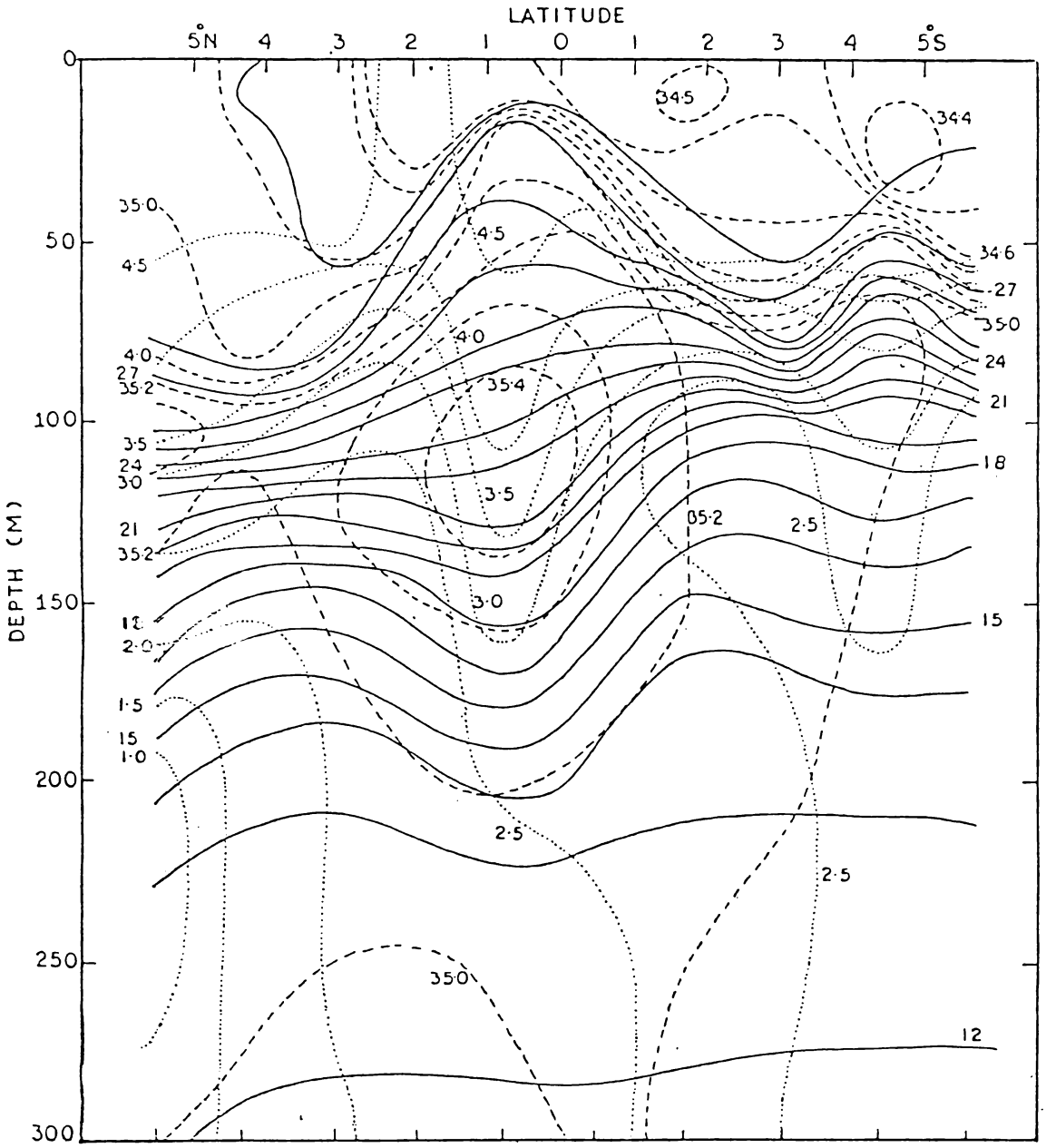

Fig. 8. Vertical section of temperature (solid lines - °C), Salinity (dashed lines - parts per mille) and dissolved oxygen (dotted lines - ml/l) at 65°E (March, 1973).

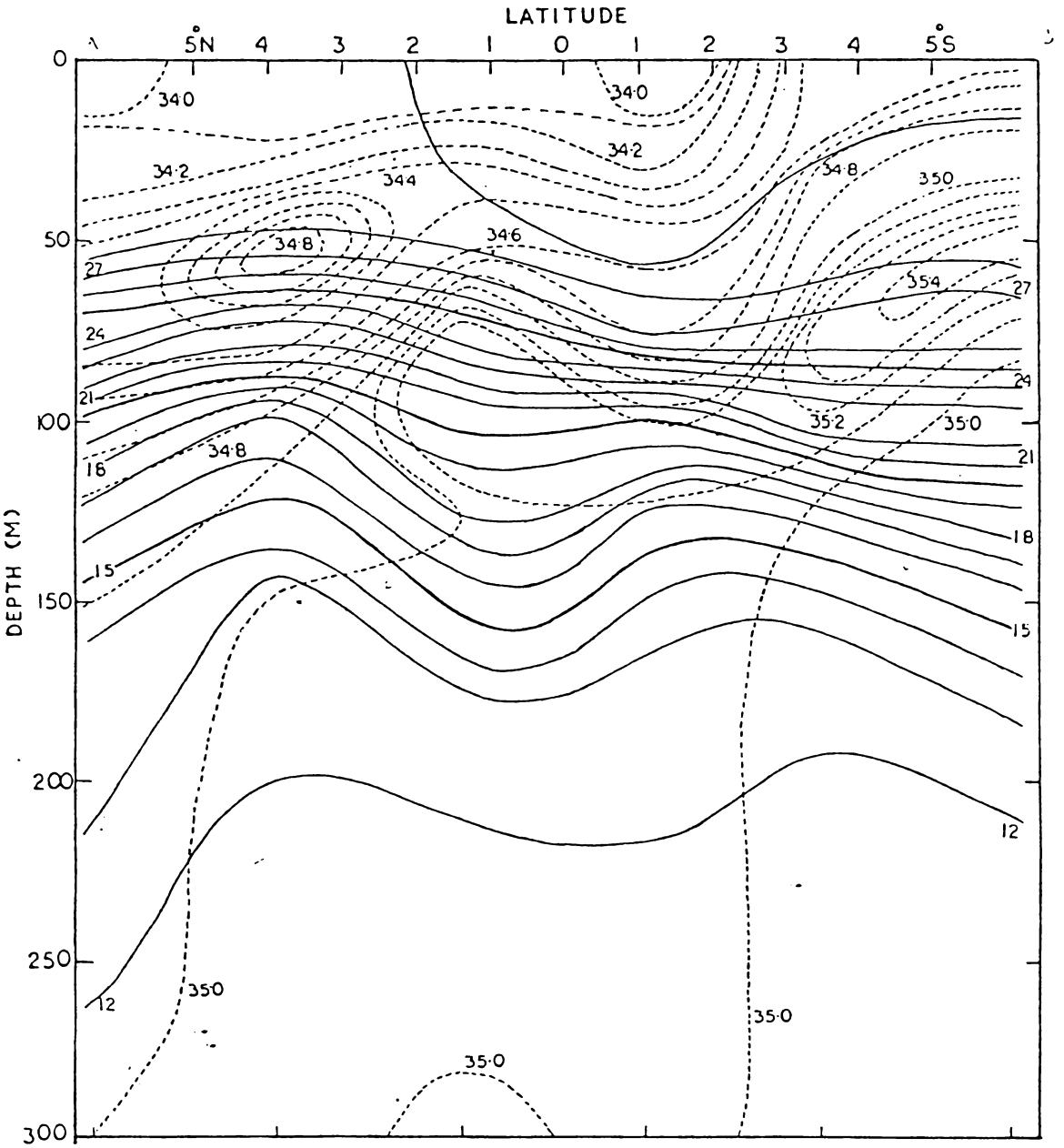

Fig. 9. Vertical section of temperature (solid lines - ^{o}C) and salinity (dashed lines - parts per mille) at 90^{o}E (March, 1959).

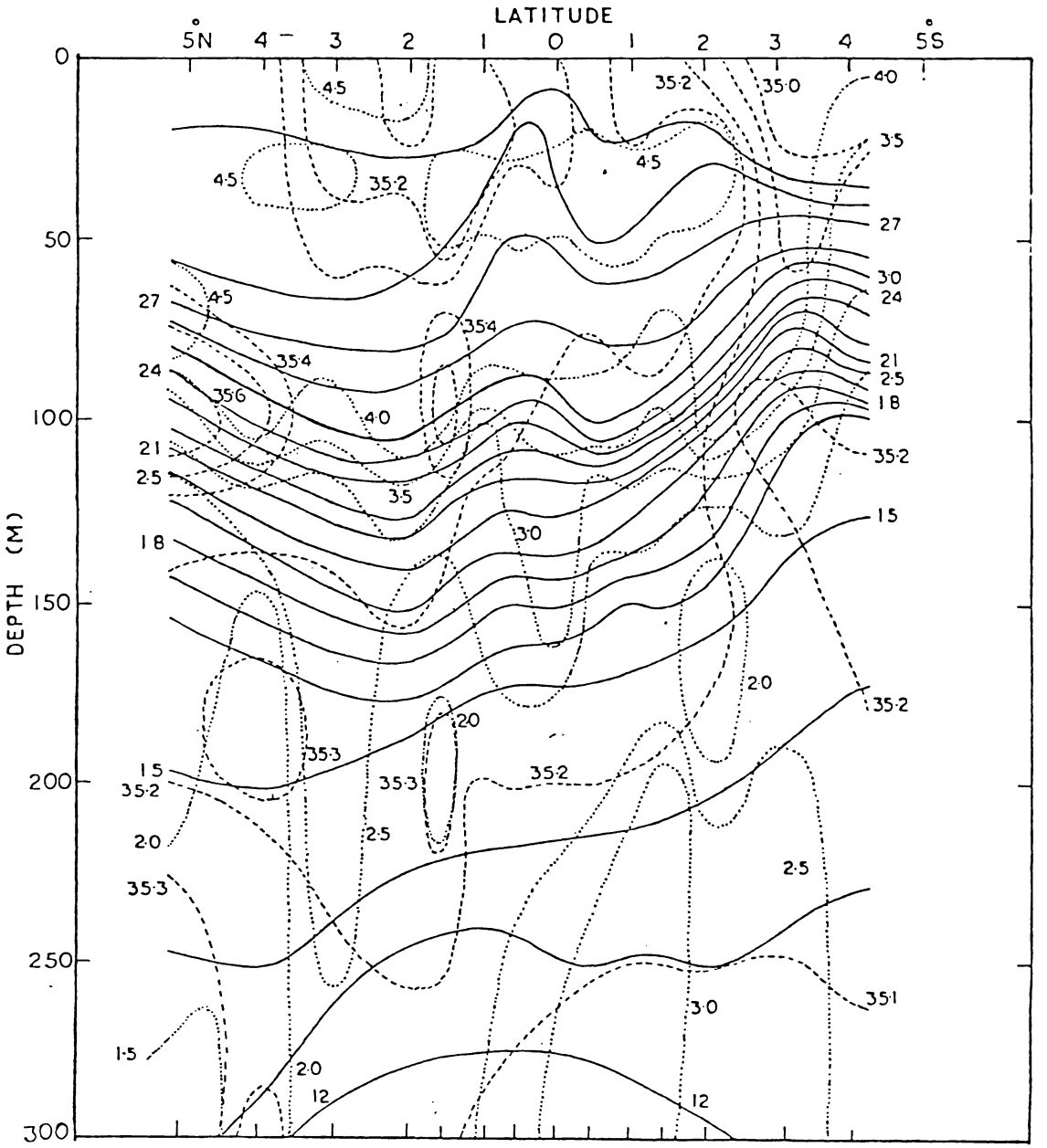

Fig. 10. Transequatorial section of temperature (solid lines - ^{o}C), Salinity (dashed lines - parts per mille) and dissolved oxygen (dotted lines - ml/l) between 49^{o} & 53^{o}E (April, 1965).

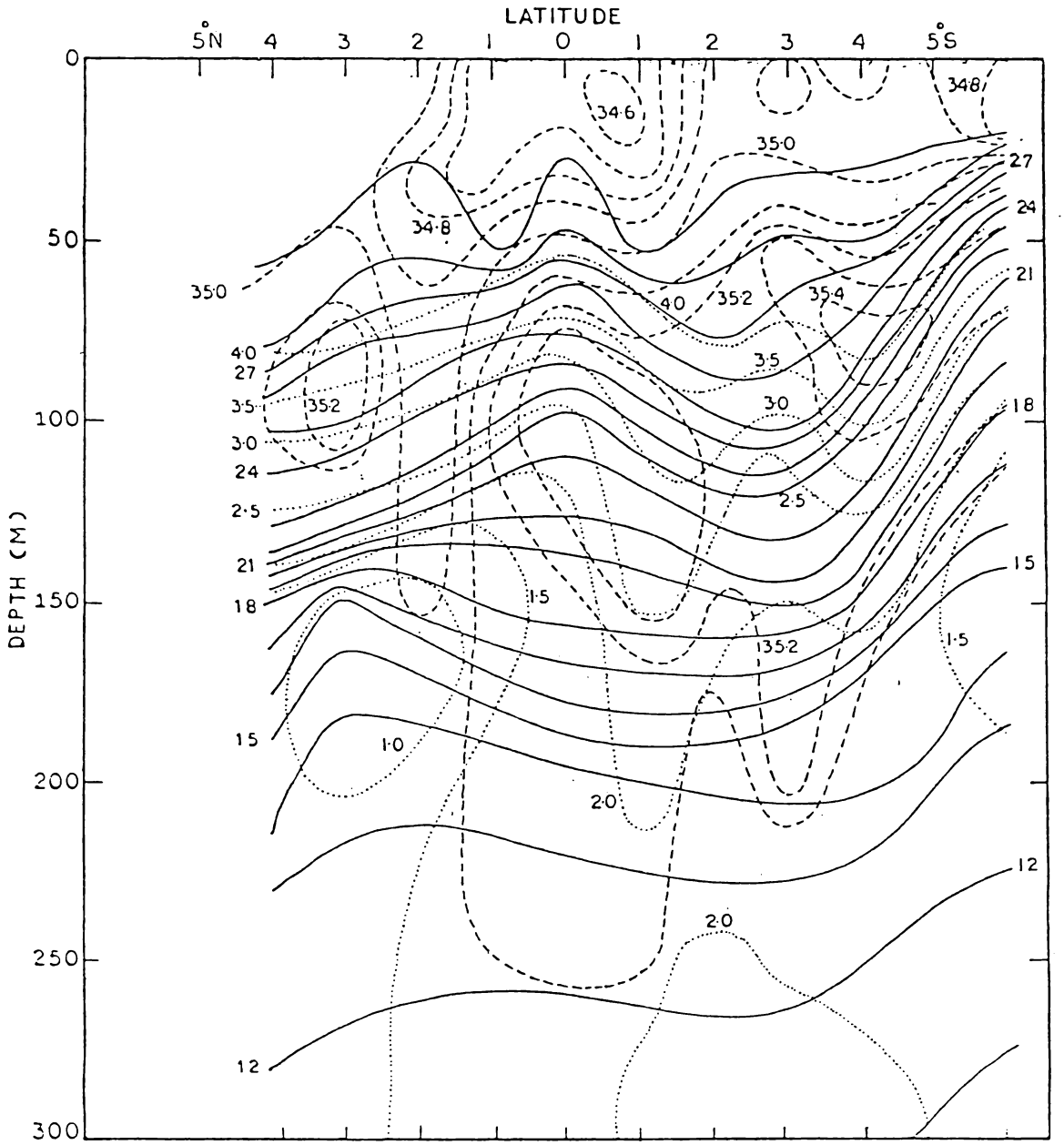

Fig. 11. Vertical section of temperature (solid lines - ^{o}C), Salinity (dashed lines - parts per mille) and dissolved oxygen (dotted lines - ml/l) at 78^{o}E (April, 1961).

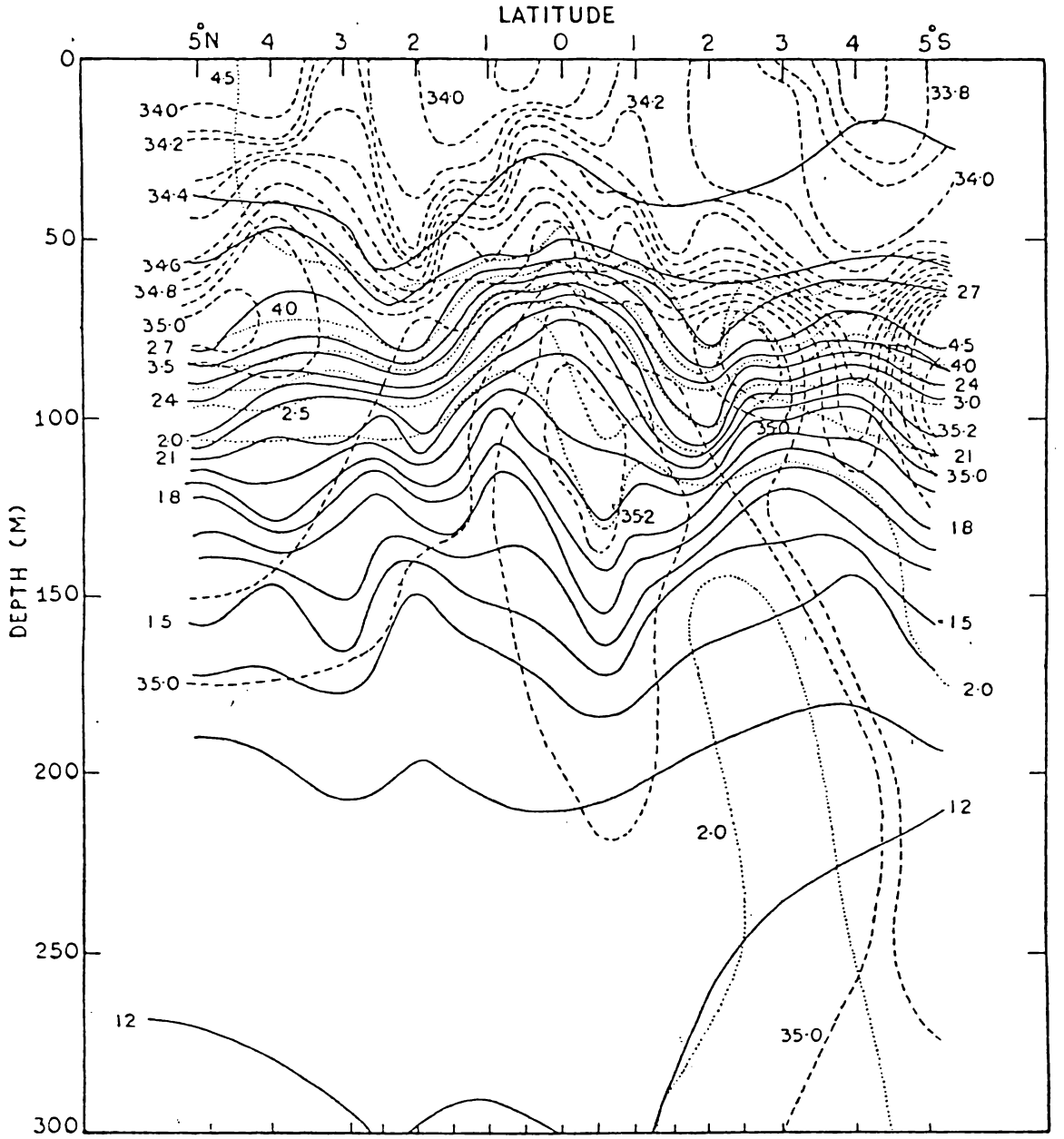

Fig. 12. Vertical section of temperature (solid lines - ^{o}C), Salinity (dashed lines - parts per mille) and dissolved oxygen (dotted lines - ml/l) at 92^{o}E (April, 1963).

been rain fall along the section when it was occupied. The isotherms, in the eastern section, show wavy nature extending to the bottom of the thermocline unlike in the other two sections where the wavy nature is confined only to the upper layer (Fig. 12). Therefore, it is not clear if the wavy nature is the influence of the internal waves as their effect is expected to be felt at the boundary of the discontinuity layer. However, the spreading of the thermocline below the equator is conspicuous. As the values of the salinity in the high salinity tongues of the southern and northern hemispheres are lower than that of the high salinity core below the equator, it can be construed that the high salinity can only be associated with the easterly flow. Based on physical properties there is a definite indication of the Equatorial Undercurrent although one may be puzzled with the wavy nature of the isotherms at the bottom of the thermocline.

The Equatorial Undercurrent continues to prevail along the width of the Indian ocean. But there is no clear indication if there is any increase in the strength of the Undercurrent from the previous months. The surface flow in the central region is easterly.

2.5. MAY

The distribution of hydrographic properties along the transequatorial section at 55°E gives a pattern of isotherms and isohalines which are more or less similar to those, in the previous month along the longitudes between 49° and 53°E, especially in the subsurface layers. At the surface, alternate high and low salinity water is observed along the section (Fig. 13). The combined effect of temperature and salinity at the surface leaves denser water on either side of 3°N and 3°S, and lighter water in between these two latitudes producing an easterly flow near the equator. The spreading of thermocline observed in the depth range 100-150 m and the high salinity core at 1°N, just above the spreading of thermocline may be associated with the Equatorial Undercurrent. The high salinity core may be originated from the southward advecting high salinity water at 5°N where the salinity exceeds 35.8%.. From the oxygen distribution it is evident that the 2.5 ml/l oxypleth runs almost vertically downward at the equator to confirm the presence of strong mixing, an associated feature of the Equatorial Undercurrent.

The wavy appearance of the isotherms along 65°E during this month may be due to the influence of the internal waves. The thermocline is compact at 5°S and spreads toward north.

The intense troughing of isotherms is noticed at $4^{o}N$ in the subsurface layers and at the equator in the surface layer. Very low salinity is observed at the surface, around $4^{o}N$ and it increases towards the equator upto $0^{o}30'N$. The low salinity water at $4^{o}N$ might perhaps be the Pacific ocean water carried by the South Equatorial Current that crossed the equator on the western side of $65^{o}E$ and join the southwest monsoon current. Within $0^{o}30'N$ and S, very low gradient of salinity is observed (Fig. 14). The surface salinity, gradually, increases southwards from $0^{o}30'S$. The isopycnal surface slopes upwards from $4^{o}N$ to $0^{o}30'N$, then it goes down at the equator and again slopes up towards south. Therefore, an eastward flow is pressumed at the surface in between $0^{o}30'N$ and S. An advection of high salinity water from north towards the equator is evident in the subsurface layers at about 75 m. It may be associated with the surface eastward flow which extends upto 100 m. Another intense troughing of isotherms is noticed at $4^{o}N$ below 100 m that covers the entire depth of the section. The oxygen distribution does not show any downward mixing of high oxyty water at the equator.

The transequatorial distribution of hydrographic properties along $84^{o}E$ gives a clear picture of the contraction of the thermocline at the equator and spreading on either side (Fig. 15). Surface salinity increases gradually from $5^{o}N$ to $5^{o}S$. Penetration of high salinity water towards the equator is observed from both the

hemispheres in the subsurface layers. The combined effect of temperature and salinity indicates an intense easterly flow at the surface symmetrical about the equator below which an equally strong westerly flow prevails. April, being the transition period, strong westerly winds prevail at the equator. Therefore, the strong easterly flow, driven by the surface westerlies, observed at the surface along the equator is distinguished as Equatorial Jet, discovered by Wyrtki (1973). The pattern of oxypleths, surprisingly coincide with the orientation of isotherms and isohalines in the upper 150 m.

It appears that the Equatorial Undercurrent in May is confined to the western Indian ocean only. The spreading of the thermocline and an isolated high salinity core is not found in the central and eastern sections. Therefore, it is seen that the Undercurrent is found to disappear in the eastern equatorial Indian ocean. An eastward flow is noticed at the surface along the equator to cover the entire width of the Indian ocean. The influence of the internal waves is observed during the previous month in the western section whereas it is detected in the central Indian ocean during May. The troughing of isotherms at the equator along $84^{o}E$ indicates the continuation of the Equatorial Jet along the equator even towards the end of May in the upper 100 m and the ridging in the subsurface depth denotes westward flow.

2.6. JUNE

The distribution of hydrographic properties along 55°E does not show any spreading of thermocline at the equator, on the contrary slight troughing is noticed within 1°N and S (Fig. 16). The high salinity water is found to be advected towards the equator from 5°N in the subsurface layer. The surface density structure denotes the high density water on either side of the equator beyond 1°N and S leaving lighter water in between these latitudes, indicating the presence of an eastward flow at the surface. The troughing of oxypleths at the equator may be associated with the surface eastward flow. There is no indication of downward mixing of high oxyty water below the equator.

Hydrographic properties along 65°E show spreading of thermocline just south of the equator associated with a high salinity core at 1°S in the depth range of 50-150 m (Fig. 17). The subsurface troughing of the thermocline is more pronounced than surface ridging indicating downward increase of easterly flow. At the surface lower salinity is observed between 1°N and 4°N, which may perhaps be the Pacific Ocean Water brought by South Equatorial Current, as already explained for the previous month. The salinity does not vary in between 1°N and 2°S. Beyond 2°S the salinity increases southwards. Since the upper 50 m is an

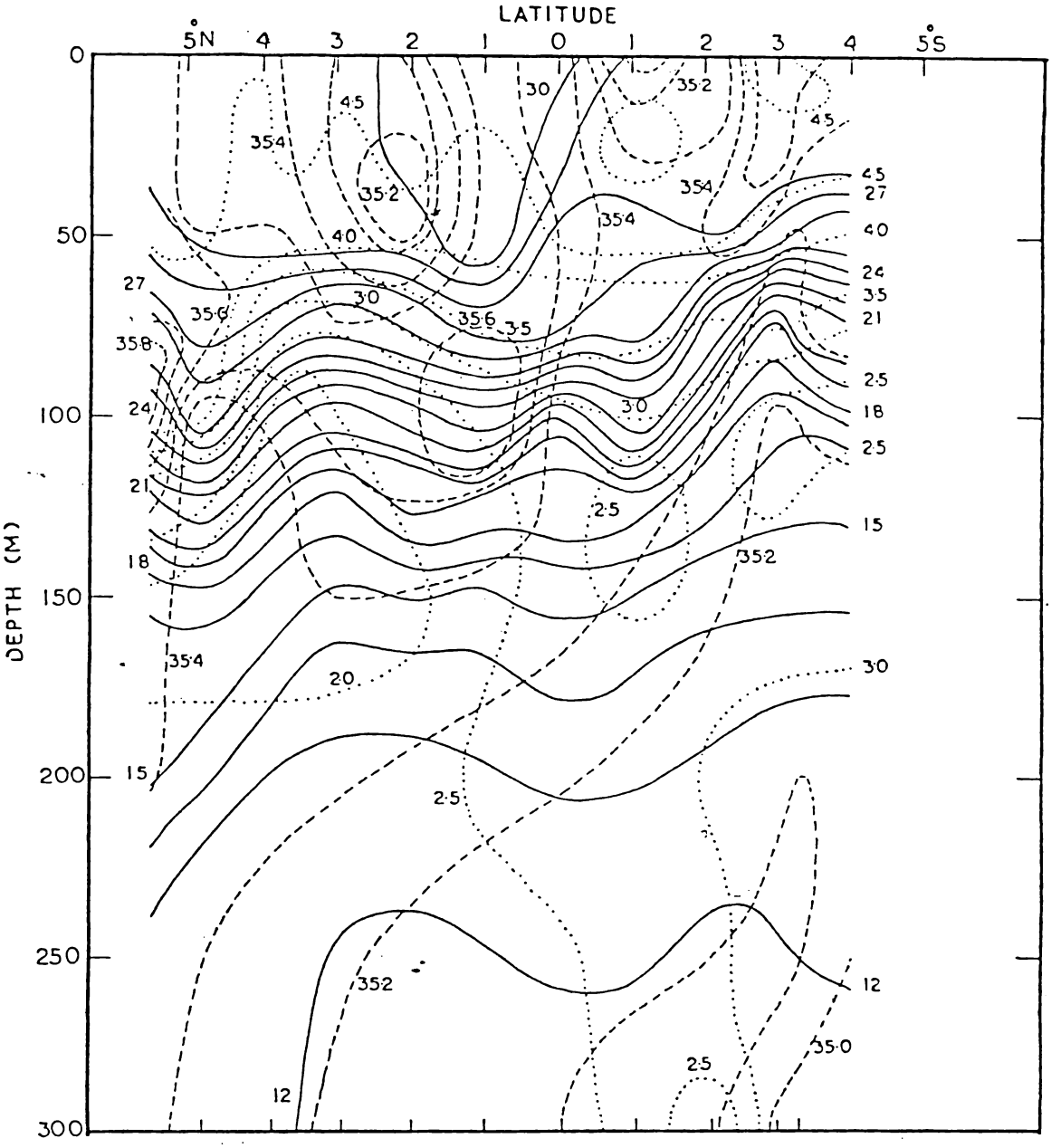

Fig. 13. Vertical section of temperature (solid lines - ^{o}C), Salinity (dashed lines - parts per mille) and dissolved oxygen (dotted lines - ml/l) at $55^{o}E$ (May, 1973).

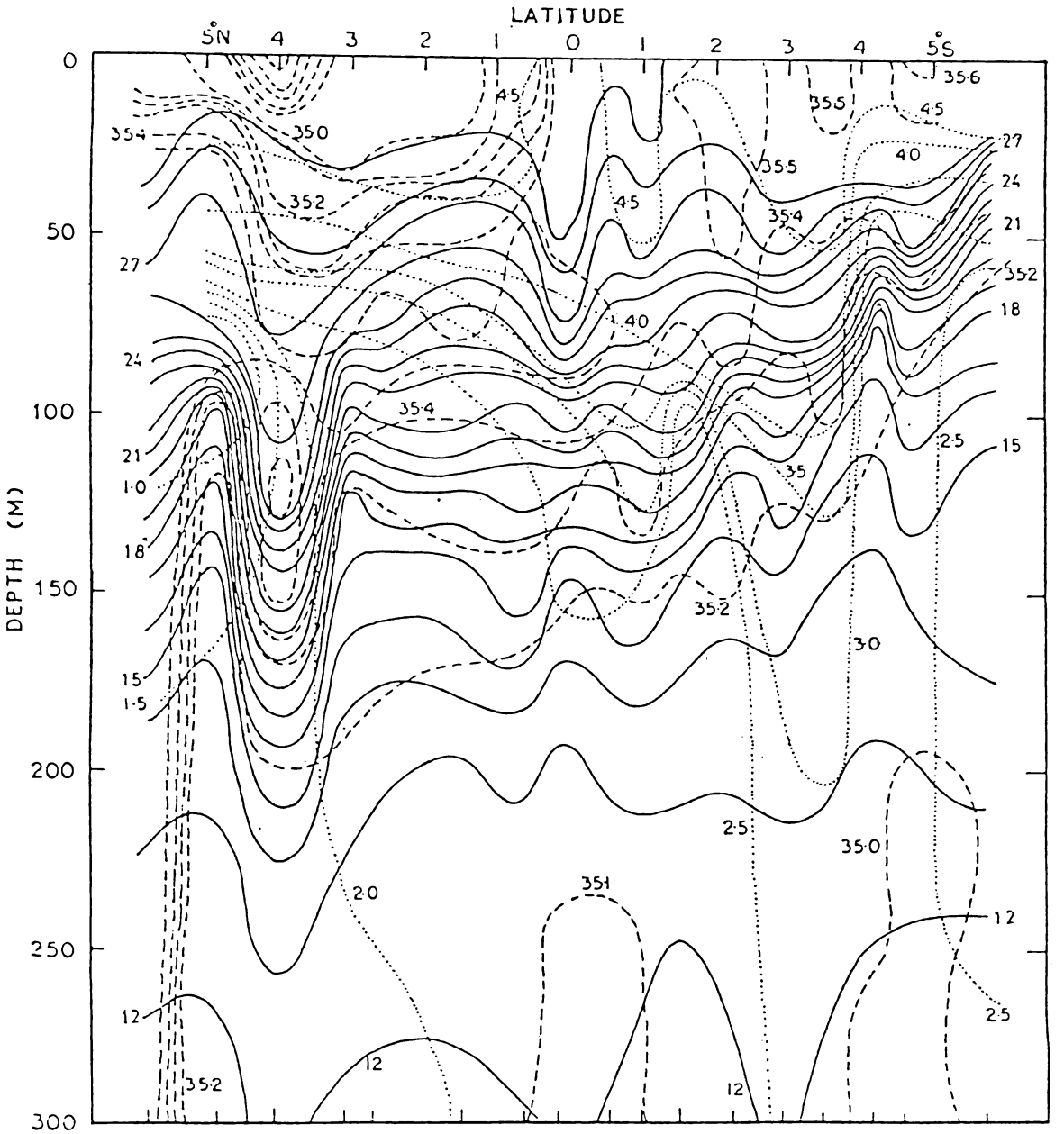

Fig. 14. Vertical section of temperature (solid lines - ^{o}C), Salinity (dashed lines - parts per mille) and dissolved oxygen (dotted lines - ml/l) at $65^{o}E$ (May, 1971).

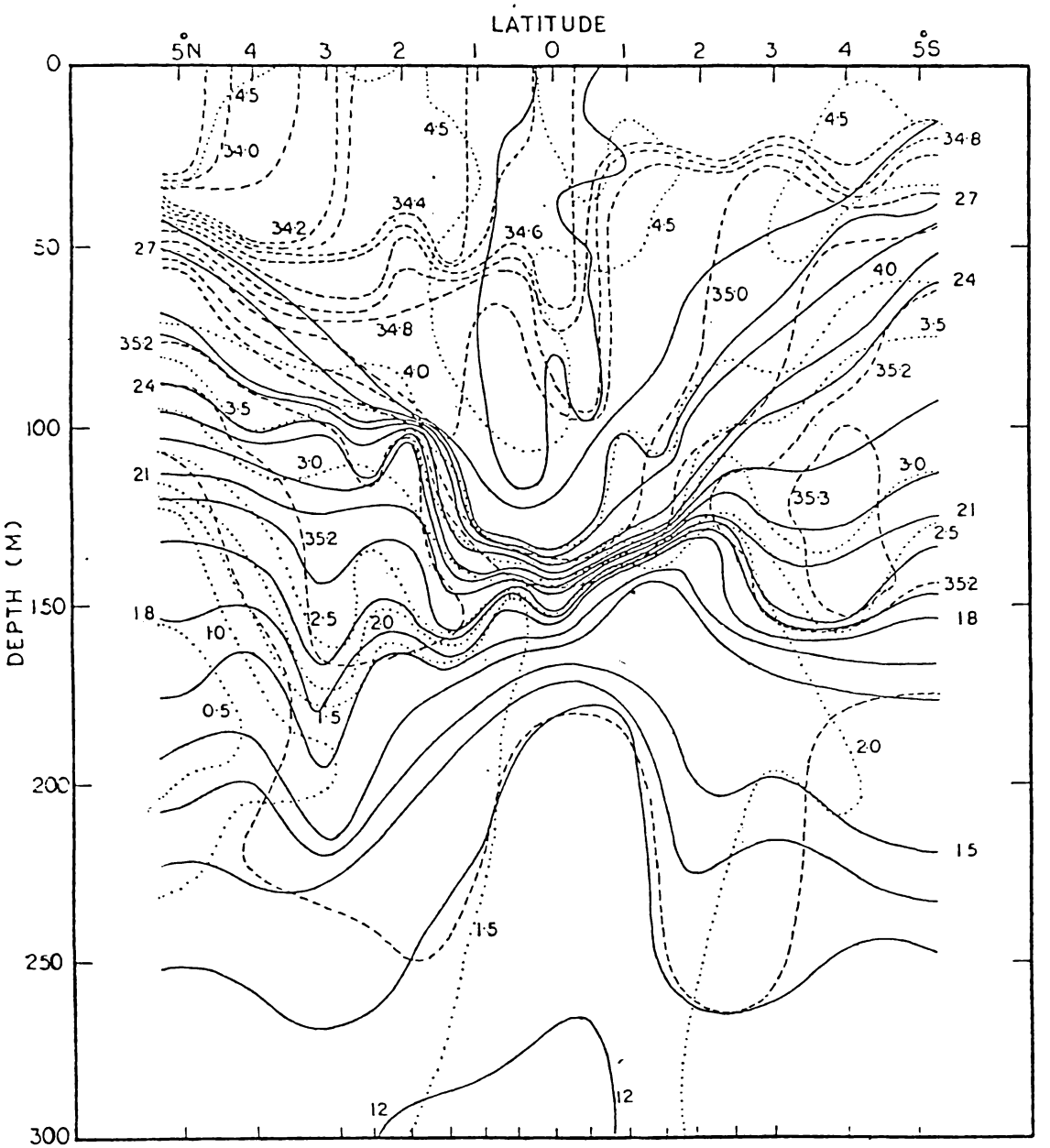

Fig. 15. Vertical section of temperature (solid lines - ^{o}C), Salinity (dashed lines - parts per mille) and dissolved oxygen (dotted lines - ml/l) at $84^{o}E$ (May, 1964).

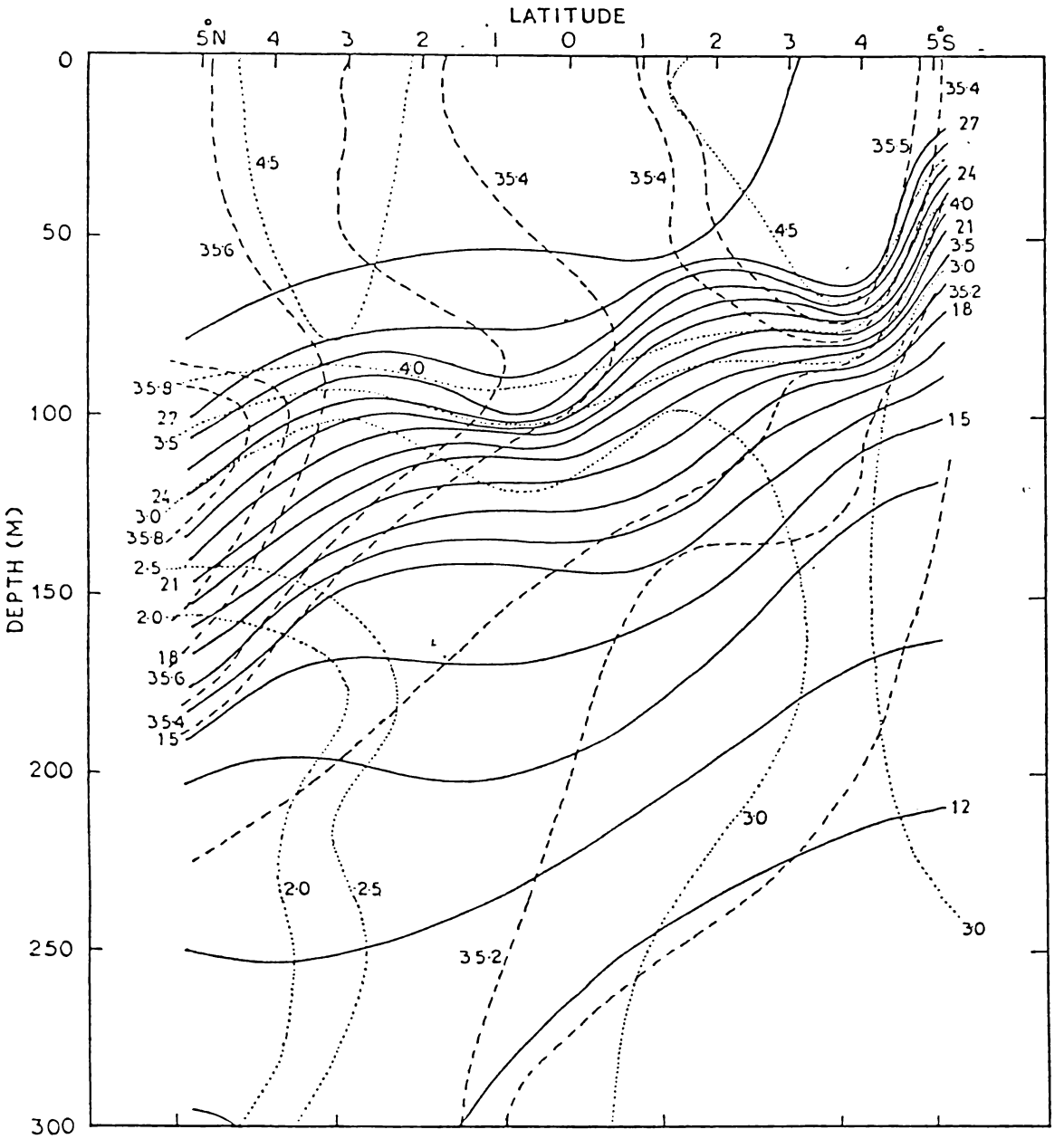

Fig. 16. Vertical section of temperature (solid lines - ^{o}C), Salinity (dashed lines - parts per mille) and dissolved oxygen (dotted lines - ml/l) at $55^{o}E$ (June, 1956).

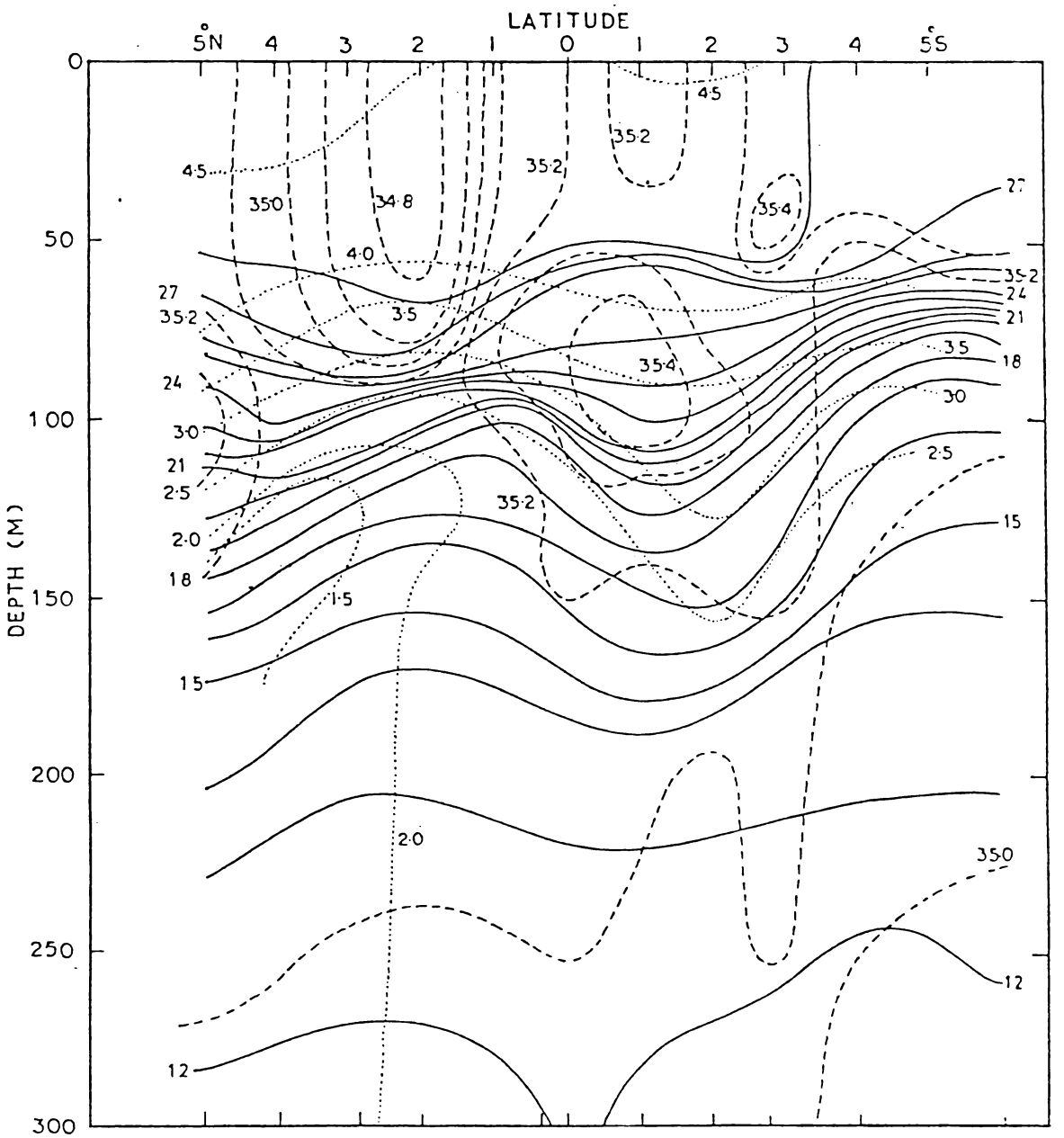

Fig. 17. Vertical section of temperature (solid lines - ^{o}C), Salinity (dashed lines - parts per mille) and dissolved oxygen (dotted lines - ml/l) at 65^{o}E (June, 1971).

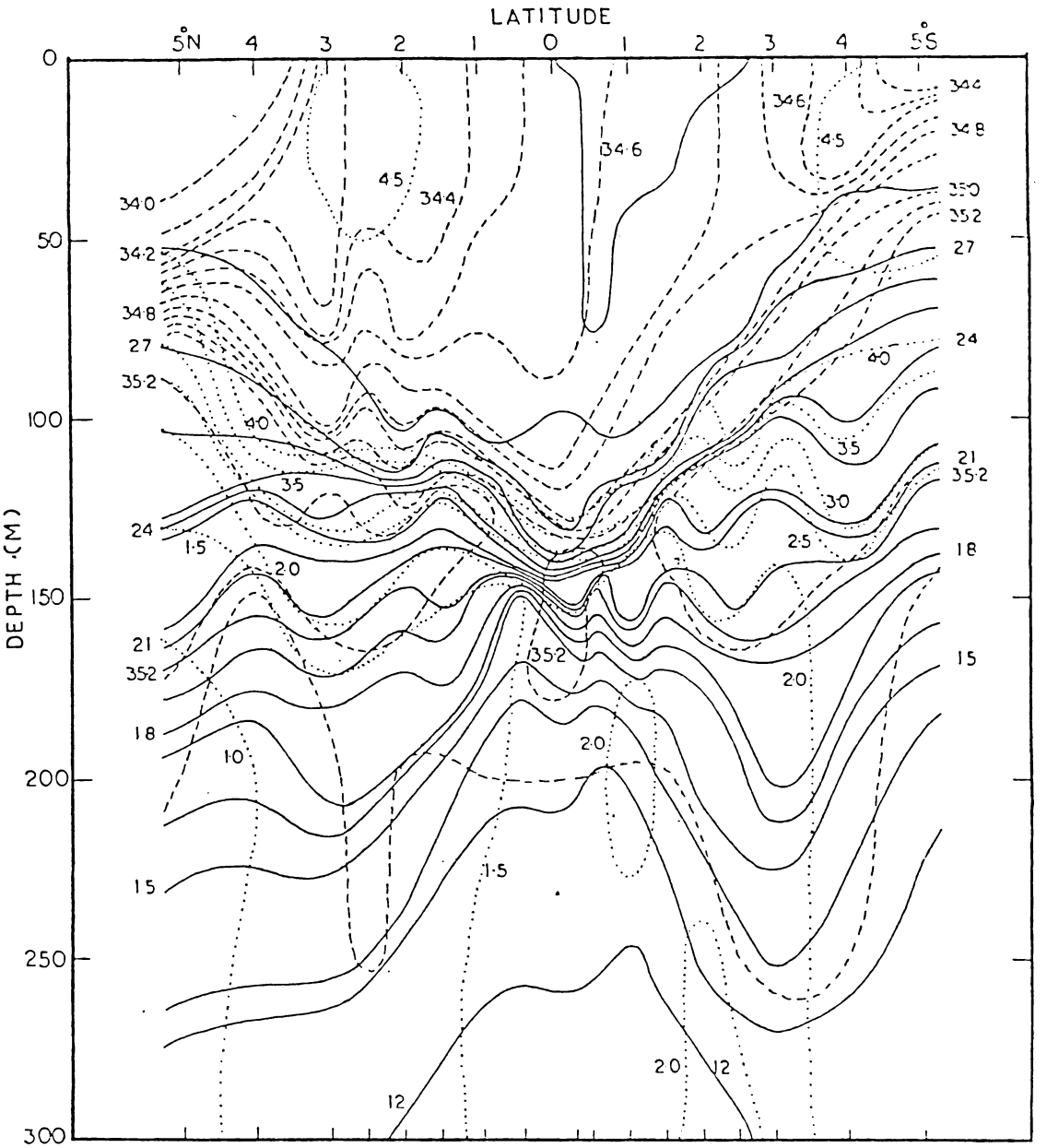

Fig. 18. Vertical section of temperature (solid lines - ^{o}C), Salinity (dashed lines - parts per mille) and dissolved oxygen (dotted lines - ml/l) at 88^{o}E (June, 1964).

isothermal layer, the density structure depends on the salinity distribution and it indicates a westerly flow north of the equator and easterly flow south of it. Mixing of high oxyty water into deeper layers is not observed at the equator except a slight troughing of oxypleths, just south of the equator.

The distribution of hydrographic properties in the eastern region (88°E) of the Indian ocean in June are almost similar to that of May except that an isolated high salinity core is observed in this month at the equator below 150 m (Fig. 18). This may be derived from the meridional advection of high salinity water from both the hemispheres. At the surface, comparatively, less saline water is observed at the extreme south of the section which may be originated from the Pacific ocean. The surface density structure indicates an intense easterly flow symmetrical about the equator. Thermal structure and oxypleths are also exhibiting contraction at the equator and spreading on either side, indicating sinking at the equator and upwelling on either side of the equator. Strong westward flow can be inferred below 150 m symmetrical about the equator. The pattern of oxypleths along the section is exactly similar to that of isotherms. Low and high oxygen values are observed below 150 m in the extreme north and south respectively.

Summing up the results of June, it can be realised that an easterly flow prevails at the surface along the equator to cover the whole width of the Indian Ocean. A definite high salinity core and the associated spreading of thermocline observed at 65°E confirms that the Equatorial Undercurrent continues to be present in the central Indian Ocean during early June. The absence of the Equatorial Undercurrent at 55°E may be due to the strong transequatorial flow in the extreme west associated with the Somali Current during this season (Bruce, Stommel and Swallow 1966; Bruce, 1968,1969; Leetmaa, 1972). The contraction of thermocline, observed at the equator in the eastern Indian Ocean indicates the absence of the Equatorial Undercurrent, and its spreading on either side shows the presence of a strong easterly flow at the surface and westerly flow below it. Wyrtki (1973) observed a similar current in the Indian Ocean during the transition periods, called the Equatorial Jet. The Equatorial Jet in the Indian Ocean is, normally, found during April and May and October and November. But, the late arrival of monsoon during the period of measurement, probably, extended this phenomenon towards the beginning of June in this particular year (Muraleedharan et al., 1980).

2.7. JULY

The section along 54°30'E is confined to 2°30'N and 2°S. Therefore, a detailed discussion about the distribution

of hydrographic properties beyond these latitudes is not plausible. The characteristics, such as spreading of thermocline and high salinity core, which are associated with the Equatorial Undercurrent are not noticed along $54^{o}30'E$ (Fig. 19). Meridional variation of temperature is much less in the surface layers. Therefore, the surface density structure depends, mainly, on the distribution of salinity alone. Low salinity water is observed at the equator surrounded by high salinity water on either side. So, the surface density structure produces high pressure near the equator and low pressure on either side, indicating an eastward flow at the equator. The subsurface high salinity tongue extending from the north may be associated with the surface easterly flow. This can be further confirmed by the troughing of the oxypleths, just south of the equator.

Section along $80^{o}E$ shows contraction of the thermocline at the equator and spreading on either side, suggesting an eastward flow at the surface and westward flow below it (Fig. 20). Since the meridional gradient of salinity at the surface is much less, temperature is the dominant factor to influence the surface density structure. Penetration of subsurface high salinity water from the southern hemisphere towards the equator is associated with the surface easterly. The troughing of oxypleths also support

the above inference. The tongue-like penetration of high oxyty water from the deeper layers just north of the equator may be associated with the oxygen rich water found south of $5^{o}S$. This is expected to be drived from South Equatorial Current carrying high oxyty Pacific Ocean water towards west.

Summing up the results, it is understood that the Equatorial Undercurrent is present neither in the western nor in the eastern region. The surface density structure in the two sections indicates the presence of an easterly flow at the surface along the equator. Along $54^{o}30'E$ the high salinity water penetrates from the northern hemisphere towards the equator, whereas in the eastern Indian Ocean it penetrates from the south. This is because in the western Indian Ocean, comparatively, higher salinity is observed in the northern hemisphere whereas in the eastern Indian Ocean the reverse is true.

2.8. AUGUST

The transequatorial distribution of hydrographic properties along $53^{o}E$ during this month exhibits a compact thermocline just north of the equator and spreading on either sides (Fig. 21). This spreading is not as conspicuous as in the section along $88^{o}E$ in June. A uniform distribution of salinity is observed at the surface but for a slight

increase beyond 4°N. Therefore, the surface density distribution depends mainly on temperature. Since the 27°C isotherm outcrops the naviface near 3°N and 2°S, the dense water occupies the region beyond these latitudes and lighter water within these latitudinal belt. Slight increase of temperature is noticed in between 3°N and 2°S towards the equator, so that an eastward flow can be inferred at the surface near the equator. The disappearance of the subsurface eastward maximum is further confirmed by the absence of the downward mixing of high oxyty water.

The thermocline contracts along 62°E at the equator while there is slight spreading beyond 2°N and 2°S (Fig. 22). A high salinity core of 35.7‰ is found at 2°N within the depth range of 50-100 m. The irregular spreading of the high salinity core in the absence of an eastward flow is due to mixing with surrounding water. Higher values of salinity are observed at the surface at 5°N and lower values at 4°S. The density differences caused by the salinity changes are compensated by the temperature distribution at these two latitudes. Slight increase in salinity is observed within 1°N and 2°S when compared to the salinity values on either side. Since the temperature is more or less uniform within 4°N and 4°S, the density structure solely depends on the salinity and it produces

westerly flow at the equator. The oxygen distribution does not show any associated features of the Equatorial Undercurrent.

Summing up the results of these sections, it can be concluded that neither of the sections indicate the presence of an Equatorial Undercurrent. The high salinity core is observed in the western and central Indian Ocean. This core, found at $1^{o}N$ along $53^{o}E$ may be associated with the surface eastward flow. In the central Indian Ocean the surface easterly disappears and a westerly develops at the equator. In the absence of the eastward momentum, the high salinity core dissipates and drifts northwards.

2.9. SEPTEMBER

The transequatorial distribution of temperature along $79^{o}E$ indicates slight spreading of the thermocline at the equator and contraction on either side and again spreading beyond $2^{o}30'N$ and $2^{o}S$ (Fig. 23). The horizontal temperature gradient is much less in the upper 50 m, whereas a slight increase is observed between $2^{o}N$ and $2^{o}S$ in the depth range 50-75 m. The surface salinity distribution indicates the presence of high salinity water beyond $2^{o}N$ and $3^{o}S$ with less saline water in between these latitudes. The thickness of this lighter water is roughly 75 m. Strong vertical gradient of temperature coincides with vertical gradient of

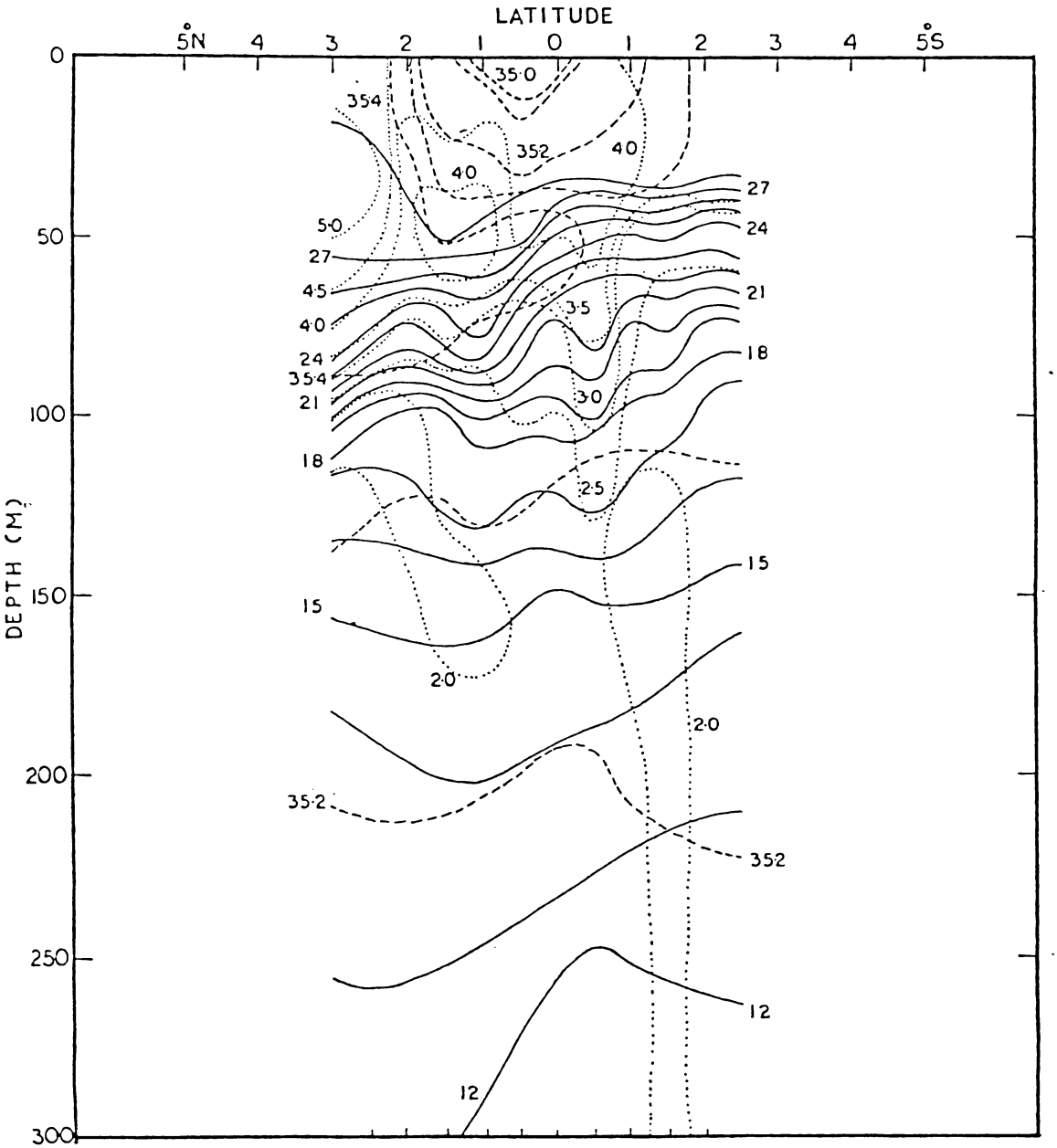

Fig. 19. Vertical section of temperature (solid lines - ^{o}C), Salinity (dashed lines - parts per mille) and dissolved oxygen (dotted lines - ml/l) at $54^{o}30'E$ (July, 1975).

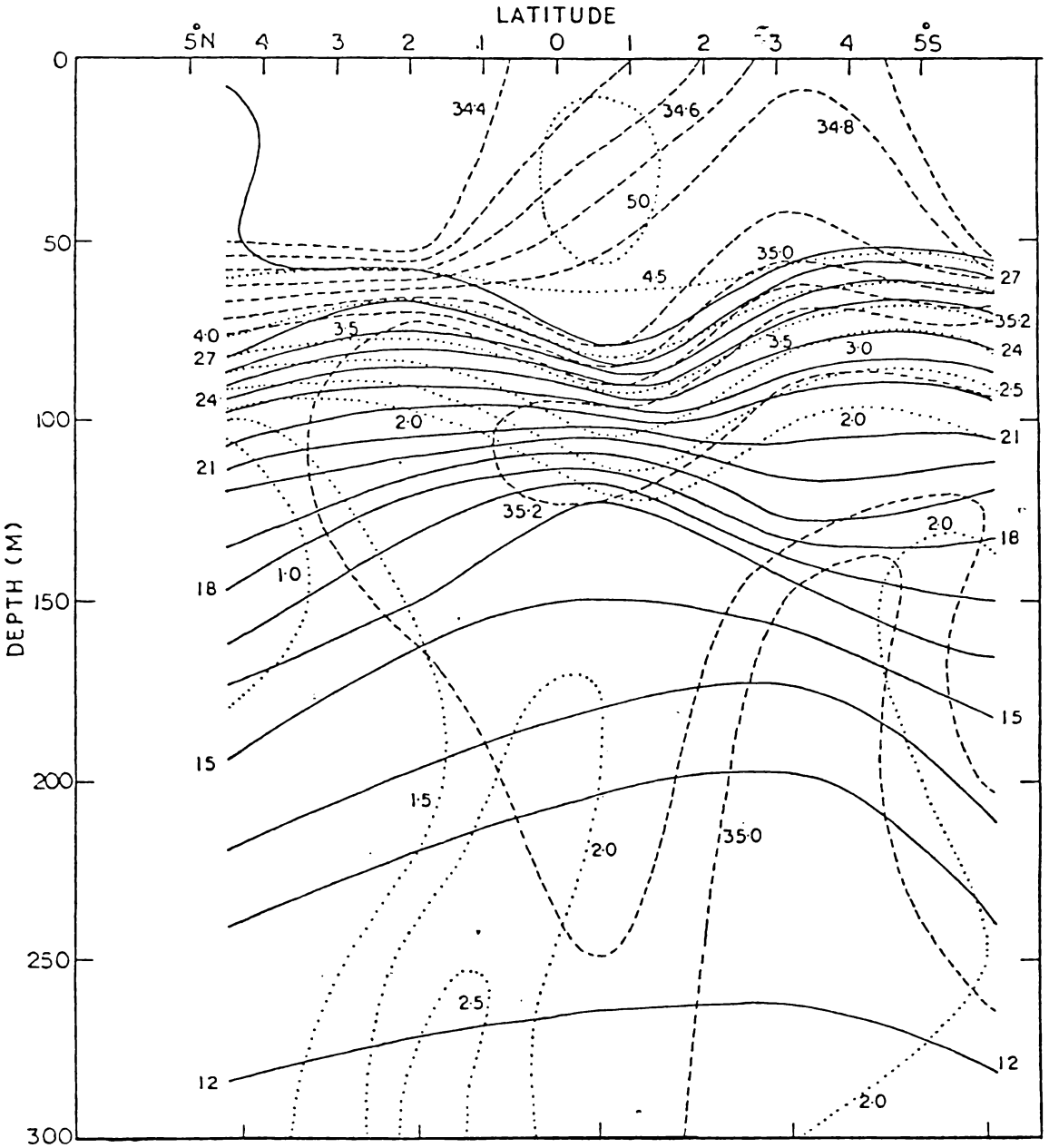

Fig. 20. Vertical section of temperature (solid lines - ^{o}C), Salinity (dashed lines - parts per mille) and dissolved oxygen (dotted lines - ml/l) at 80^{o}E (July, 1963).

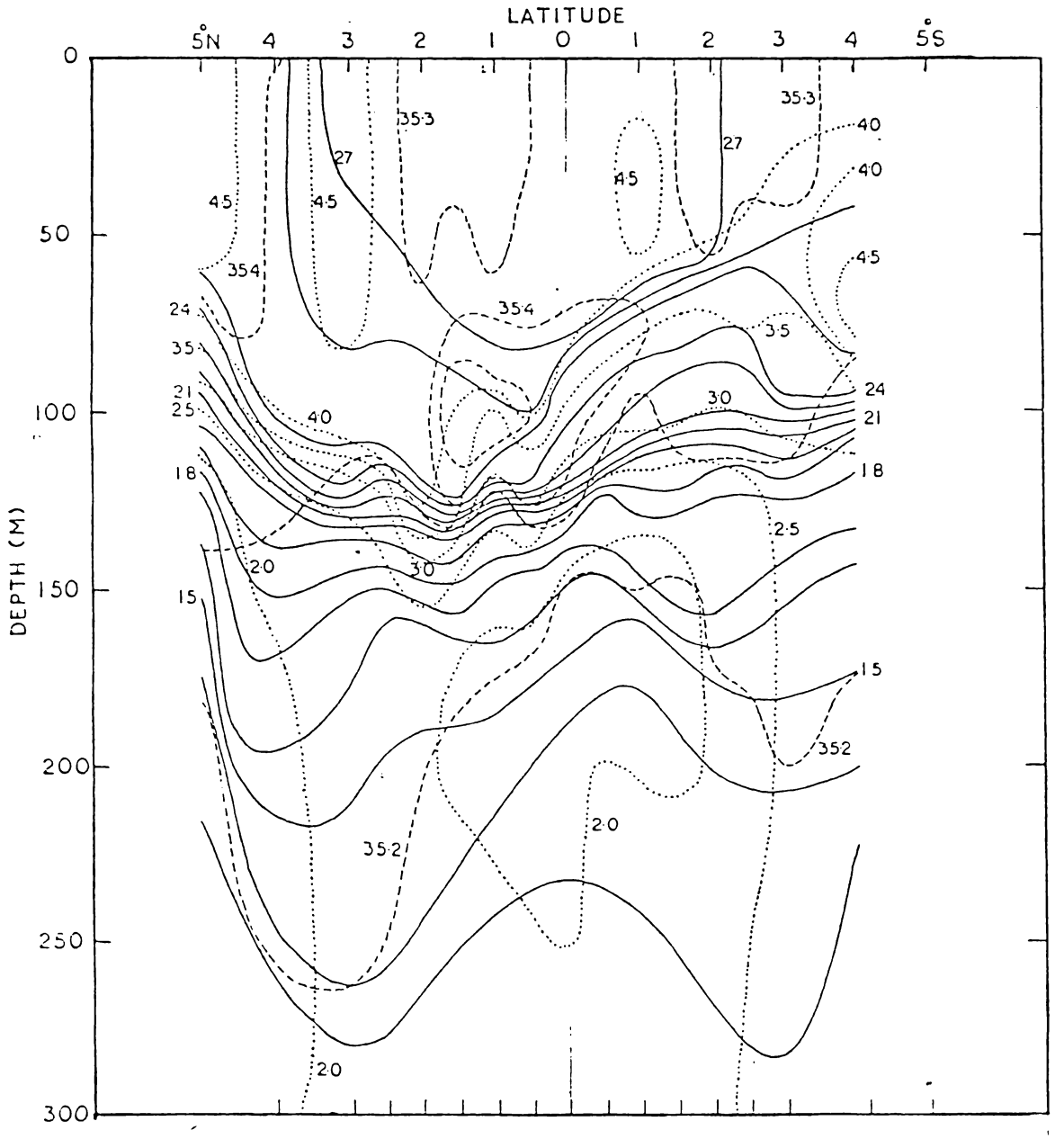

Fig. 21. Vertical section of temperature (solid lines - ^{o}C), Salinity (dashed lines - parts per mille) and dissolved oxygen (dotted lines - ml/l) at 53^{o}E (August, 1962).

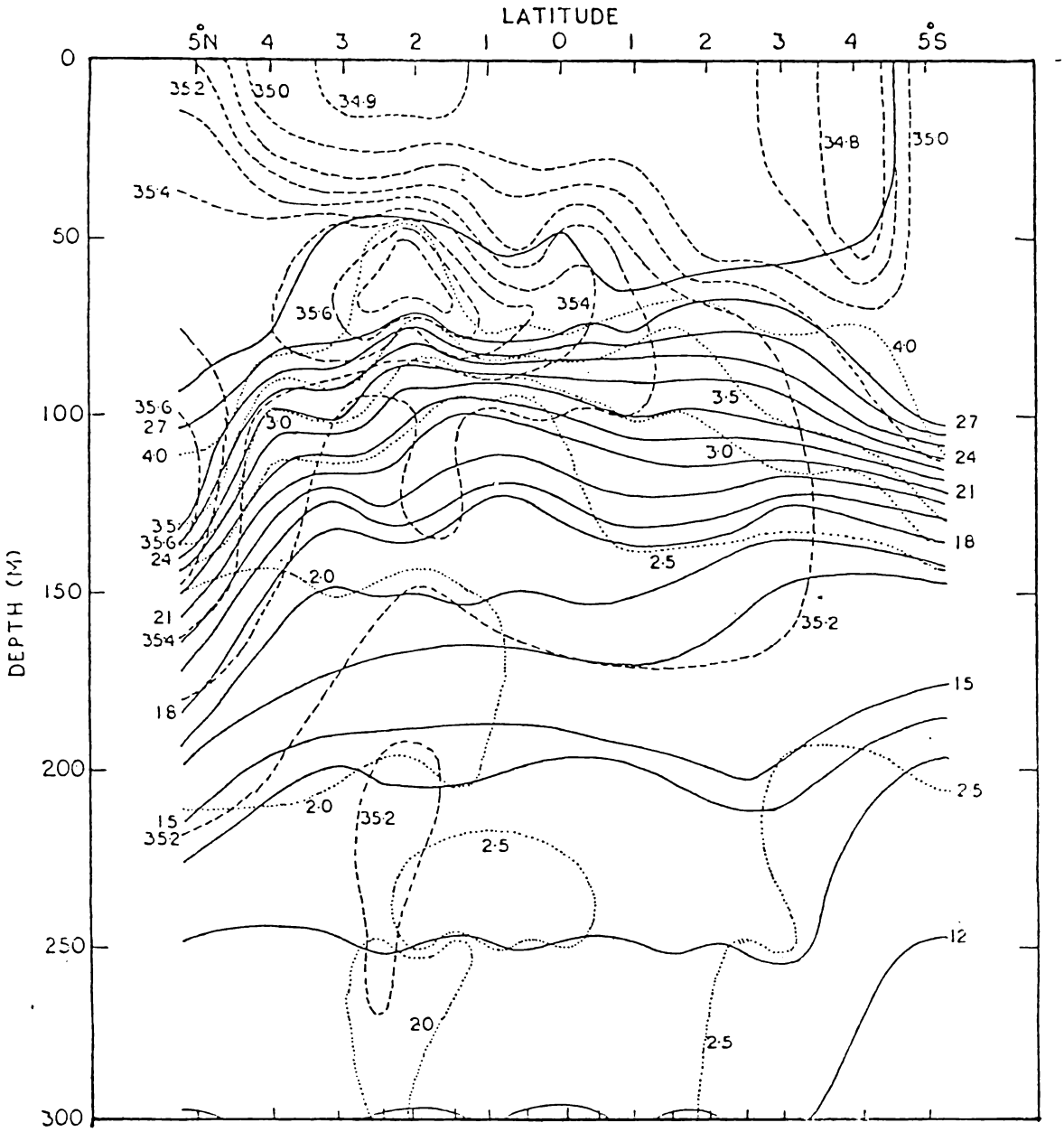

Fig. 22. Vertical section of temperature (solid lines - ^{o}C), Salinity (dashed lines - parts per mille) and dissolved oxygen (dotted lines - ml/l) at $62^{o}E$ (August, 1962).

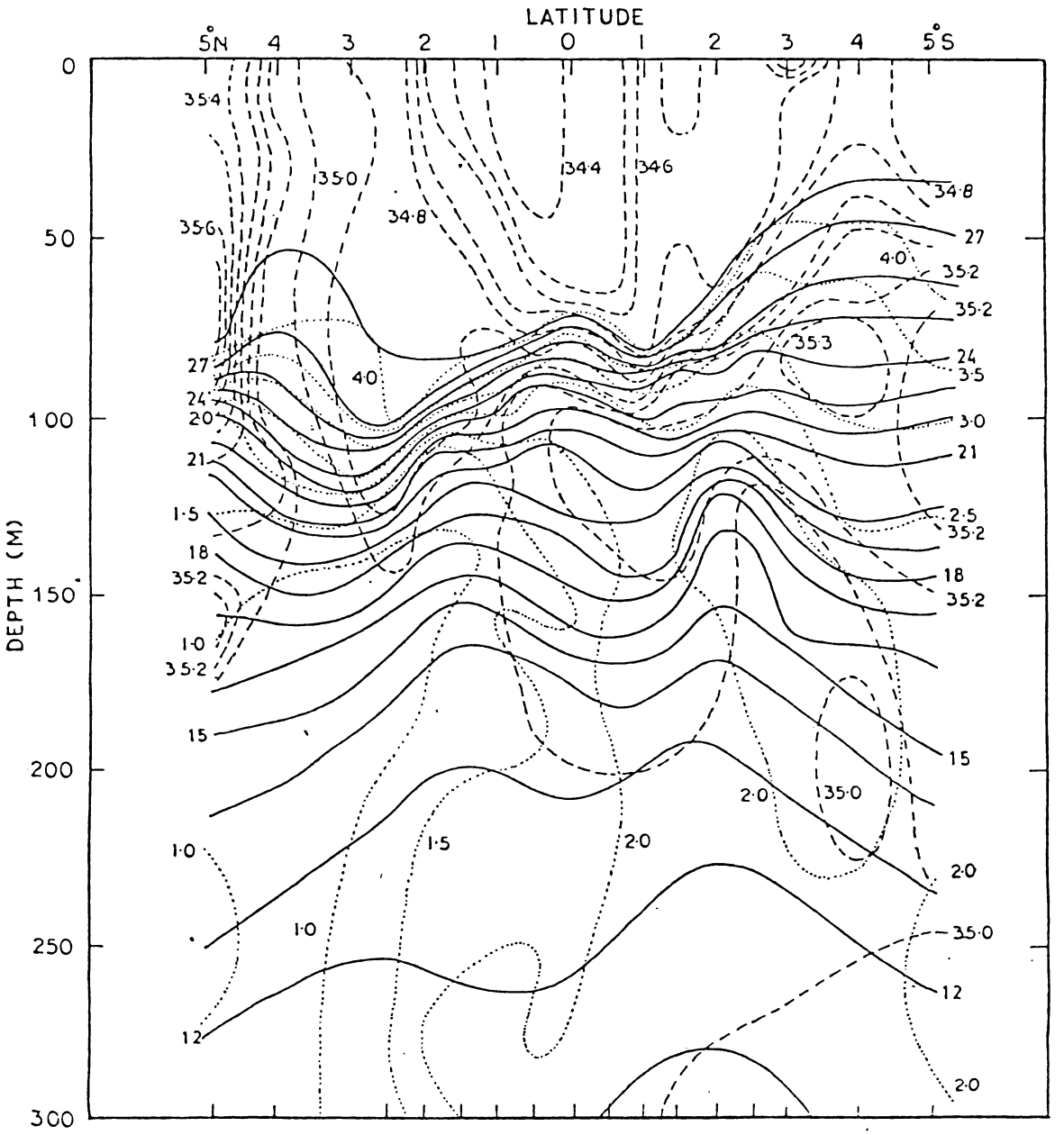

Fig. 23. Vertical section of temperature (solid lines - ^{o}C), Salinity (dashed lines - parts per mille) and dissolved oxygen (dotted lines - ml/l) at 79^{o}E (September, 1962).

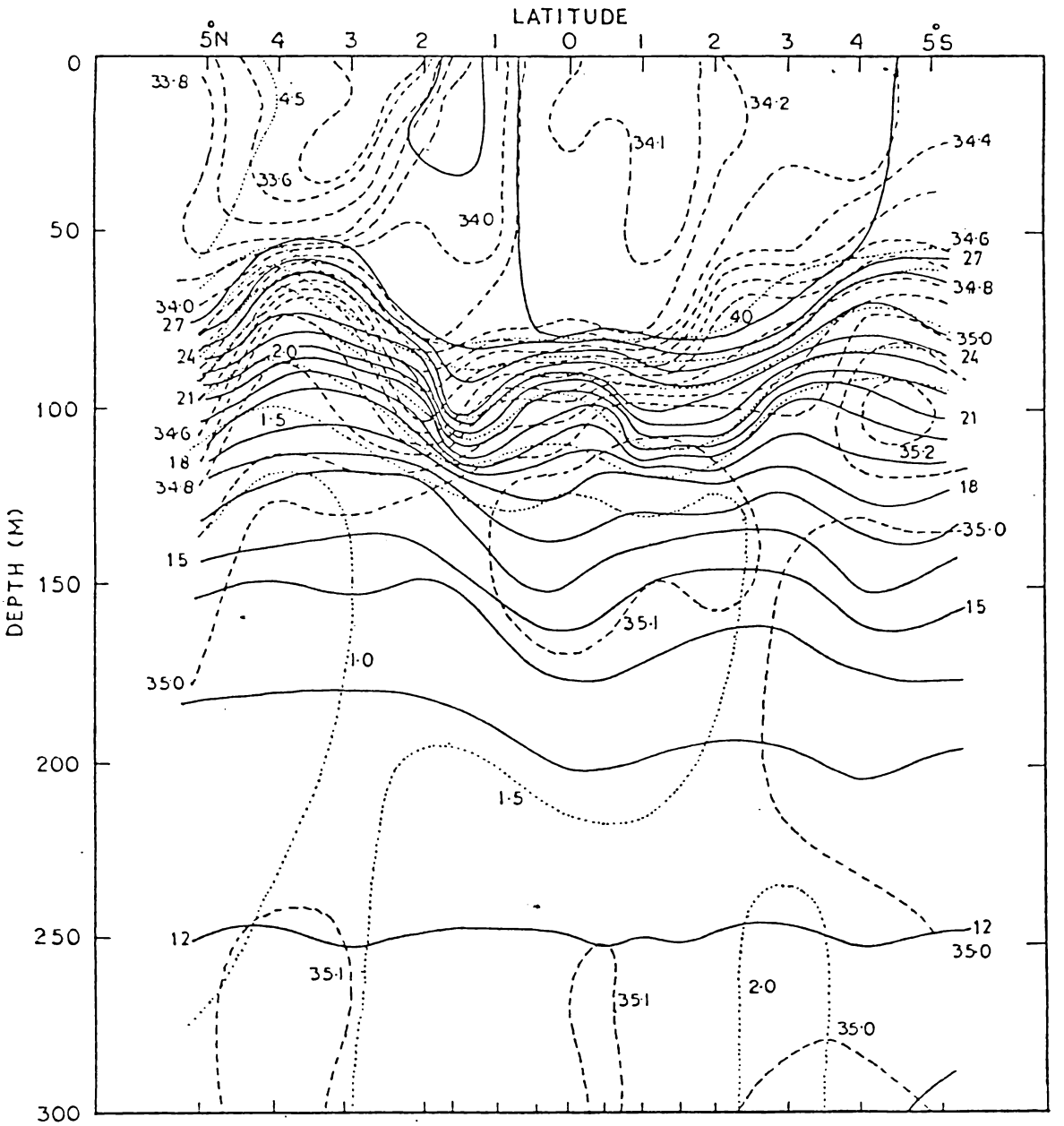

Fig. 24. Vertical section of temperature (solid lines - ^{o}C), salinity (dashed lines - parts per mille) and dissolved oxygen (dotted lines - ml/l) at 91°30'E (September, 1962).

salinity below 75 m within $1^{o}N$ and $1^{o}S$ (Fig. 23). High salinity water of 35.2‰ is observed below 100 m at the equator which is found to be extended from the southern hemisphere. The combined influence of temperature and salinity results the deepening of pycnocline at the equator and rising towards higher latitudes producing a strong surface eastward flow at the equator. The surface eastward flow is confined to the upper 75 m because of strong vertical density gradients beneath. The troughing of isotherms below 100 m near the equator coincides with high salinity water resulting in weak horizontal density gradients and weakens the current within the thermocline.

The low oxyty water is found to be advancing towards south from extreme north in the subsurface depth. The downward transport of oxygen rich water is not observed at the equator. It is an indication of the absence of vertical mixing and in turn absence of Undercurrent.

Isolated patches of warm water is noticed in the surface layers along $91^{o}30'E$ with cold water separating these two at about $1^{o}N$ (Fig. 24). In the subsurface layer the temperature distribution is almost similar to that of the previous section. The surface salinity is lowest between $2^{o}N$ and $3^{o}N$ and increases southward. Of the two factors that

control the density, namely salinity and temperature, the latter dominates resulting in the decrease of density southward from $2^{o}N$ upto the equator beyond which it increases in the surface layers. In the subsurface layers a high salinity core is observed at the equator which may be the continuation of the high salinity water observed at $5^{o}S$. As in the previous section, here also a strong vertical density gradient below 75 m is noticed at the equator. Therefore, a troughing of the pycnocline is expected at the equator favouring an easterly flow at the surface. The surface eastward flow does not penetrate beyond 75 m as there is a strong density gradient below that depth. The high salinity water observed beneath 100 m at the equator nullifies the effect of temperature to produce either a weak current or a layer of no motion.

In the previous section the low oxyty water is confined only in the northern hemisphere. At this longitude, it advances further to the southern hemisphere in the depth range 100-200 m.

Due to nonavailability of the hydrographic data in the western Indian Ocean no comment is being made regarding the current structure in that region during this month. In the central and eastern Indian Ocean the Equatorial Undercurren could not be identified in the absence of any associated

hydrographic characteristics. The high salinity water, observed in both the regions below the thermocline might be originated from the southern hemisphere. From the combined influence of the salinity and temperature distributions in the surface layers, an eastward flow can be expected along the equator in the central as well as eastern Indian Ocean. The subsurface low oxyty water in the central Indian Ocean is confined to the northern hemisphere, whereas in the eastern Indian Ocean it extends further to the south. Similar feature is also noticed in International Indian Ocean Expedition Atlas (Wyrtki, 1971) along 91°30'E.

2.10. OCTOBER

An intense troughing of isotherms, isohalines and oxypleths is noticed at the equator along 77°E (Fig. 25). The surface salinity decreases from 5°N to 5°S. The surface density north of the equator is mainly controlled by the salinity as the temperature gradient is less, whereas in the southern half of the section temperature plays a major role in the density distribution. The low density water at the equator is surrounded by high density water on either side developing a meridional pressure gradient that causes an eastward flow at the surface. A high salinity core is noticed around 4°N at about 50 m depth. Besides, a meridional advection of high salinity water is observed in the subsurface

layer from either side, towards the equator. The meridional convergence of the water indicates strong and narrow eastward flow at the equator. The oxygen rich water does not penetrate to deeper layers at the equator as a result of higher vertical stability in the upper layers.

The troughing of isotherms is more conspicuous along 84°E than in the previous section and the axis shifts towards north by 0°30' (Fig. 26). The surface temperature and salinity increase equatorward from either side. Of the two, the temperature dominates the other and controls the density structure providing a condition for an easterly flow at the surface near the equator. A high salinity core of 35.6‰ is noticed at 1°N around 50 m. Meridional advection of high salinity water observed from either side of the equator in the previous section might have formed into a single water mass in its due course towards east. Comparatively, less oxyty water is observed below the thermocline which indicates the absence of vertical mixing.

Since the data is not available in the western Indian Ocean, the current structure in that region is not discussed. An intense easterly flow is inferred in the central and eastern Indian Ocean along the equator whose axis

shifts slightly northward when it reaches the eastern region. The high salinity core noticed at $4^{o}N$ in the central Indian Ocean is drifted southward to about $1^{o}N$ in the eastern Indian Ocean. The meridional advection of high salinity water towards the equator from either side is indicated in the central Indian Ocean where the converging water masses mix together to form a single water mass near the equator, as shown in the section along $84^{o}E$. All the above features are associated with the intense surface eastward flow.

2.11. NOVEMBER

Since the section taken between $54^{o}E$ and $58^{o}E$ covers a few stations, the conclusions drawn may not be completely valid. Warm water is noticed between $1^{o}S$ and $5^{o}S$ at the surface. The $27^{o}C$ isotherm shoals to 10 m at $4^{o}N$ and sinks to a maximum depth of 75 m just south of the equator and again rises southward (Fig. 27). The thermocline weakens, considerably, in the northern half than southern in the subsurface layers. The pattern of isotherms in the subsurface layers is entirely different from that of the surface. The isotherms slope down from $5^{o}S$ to $5^{o}N$. For example the $20^{o}C$ isotherm is observed at 50 m at $5^{o}S$ whereas it is found below 150 m at $5^{o}N$. Horizontal salinity gradient north of the equator remains constant in the surface layers while it

decreases gradually southward from the equator. But in the subsurface layers highest salinity values are observed in the extreme north and it decreases southward. Combined effect of temperature and salinity produces a horizontal density gradient at the surface leaving denser water north of the equator and lighter water in the south (Fig. 27). Therefore, an easterly and westerly flows are expected in the northern and southern hemisphere respective Though a strong horizontal temperature and salinity gradien prevail in the subsurface layer, they counter balance the influence of one on the other. Therefore, a subsurface current is not expected at the equator. Unfortunately oxygen data is not available to confirm these inferences.

The isotherms trough at the equator and are associated with high salinity core just below the surface along $64^{o}E$, indicating the presence of an easterly flow (Fig. 28). If the salinity alone is taken into account, the current would have been westerly but the combined influence of the temperature and the westerly wind gives rise to an easterly flow, obviously, indicating the combine effect of the wind and temperature overweighs that of the salinity as the strong Equatorial Jet is noticed during th month. The boundary of this easterly flow is shown by the ridging of isotherms at $2^{o}N$ and $2^{o}S$ beyond which westerly

flows are expected. Therefore, cyclonic eddies develop at $2^{o}N$ and $2^{o}S$, as a result, water from subsurface depth rises bringing less oxyty water to the surface. Due to convergence at the equator the high oxyty water is surrounded by low oxyty water.

Along $86^{o}E$ the isotherms ridge at $1^{o}S$ in the surface layers and trough just north of the equator at the bottom of the thermocline (Fig. 29). Salinity, greater than 35.2‰ is noticed at $1^{o}S$ in the depth range of 100-150 m, and it is less than 33.3‰ at the equator in the surface layers with an increase on either side. Probably, such a low salinity value may be an isolated one caused by rain fall at the time of occupation of the station at the equator. The density structure in the surface layer is, mainly, controlled by salinity alone as the temperature does not vary much. The lighter water at the equator with denser water on either side produces easterly current. The high salinity core observed near the surface in the previous section might have sunk to deeper layers of more than 100 m at $86^{o}E$ in its course towards east. Very low oxyty water is noticed in the subsurface layers on either side of the equator due to the absence of vertical mixing below the equator.

Sections along $64^{o}E$ and $86^{o}E$ indicate a surface easterly flow along the equator which may not be as strong

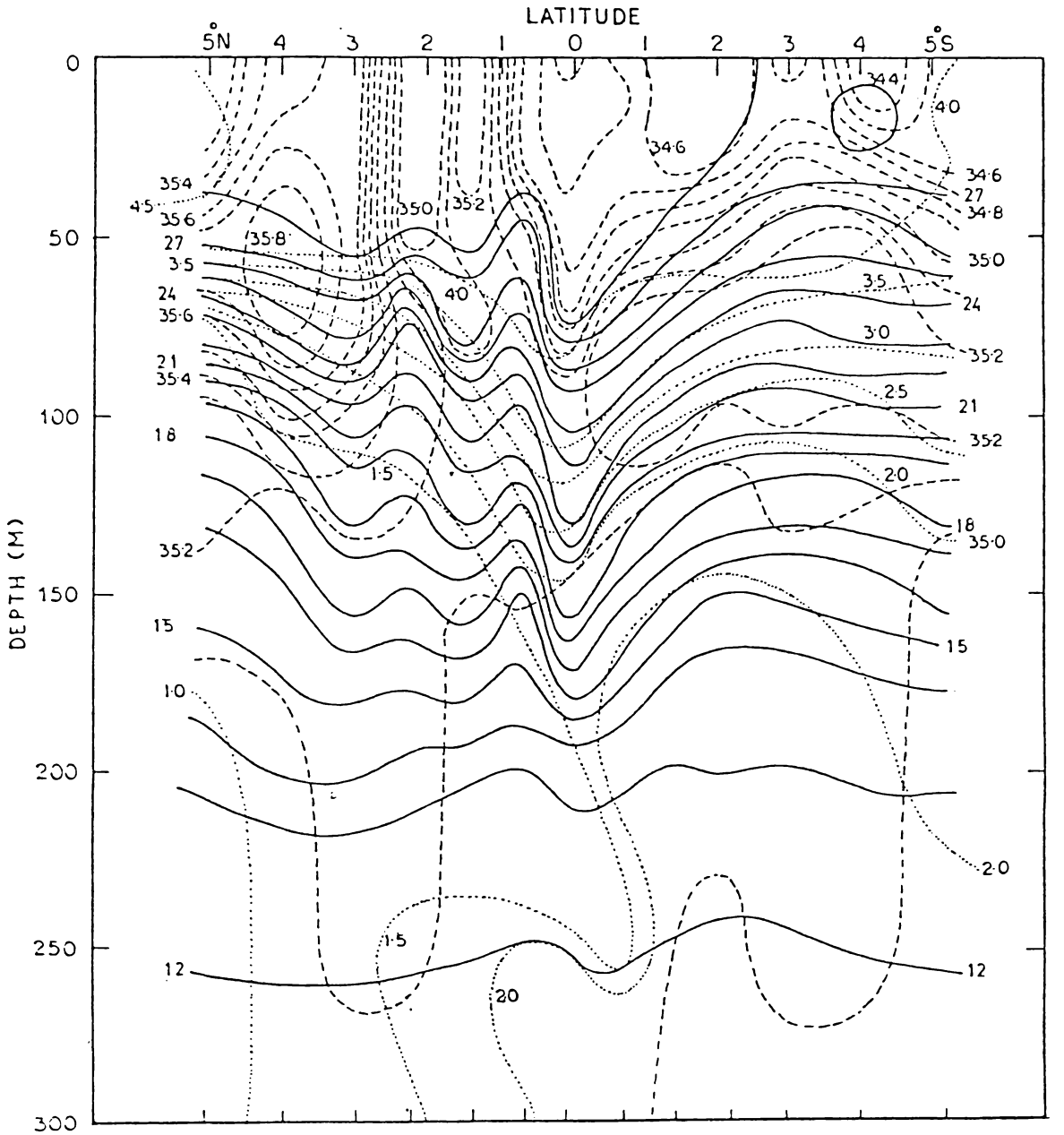

Fig. 25. Vertical section of temperature (solid lines - ^{o}C), Salinity (dashed lines - parts per mille) and dissolved oxygen (dotted lines - ml/l) at 77°E (October, 1962).

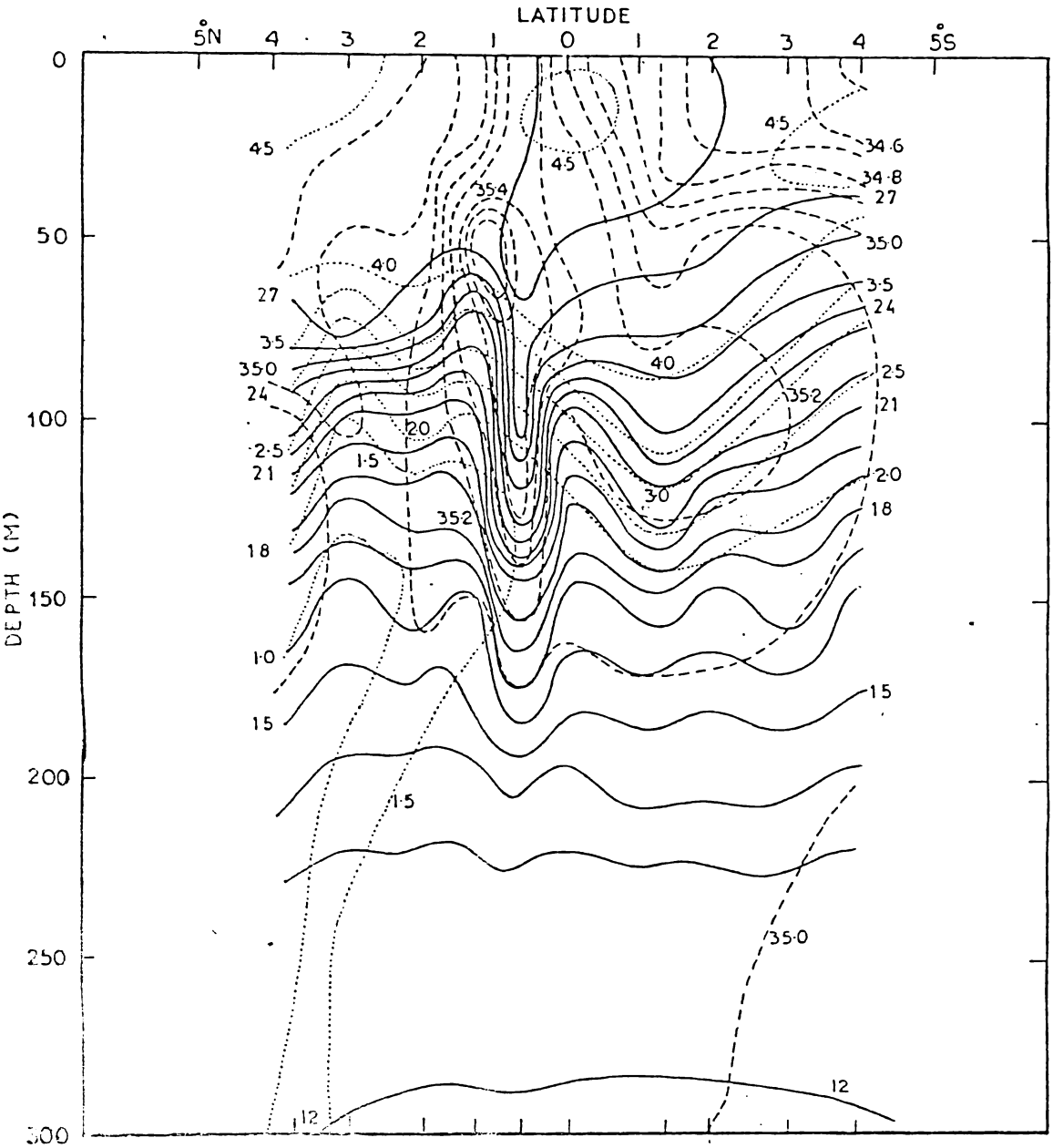

Fig. 26. Vertical section of temperature (solid lines - °C), salinity (dashed lines - parts per mille) and dissolved oxygen (dotted lines - ml/l) at 84°E (October, 1962).

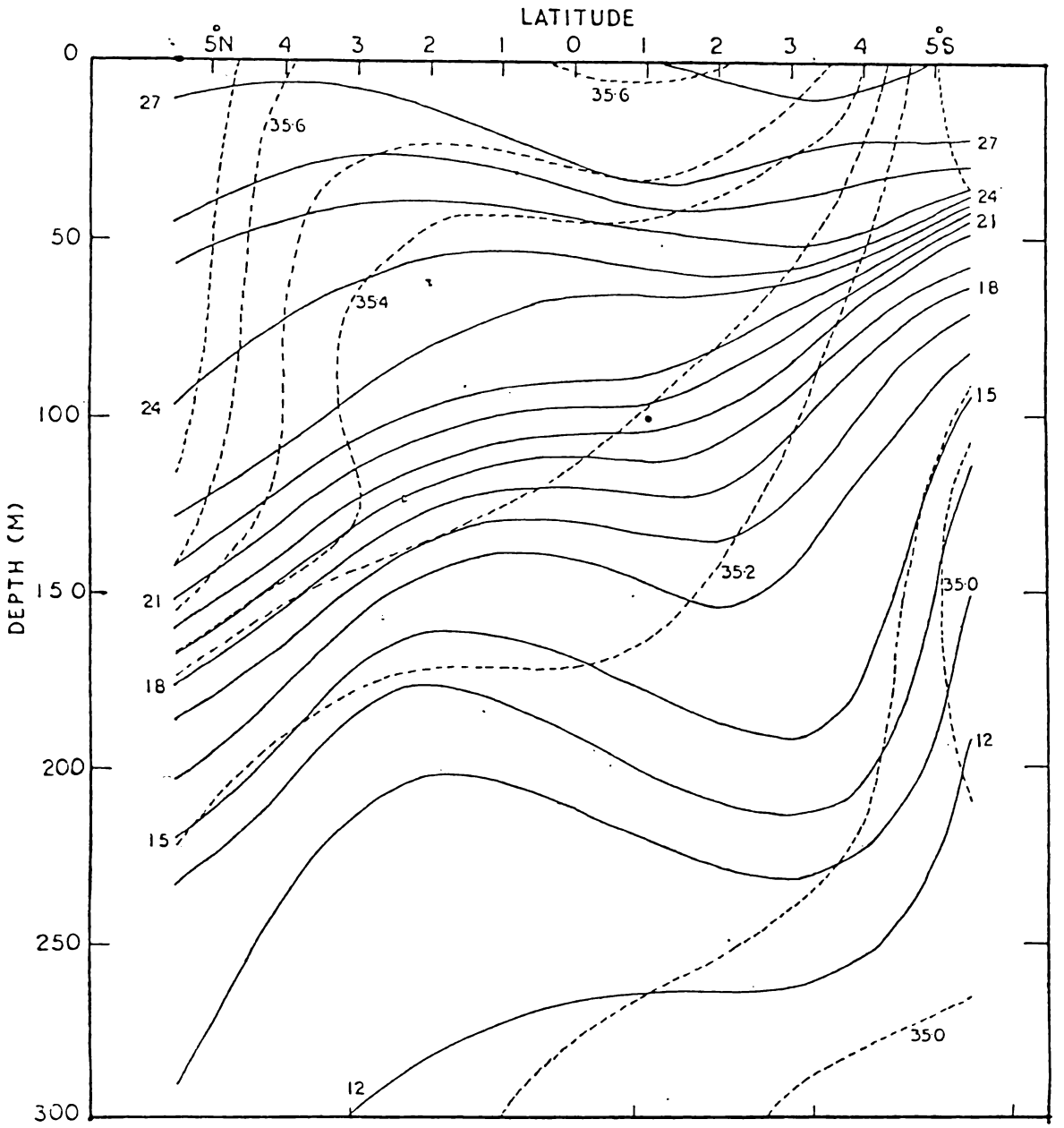

Fig. 27. Transequatorial section of temperature (solid lines - ^{o}C) and salinity (dashed lines - parts per mille) between 54° & 58°E (November, 1955).

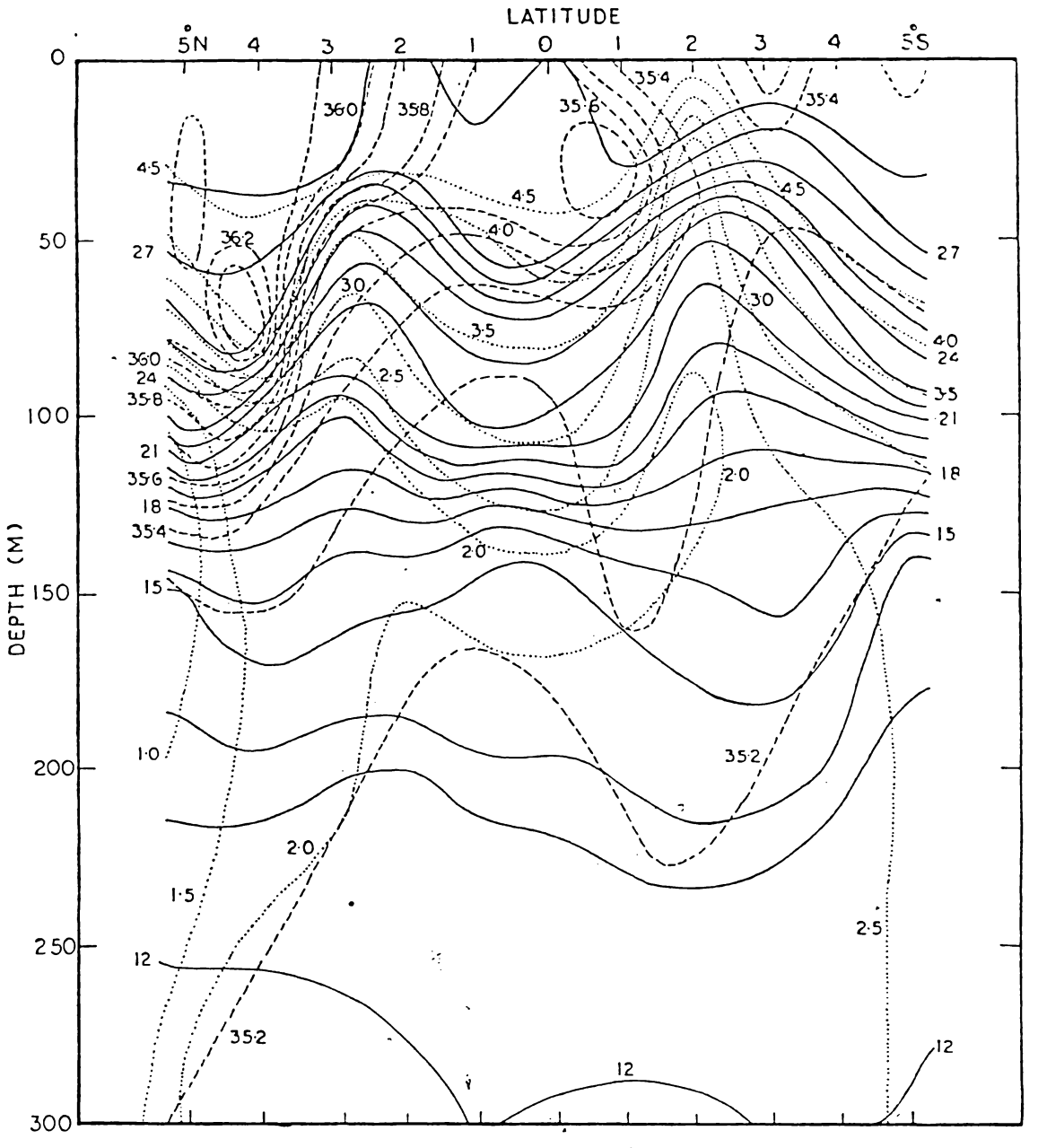

Fig. 28. Vertical section of temperature (solid lines - ^{o}C), Salinity (dashed lines - parts per mille) and dissolved oxygen (dotted lines - ml/l) at 64^{o}E (November, 1976).

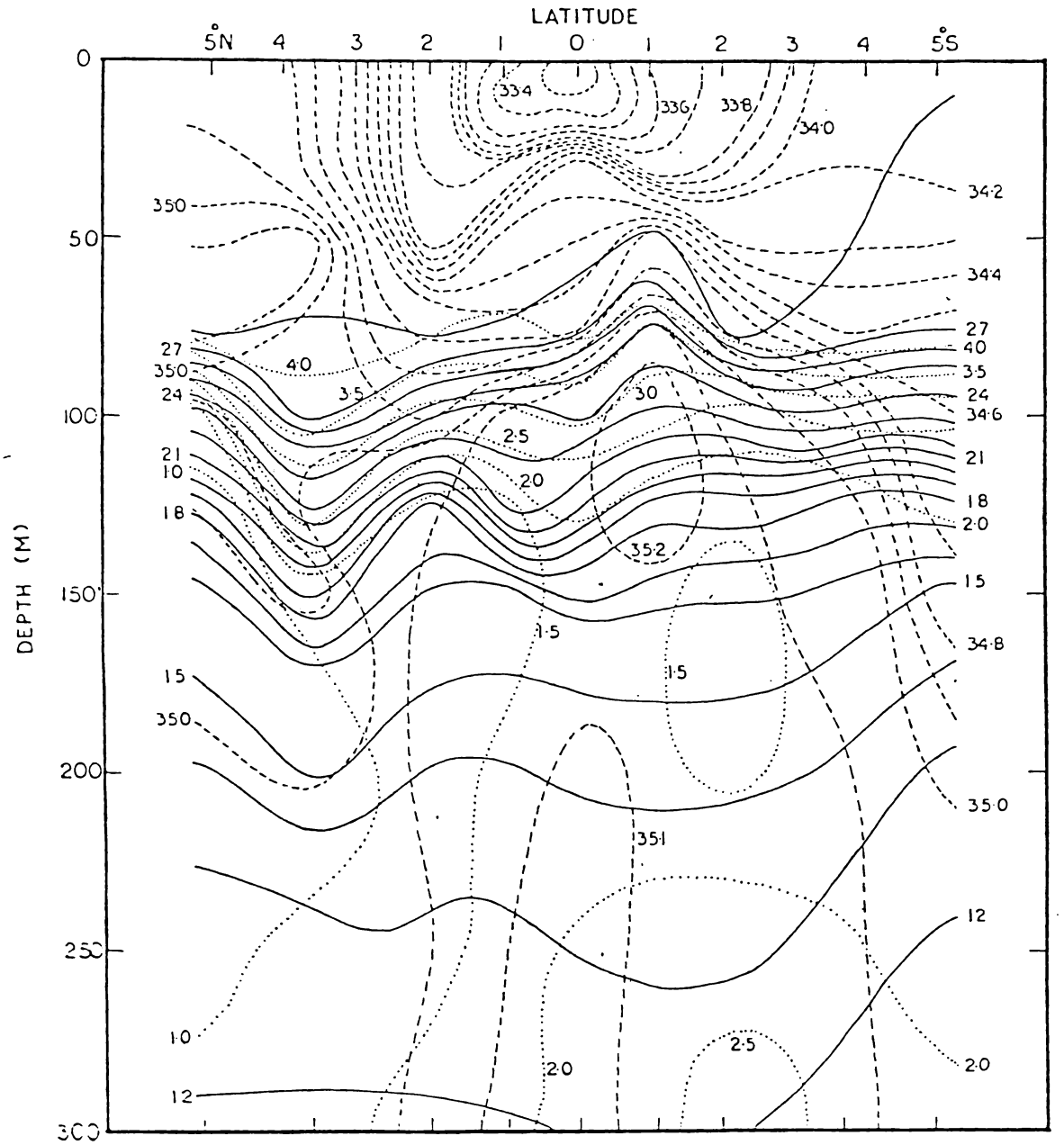

Fig. 29. Vertical section of temperature (solid lines - ^{o}C), Salinity (dashed lines - parts per mille) and dissolved oxygen (dotted lines - ml/l) at 86^{o}E (November - December, 1963).

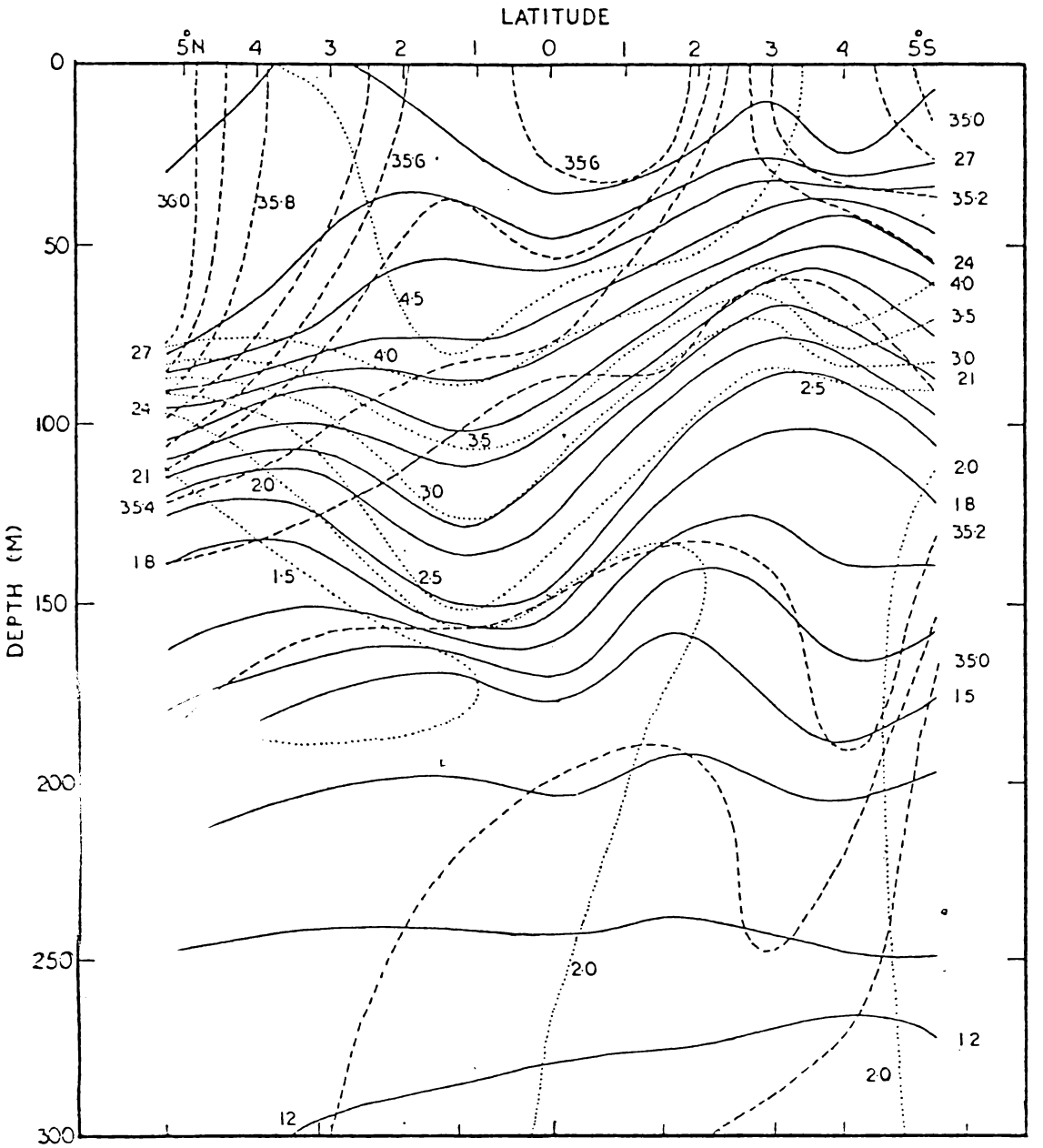

Fig. 30. Vertical section of temperature (solid lines - ^{o}C), Salinity (dashed lines - parts per mille) and dissolved oxygen (dotted lines - ml/l) at 71^{o}E (December, 1960).

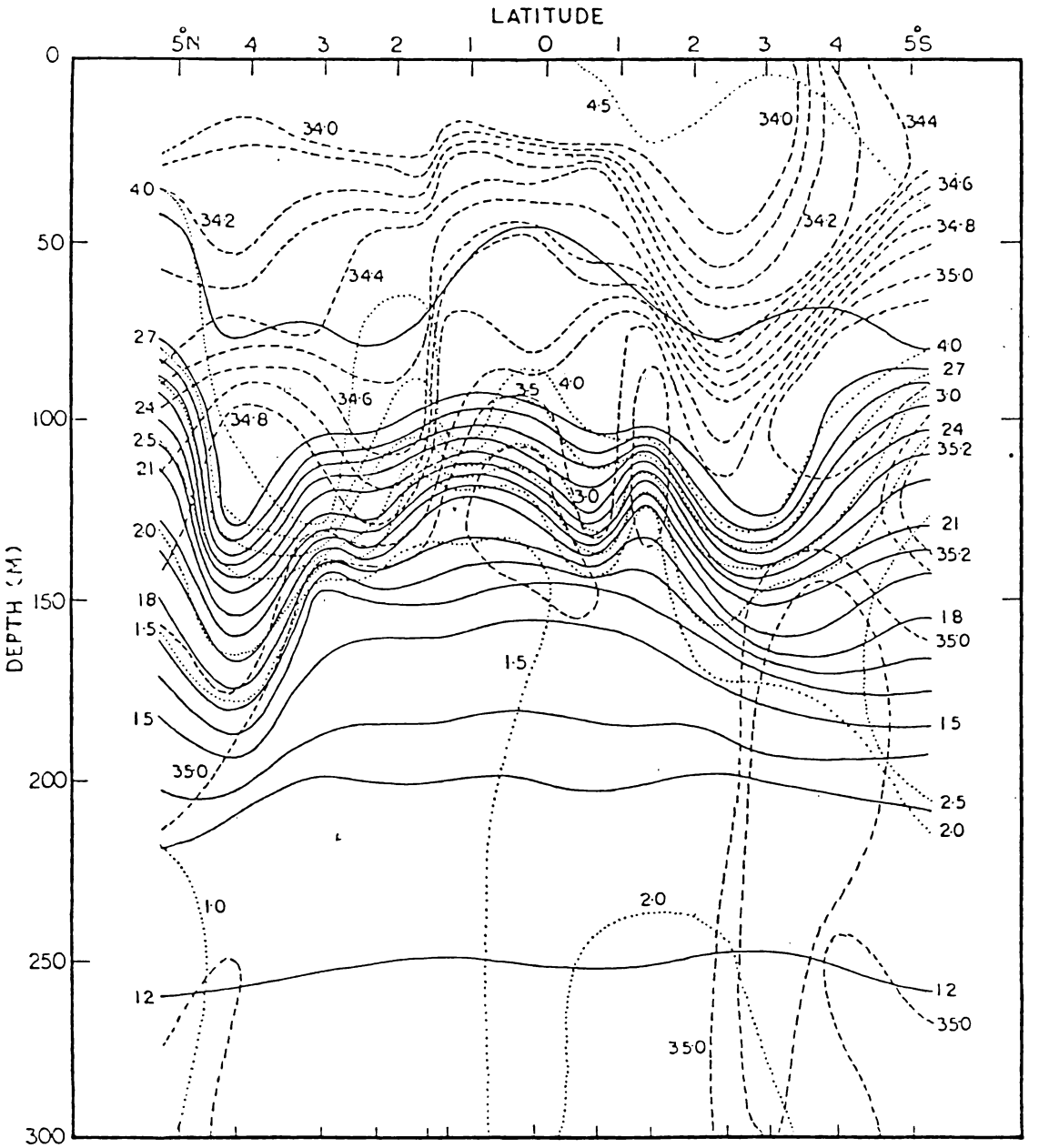

Fig. 31. Vertical section of temperature (solid lines - ^{o}C), Salinity (dashed lines - parts per mille) and dissolved oxygen (dotted lines - ml/l) at 94^{o}E (November - December, 1962).

as it is in the previous month. In the eastern section, i.e. along 86°E, the eastward current does not carry high salinity water, on the contrary a very low salinity is observed at the equator. The only plausible explanation for such a very low value is the rain fall at the time of occupation of the station.

2.12. DECEMBER

Unfortunately there are oceanographic data available only for two sections during this month, one in the central Indian Ocean along 71°E and the other along 94°E in the eastern region under study.

The thermal structure along 71°E, in general, shows an upward sloping of the thermocline from north to south. But, there is an indication of the spreading of the thermocline between the equator and 2°N with the doming of isotherms at 2°N while troughing of the isotherms at the bottom of the thermocline takes place around the equator. Water in the surface layers is warmer than 28°C except around 3°N.

Strong horizontal gradients of salinity are conspicuous upto a depth of about 75 m with highest salinity around 5°N with a value of about 36‰ and the lowest value of 35‰ is around 5°S. Another interesting feature in the salinity is that it is almost homogeneous between 2°N and 2°S

upto a depth of 40 m. Similar to that of the thermocline, halocline also indicates a general upsloping southwards. It is, therefore, not clear immediately how the pycnocline slopes unless the major controlling factor in deciding the density distribution is identified. As the horizontal gradients of salinity are definitely showing more conspicuous variation in the surface layers, the structure of the pycnocline should be judged, mainly, from the haline structure. Therefore, at the equator the pycnocline should show a trough structure while it slopes down northward in the northern hemisphere, whereas the reverse condition prevails in the southern hemisphere. As a result the flow pattern should be eastward along the equator surrounded by westerlies on either side in the upper layers.

The spreading of the thermocline between the equator and $2^{o}N$ in the depth range of 40-160 m confirms an easterly flow which may be relatively stronger compared to that at the equator because of comparatively stronger horizontal gradients of temperature and salinity. It is interesting to note that the westerly flow beyond $3^{o}N$ and S towards higher latitudes should be associated with strong westerlies as evidenced by strong horizontal gradients of temperature in the depth range of 75-140 m, north of $3^{o}N$ and 25-75 m, south of $3^{o}S$. The oxypleths are almost running parallel to the isotherms in the

subsurface layers as normally expected that the thermocline and oxycline coincide.

The distribution along 94°E shows an anomalous nature compared to the other section, as the salinity distribution dominates over the thermal structure, particularly, above the thermocline. Thermal structure, in general does not convey any interesting features. The vertical gradients are very strong both in the temperature and salinity distribution with a distinction that the halocline is shallower than the thermocline. A very prominent feature of the salinity distribution is that high salinity water is sandwitched between 1°N and S in the depth range of 50-150 m. Based on the salinity distribution alone, the Equatorial Undercurrent is conspicuous with a westerly flow in the surface layers at the equator as the meridional sloping of sea surface is indicated by the isohalines.

A cursary glance of the hydrographic conditions in the central and eastern regions of the Indian Ocean during December reveals a definite contrast in the salinity structure between the two. The Equatorial Undercurrent is identified by the thermal structure in the latter while it is done by salinity structure in the former. Further, the Undercurrent in the eastern region is separated by a westerly flow at the surface while it is not so in the central region where the surface flow at the equator is also easterly,

although very weak. It can, therefore, be concluded that the Equatorial Undercurrent shows its appearance definitely by December even though all the associated hydrographic features could not conclusively be identified. The oxypleths show downward mixing with higher values near about the equator which may confirm the presence of the Undercurrent.

CHAPTER - III

CHAPTER - III

DISTRIBUTION OF ZONAL FLUX

Zonal flux has been calculated across eleven selected transequatorial sections along various longitudes. The sections are selected in such a way that they occupy western, central and eastern Indian Ocean, so that the longitudinal variation of the mass transport within the Undercurrent can be studied. Of these, a few sections have been selected for the later part of the northeast monsoon in order to confirm its presence inferred from the hydrographic properties. The sections along $84^{o}E$ in May, $88^{o}E$ in June and $84^{o}E$ in October are mainly chosen to estimate the transport of the Equatorial Jet. The zonal flux is computed only between a maximum of $3^{o}N$ to $3^{o}S$, as the objective of the author is to study the Equatorial Undercurrent and Equatorial Jet, although, the distribution of the properties is extended upto $5^{o}N$ and S. Since, the study is mainly concerned with the Equatorial Undercurrent and Jet, the eastward zonal flux alone is demarkated with the 50% and 75% frequencies, while no such attempt is made for the westward flux.

3.1. The distribution of the flux is presented in figures 32 to 42. In these figures, the 50% and 75% frequencies are demarkated by the solid and dashed lines respectively. These diagrams, besides giving the bivariate distribution of salinity and thermosteric anomaly at

intervals of 0.2‰ and 40 cl/t respectively, they also give the temperature variation as the isanosteric surface is dependent only on temperature and salinity. Therefore, for any single salinity interval there is bound to be only single temperature interval. By comparing the interval of temperature with the corresponding diagram of the distribution of temperature, it is possible to delineate the depth distribution of each frequency.

3.2. Since the meridional section at $54^{o}30'E$ during February is limited to $2^{o}N$ and $2^{o}S$, the transport is calculated in between these latitudes. The estimated transport is $19.34 \times 10^{6}\ m^{3}\ s^{-1}$ (Fig. 32). The distribution of the eastward flux exhibits three modes. The primary is at an isanosteric surface of 300 cl/t and salinity 35.5‰ representing the water just below the high salinity core (Fig. 4). Although, this mode appears below the high salinity core, it is having a temperature around $20^{o}C$ which implies that this is a mode within the Equatorial Undercurrent. An intrusion of similar water from Arabian Sea towards the equator at $55^{o}E$ along 300 cl/t surface is depicted in the figure presented by Sharma et al. (1982). Two classes of high salinity, ranging from 35.4‰ to 35.6‰ and at 440 cl/t isanosteric surface form the secondary mode. This water with a temperature around $26^{o}C$ indicates the one that is found just above the high salinity

core (Fig. 4). This is also derived from the Arabian Sea (Sharma et al., 1982). The tertiary model in the zonal flux within 50% distribution, having a value of 2.36 x 10^6 m^3 is of a low salinity water around 35.3‰ and 220 cl/t. This water might have been from the southern hemisphere converging towards the equator and flowing eastward. An examination of the distribution of hydrographic properties (Fig. 4) with the flux shows that the eastward flow appears to have been confined to the subsurface layers. The Undercurrent with salinity greater than 35.6‰ is mainly confined to two frequencies of 1.82 and 1.87 x 10^6 m^3 s^{-1} and 360 cl/t within the 75% zonal flow. The tertiary mode under 75% of the zonal flux falls between 160 and 200 cl/t surface with an average salinity of 35.3‰. The temperature of this water is around 15°C which forms the easterly flow at the bottom of the thermocline.

About 25% of the total eastward flux is of salinity greater than 35.6‰ and constitutes the high salinity core in between the isanosteric surfaces 280 and 440 cl/t. Since the primary mode lies just below the high salinity core (Fig. 4 and 32), it can be presumed that the maximum velocity does not coincide with the high salinity core, instead it is found just below it. Similar structure is also observed by Voigt et al. (1969) in the Atlantic Ocean.

3.3. The bimodal distribution of the flux along 58°E in March reveals the primary mode of easterly flow around 240 cl/t and 35.3‰ salinity. This mode has two frequencies with values 4.06 and 3.78 x 10^6 m^3 s^{-1}. The secondary mode within 50% level is around 180 cl/t and 35.1‰ . The temperature of the primary mode ranges from 15° to 19°C, obviously, indicating the flow within the thermocline as a result of the Equatorial Undercurrent. It is further confirmed with the high salinity water associated with that. A close examination reveals that there is westerly flow with higher salinities and also at higher isanosteric surfaces. The inference drawn from the distribution of hydrographic properties is confirmed from the flux pattern in the upper layer with a wide range of salinity distribution from 34.8 to 35.8‰. The easterly flow, below this layer, builds upto a maximum value at 220 cl/t and 35.2‰ . Such a situation precludes that the maximum flux is not closely associated with the high salinity core but below it. A similar feature is also noticed in the previous month. Sharma et al. (1982) identified it as due to the advection of the Arabian Sea Water towards the equator. It is, therefore, interesting to note that the Equatorial Undercurrent in the western Indian Ocean is mainly fed from the water of the central Arabian Sea.

There are two frequencies of easterly flow within 75% flux level at about 180 and 300 cl/t with the salinity of 35.3‰ . These two frequencies, mainly, constitute the downward and upward extension of the Equatorial Undercurrent.

The total estimated eastward and westward fluxes at $58^{o}E$ in March within $2^{o}N$ and $2^{o}S$ are 20.34×10^{6} m^{3} s^{-1} and 11.27×10^{6} m^{3} s^{-1} respectively. The westward flux is mainly derived from the surface flow. A part of it is noticed below the high salinity core. Only 15% of the total eastward flux constitutes the high salinity core whereas more than 50% of the flux represents the two modes underneath it. As in the previous section the velocity core is also found to be present just below the high salinity core.

A comparison of distribution of the flux between February and March reveals that the Equatorial Undercurrent is not only strengthened but also deepened as a result of which there is a slight decrease in its salt content. Further, it is interesting to note that unlike in the previous month the surface westerly flow in March is well demarkated from the Equatorial Undercurrent with more frequencies.

3.4. The zonal flux distribution along $65^{o}E$ in March which represents the central region of the Indian Ocean is

shown in figure 34. Within 50% limit of the total eastward flux, there are two modes with three frequencies in the primary and two in the secondary. The primary mode is mainly limited to the salinity of about 35.3‰ and 400 cl/t with values of 3.30 and 2.65 x 10^6 m^3 s^{-1}. The third frequency in the primary mode is of 35.5‰ salinity and 320 cl/t thermosteric anomaly. Obviously, the third frequency is the water within the high salinity core. The secondary mode within 50% limit is also around 35.3‰ salinity within the isanosteres of 200 and 280 cl/t. It is conspicuous to note that the frequencies of the 75% limit are adjacent to the primary and secondary modes. The highest eastward flux in the salinity distribution is limited to 35.2 and 35.4‰ with a value of 18.63 x 10^6 m^3 s^{-1} while the flux at different thermosteric levels has almost uniform distribution except between 320 and 400 cl/t. Thus, of the bivariate distribution, salinity appears to be dominating.

The total flux of the Undercurrent within 3^oN and 3^oS at 65^oE in March is 28.98 x 10^6 m^3 s^{-1}. The characteristics of the water within the primary mode reveal that it is of Arabian Sea Water except the one below 240 cl/t surface which is from the Equatorial Indian Ocean (Sverdrup et al., 1942).

During March, a comparison of the sections at 58^{o} and 65^{o}E reveals a conspicuous heterogeneity in salinity structure at 58^{o}E while there is a homogeneity of salinity along 65^{o}E. Further, it is also interesting to note that the maximum eastward flux is around 180 cl/t at 58^{o}E while it is at 380 cl/t along 65^{o}E. A comparison of the fluxes along these two sections shows that the total eastward flux increases from 20.34 x 10^{6} m^{3} s^{-1} at 58^{o}E to 28.88 x 10^{6} m^{3} s^{-1} at 65^{o}E. Thus, confirming the previous inference that the strength of the Equatorial Undercurrent increases from west to east and also from February to March.

3.5. The distribution of the zonal flux within 2^{o}N and S in figure 35 across 92^{o}E in April represents that of the eastern region. Within 50% level, there is only single mode in the salinity range 35.0 to 35.2‰ with two frequencies of 9.53 and 5.34 x 10^{6} m^{3} s^{-1}. Of the total flux of 28.53 x 10^{6} m^{3} s^{-1}, 24.45 x 10^{6} m^{3} s^{-1} constitutes the flux within the salinity range of 35.0 to 35.2‰ , revealing a homogeneous nature of the water in its bivariate distribution. Even the two frequencies within the 75% level also fall under the same salinity range. While the primary mode within 50% level is around 200 cl/t, the two frequencies within 75% level is around 280 cl/t. Evidently, the major eastward flux is at the bottom of the

thermocline in the temperature range of $13^{o}-16^{o}C$ (Fig. 35). The two frequencies with values of 1.17 and 1.61 x 10^{6} m^{3} s^{-1} constitutes the main zonal flux within the high salinity core. Although the distribution of hydrographic properties in figure 12 along $92^{o}E$ show low salinity water between $2^{o}N$ and S from which it can be inferred that there should be surface easterlies, and from the flux distribution it could be noticed that there is not a major eastward flow below the salinity of 34.8‰ . Perhaps, the surface flow may not be strong enough to give a significant amount of any frequency in the upper layers. Further, the vertical stratification may also be responsible for a weak easterly in the surface. Normally, during April the Equatorial Jet is expected to be present but this section, being in the eastern most region, the Jet might have its terminal point much on the western side of the section. Just as in the western region in March, the eastern most region in April also shows the major part of the flux is confined around a single salinity interval, whereas in the central region the distribution is uniform over a wider range of salinity.

The total eastward flux in the month of March along $65^{o}E$ and that of April along $92^{o}E$ is almost same and

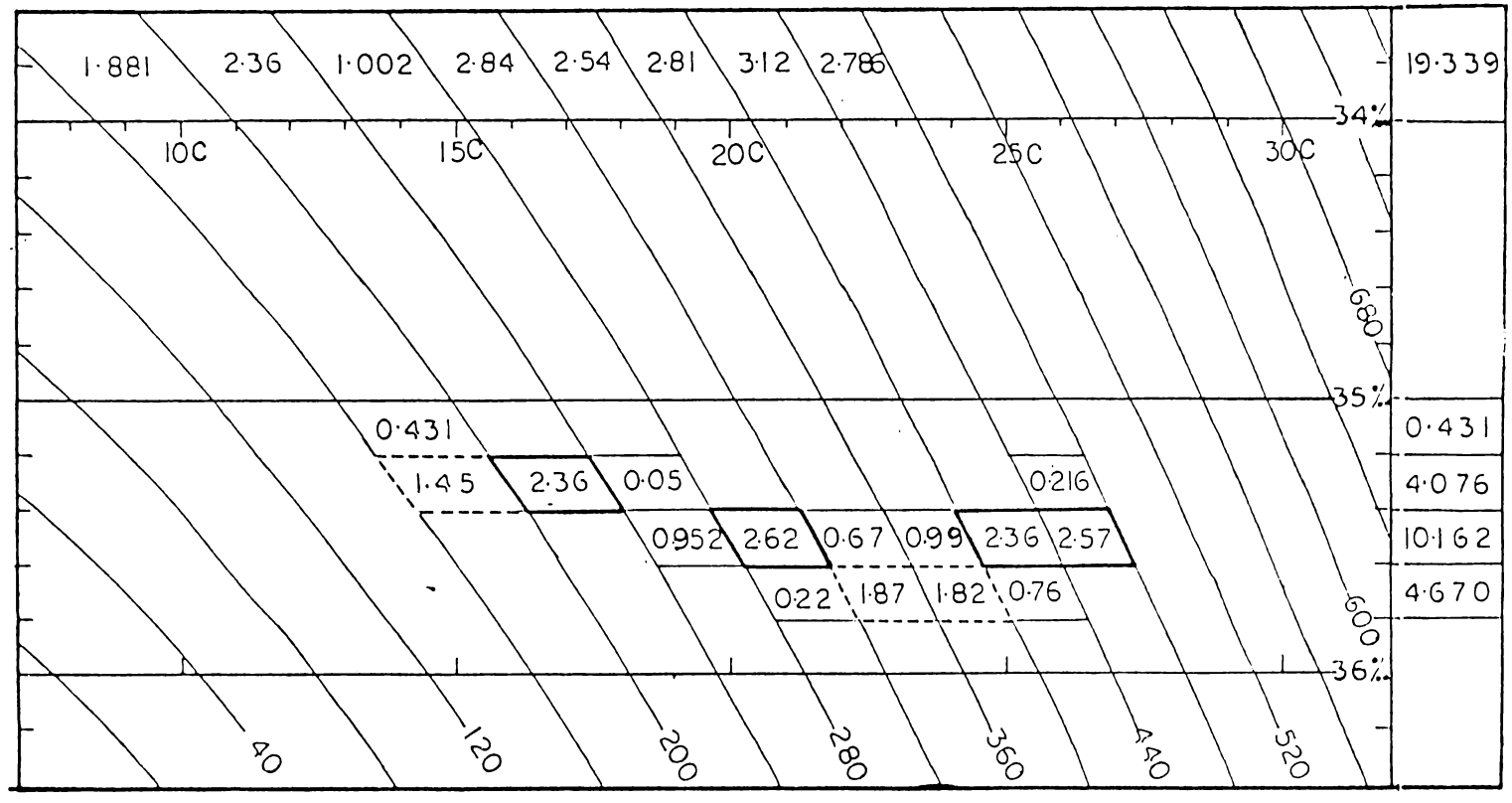

Fig. 32. The zonal flux within 2^{o}N and S (excluding westward flux) at $54^{o}30'$E in February, 1975.

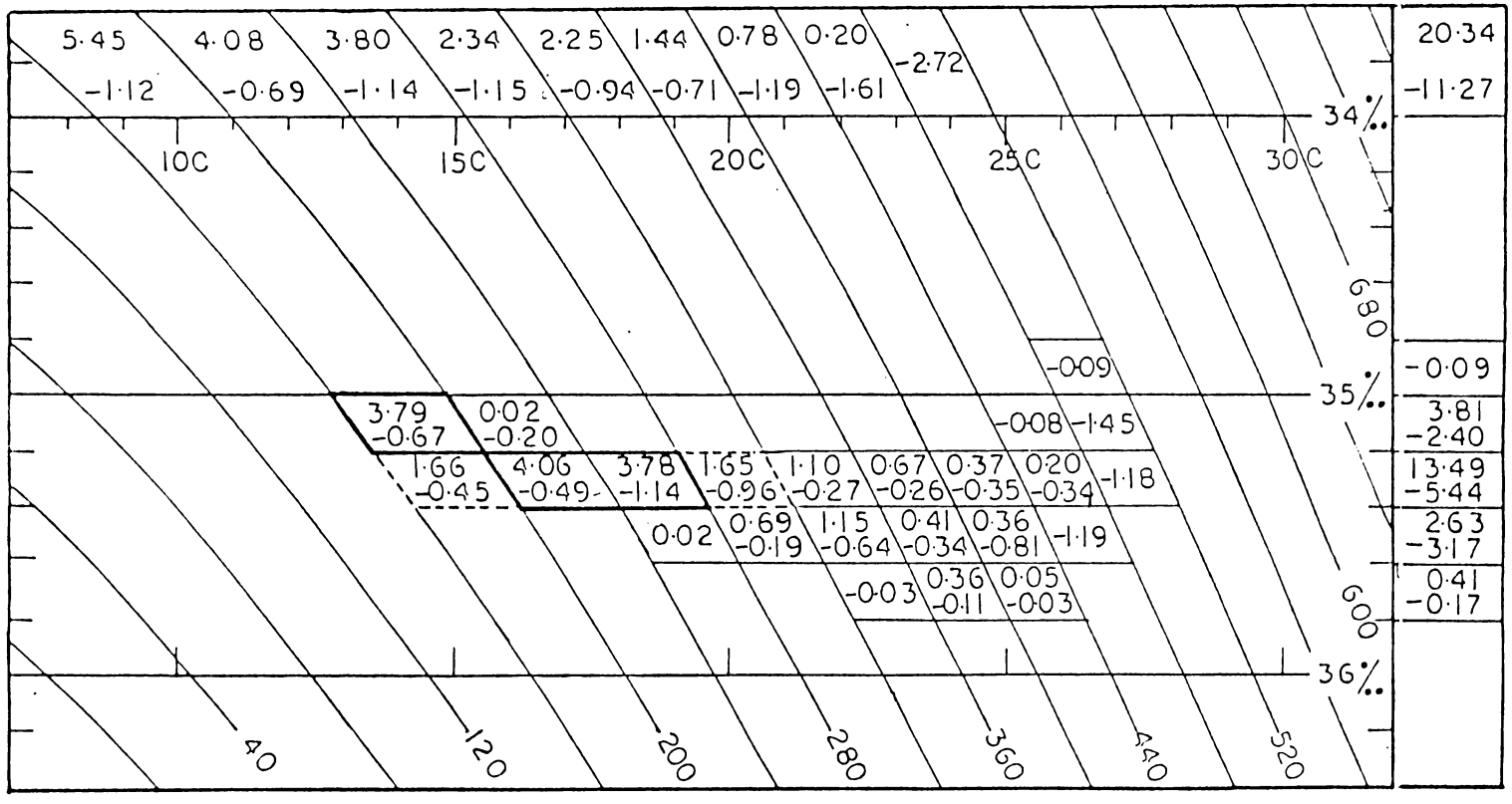

Fig. 33. The zonal flux within 2^{o}N and S at 58^{o}E in March, 1964.

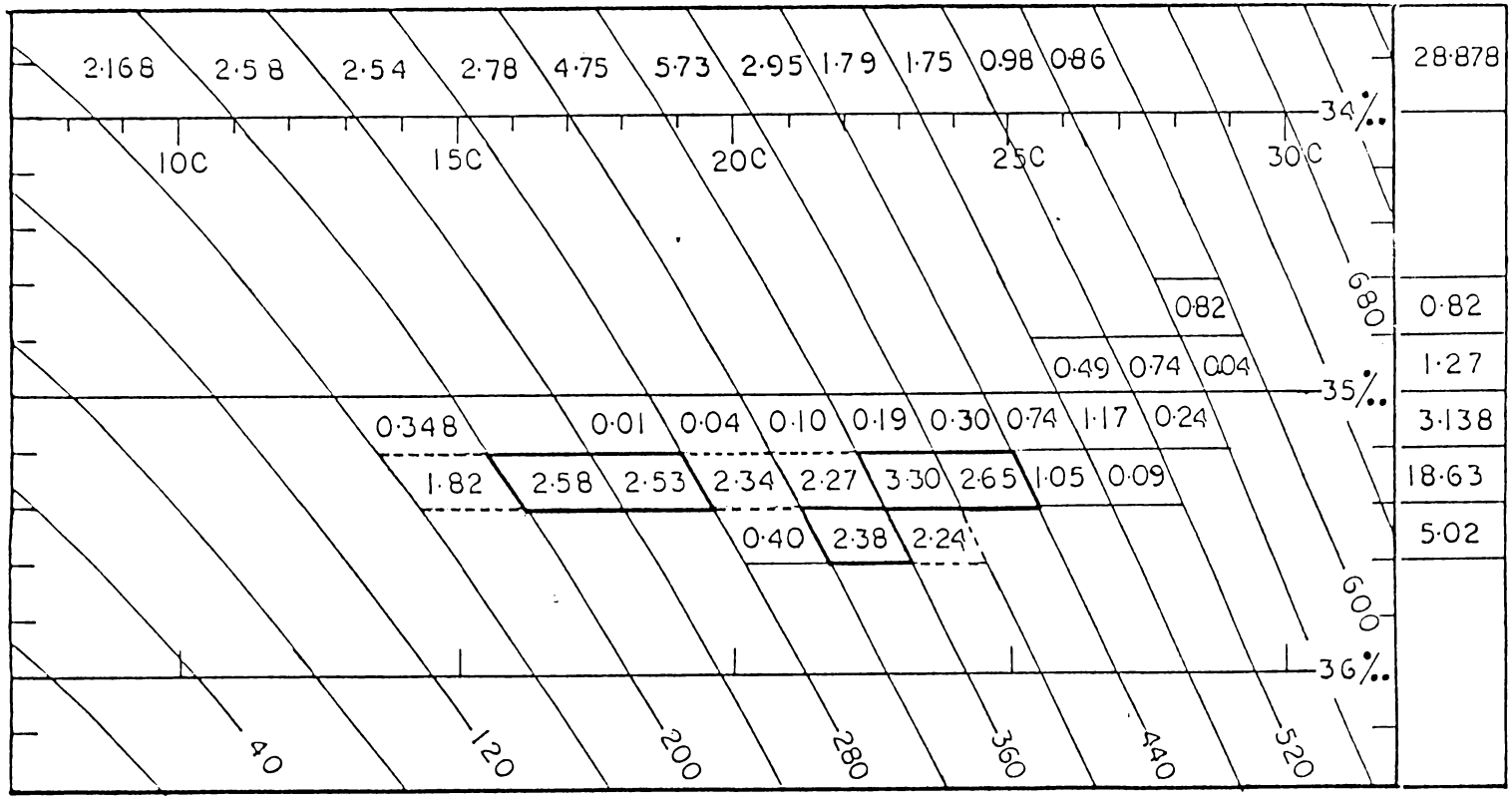

Fig. 34. The zonal flux within 3^{o}N and S (excluding westward flux) at 65^{o}E in March, 1973.

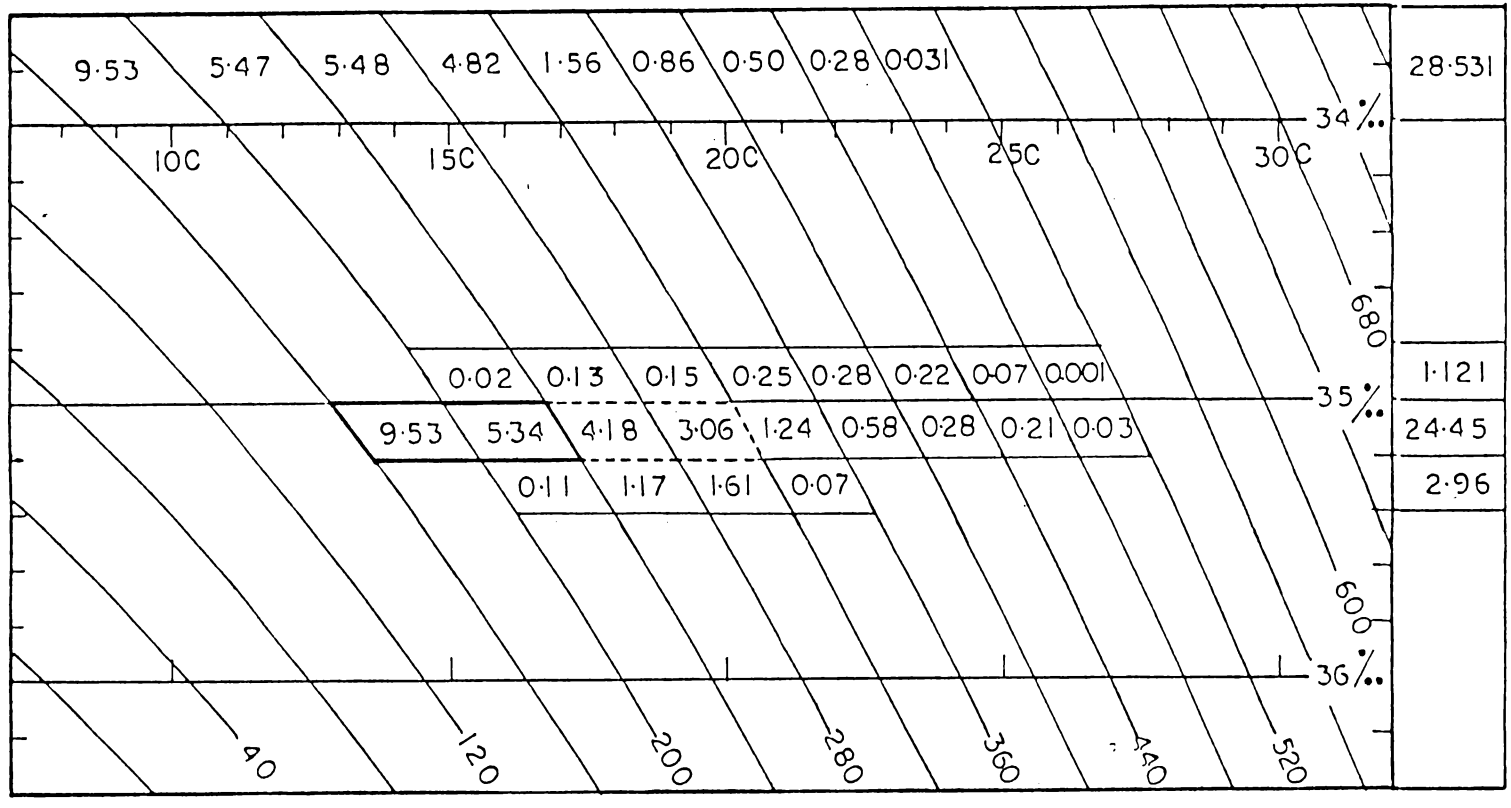

Fig. 35. The zonal flux within 2°N and S (excluding westward flux) at 92°E in April, 1963.

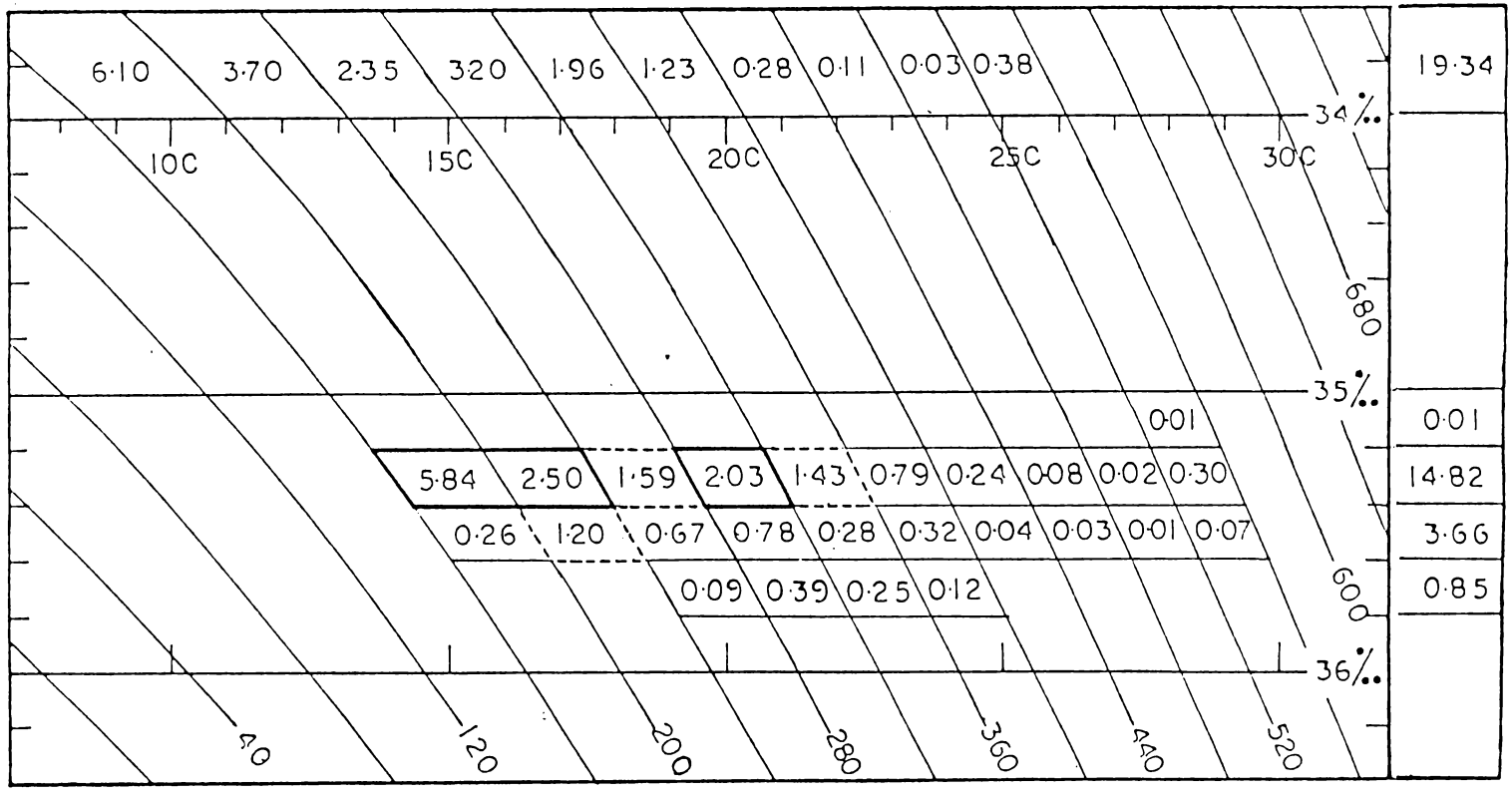

Fig. 36. The zonal flux within 3°N and S (excluding westward flux) at 55°E in May, 1973.

its primary mode is further deepened compared to that of February and March. It can, therefore, be inferred that the Equatorial Undercurrent deepens towards the east.

3.6. In view of the presence of Equatorial Jet in the Indian Ocean during May, two transequatorial sections, one along $55^{o}E$ and another $84^{o}E$ are used for computing the zonal flux between $3^{o}N$ and S, so as to understand the magnitude of the flux in the western and eastern regions of the Indian Ocean.

Along $55^{o}E$, the primary mode within 50% level has two frequencies with values 5.84 and 2.50 x 10^{6} m^{3} s^{-1} at 200 cl surface and 35.3‰ salinity (Fig. 36). The secondary mode has only one frequency with a value of 2.03 x 10^{6} m^{3} s^{-1} at the same salinity but at a higher thermosteric level of 300 cl/t. The three additional frequencies within 75% lie adjacent to the primary and secondary modes within 50% level. Of these, the one at 220 cl/t has a higher salinity of 35.5‰. This water may, perhaps, represent the water below the high salinity core around $17^{o}C$ isotherm at the bottom of the thermocline. Below this water, the primary mode of 5.84 x 10^{6} m^{3} s^{-1} constitutes the major easterly flow at the bottom of the thermocline below $15^{o}C$. From the figure it is evident that the total flow within the high salinity core in the temperature range of 18^{o} to $24^{o}C$

comprises only 0.85 x 10^6 $m^3 . s^{-1}$, which is comparatively insignificant. The secondary mode within 50% level around 300 cl/t appears to be the easterly flow associated with a steep upward inclination of the isotherms (Fig. 13) around 2^oS. Of the total easterly flux of 19.34 x 10^6 m^3 s^{-1} 14.82 x 10^6 m^3 s^{-1} constitute the water within the salinity range of 35.2 to 35.4‰ whereas such a uniform distribution is not noticed in the isanosteric level distribution which means that of the bivariate distribution of the water, the salinity is homogeneous and it is sterically heterogeneous.

Though the distribution of hydrographic properties show strong horizontal gradient of salinity which should have given rise to relatively stronger current, it appears to have been counter balanced by the warm waters prevailing in the surface layers between 3^oN and S, resulting in the absence of any frequency in the temperature range of 29 to 30^oC.

3.7. The zonal flux along 84^oE (Fig. 37) shows heterogeneous nature in its bivariate distribution. Within 50% level the primary mode with three frequencies lies around 620 cl/t without any secondary mode present at all. Of the total easterly flux of 48.15 x 10^6 m^3 s^{-1}, 33.48 10^6 m^3 s^{-1} covers the water around 620 cl/t, indicating the presence of the surface Equatorial Jet in the Indian

Ocean during May. Westerly flow along this section in the upper levels surrounding the Equatorial Jet is not significant. The subsurface flow below 400 cl/t is mainly westerly which is also depicted in the distribution of hydrographic properties (Fig.15). An interesting distinction that can be drawn between the fluxes along $55^{o}E$ and $84^{o}E$ is that the major flux along $55^{o}E$ is in the salinity range of 35.2 to 35.4‰ while it is between 600 and 640 cl/t isanosteric surfaces along $84^{o}E$. Another interesting feature between these two sections is that there is only frequency covering the additional 25% over and above 50% level.

3.8. As the zonal flux distribution along $88^{o}E$ is covered in the early June, there is not much variation in the distribution pattern between that of May along $84^{o}E$ and the present one. Similar to the previous one, of the total easterly flux of $43.52 \times 10^{6}\ m^{3}s^{-1}$, $21.40 \times 10^{6}\ m^{3}\ s^{-1}$ covers the primary mode within 50% level while $10.12 \times 10^{6}\ m^{3}\ s^{-1}$ comprises the single frequency of additional 25% level. Thus, the major easterly flow is spread within the salinity variation of 34.4 to 34.8‰ , and 600 cl/t to 640 cl/t. The only difference between these two is that the primary mode in 50% level is about 34.5‰ while the additional frequency within 75% level is at 34.7‰ . The salinity appears, in general, to be heterogeneous in bivariate distribution for

both westerly and easterly flows. While the surface flow is dominated by easterly, the subsurface flow, particularly, below the top of the thermocline is westerly. With regard to the westerly flow, it is mainly constituted within the salinity range of 35.0 and 35.2‰ . As far as the steric level variation is concerned, it is uniformally spread over a wider range. Obviously, the two frequencies of easterly flow along the equator are sandwitched by the weak westerlies.

3.9. The distribution of zonal flux along $54^{o}30'E$ during July is depicted in figure 39. During this month, the total westerly flux of 30.33 x 10^{6} m^{3} s^{-1} dominates over the easterly flux of 21.10 x 10^{6} m^{3} s^{-1}. Of the total flux, 75% comprises around 35.3‰ salinity. While there are only two frequencies within 50% level with values 8.04 and 2.26 x 10^{6} m^{3} s^{-1} around 200 cl/t, there are four frequencies involved in the additional 25% of the total flux indicating that the main zonal eastward flow is confined to around an isanosteric surface of 200 cl/t and 35.3‰ salinity. The primary mode of the easterly flow is much below the thermocline. Although the easterly flux is conspicuous at this level, it does not appear to be associated with the Equatorial Undercurrent, as its normal position is at much higher level.

The predominance of the westerly flow above the salinity of 35.4‰ , mainly, constitutes the influx of high salinity water from the north towards the equator. Of these, nearly 45% of the westerly flux is within the isanosteres of 480 and 520 cl/t. The westerly flux decreases with depth in the salinity range of 35.4 to 35.6‰ , whereas it increases with depth below the isanostere of 480 cl/t in the salinity range of 35.2 to 35.4‰ .

3.10. The transequatorial distribution of hydrographic properties at $91^{o}30'E$ in September exhibits a strong vertical gradient of temperature coinciding with the vertical change in salinity (Fig. 24). As a result the transport is distributed among a large number of characteristic classes (Fig. 40). The primary mode at 180 cl/t with modal salinity 35.1‰ represents the water just below the thermocline between $2^{o}N$ and $2^{o}S$. The average temperature of this water mass is around $14^{o}C$ and this water appears to be from the Equatorial Indian Ocean. The modal class at 260 cl/t, 35.1‰ and $18^{o}C$ in Fig. 40 represents the water within the thermocline and forms the secondary mode within 50% level. This water is expected to be derived from the Bay of Bengal as there is no evidence to prove its path from the west. More than 50% of the total flux of 16.46×10^{6} m^{3} s^{-1} comprises the two dominant modes. Most of the frequencies beyond 75% level cover the low salinity water with values

less than 35.0‰ in addition to two more frequencies adjacent to the frequencies of the primary mode at 35.1‰ and 580 cl/t isanosteric surface.

3.11. The zonal flux during October between $3^{o}N$ and S along $84^{o}E$ that represent almost the central region is presented in Fig. 41. The most interesting feature is an unusually very high eastward flux of $70.05 \times 10^{6}\ m^{3}\ s^{-1}$. 50% of the total eastward flux is covered within five frequencies. Of these four are around 540 cl/t while the other one is covered around 500 cl/t. The additional frequencies that account for 75% level are four. It is interesting to note that 75% of the total easterly flux is above 400 cl/t surface. Obviously, this must constitute the Equatorial Jet. The westerly flux that computed is relatively much lower and is mainly concentrated at 35.1‰ salinity, covering nearly 90% of the total westward flux. The maximum westward flux of $6.5 \times 10^{6}\ m^{3}s^{-1}$ is around 180 cl/t surface. In fact this value alone covers nearly 60% of the westward flux. This maximum is mainly due to the geometrical vertical extent rather than due to the intensity of the flow.

From a comparison of the distribution of hydrographic properties with that of the flux, it can be construed that

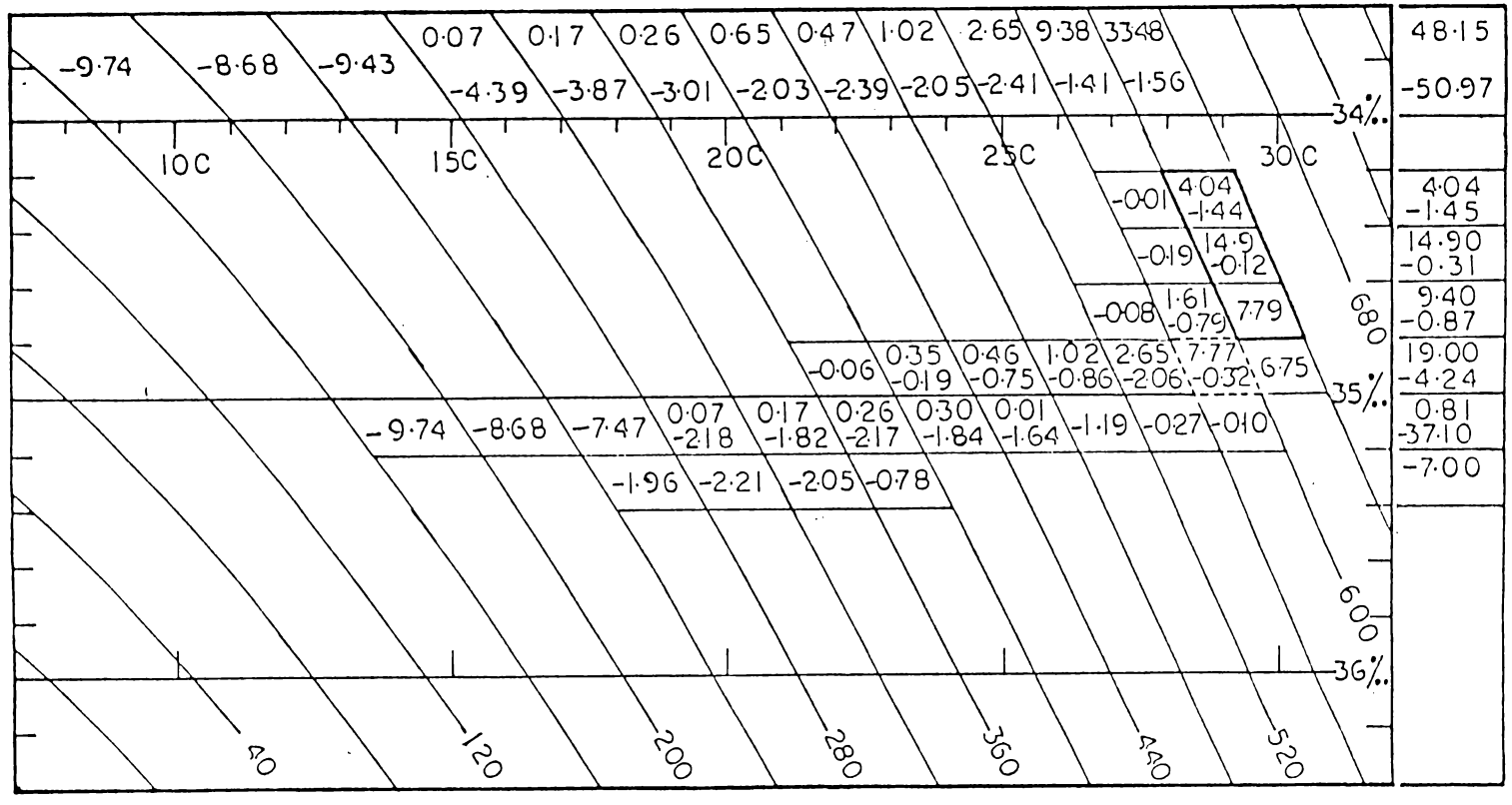

Fig. 37. The zonal flux within 3^{o}N and S at 84^{o}E in May, 1964.

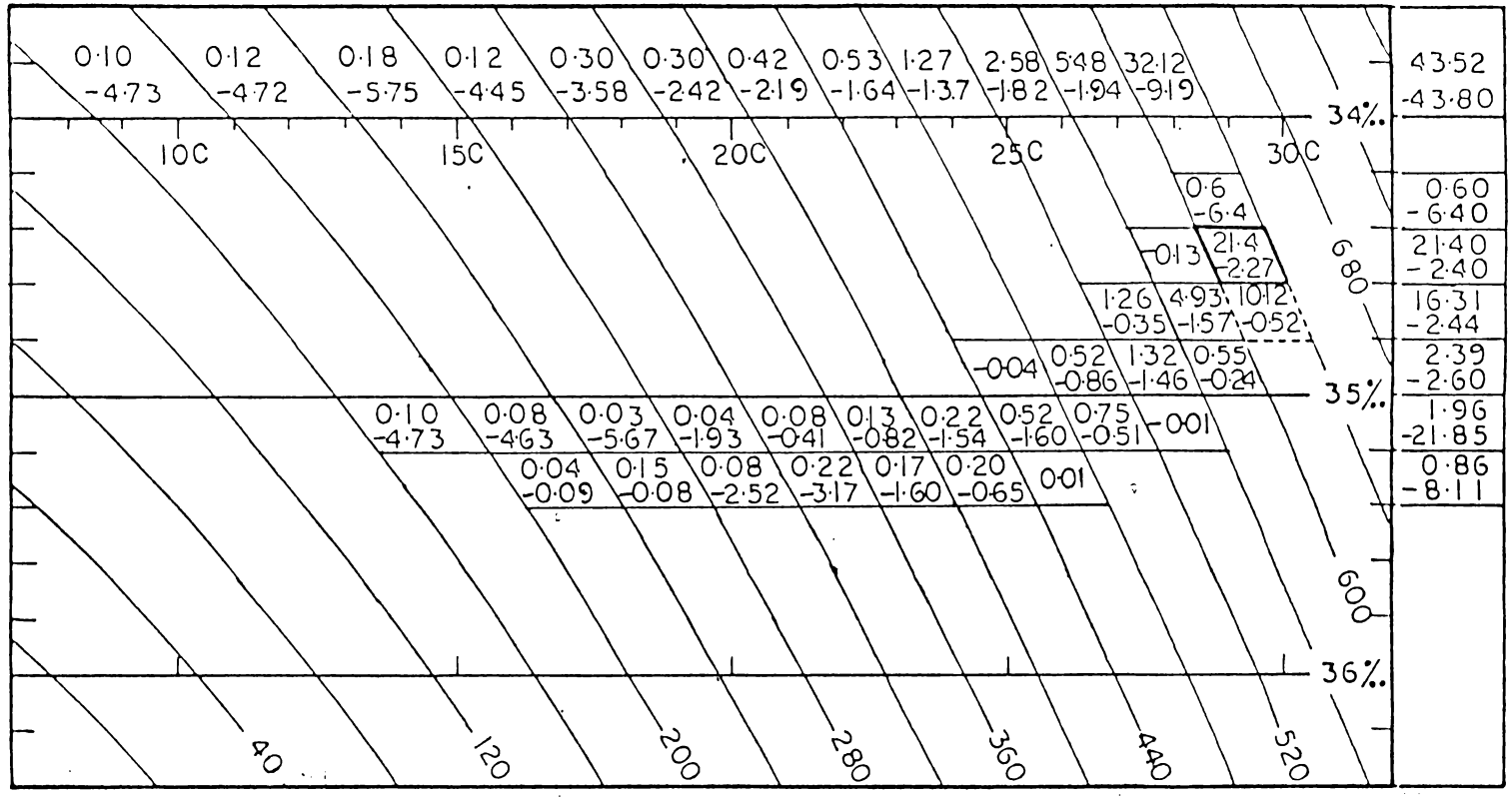

Fig. 38. The zonal flux within 3°N and S at 88°E in June, 1964.

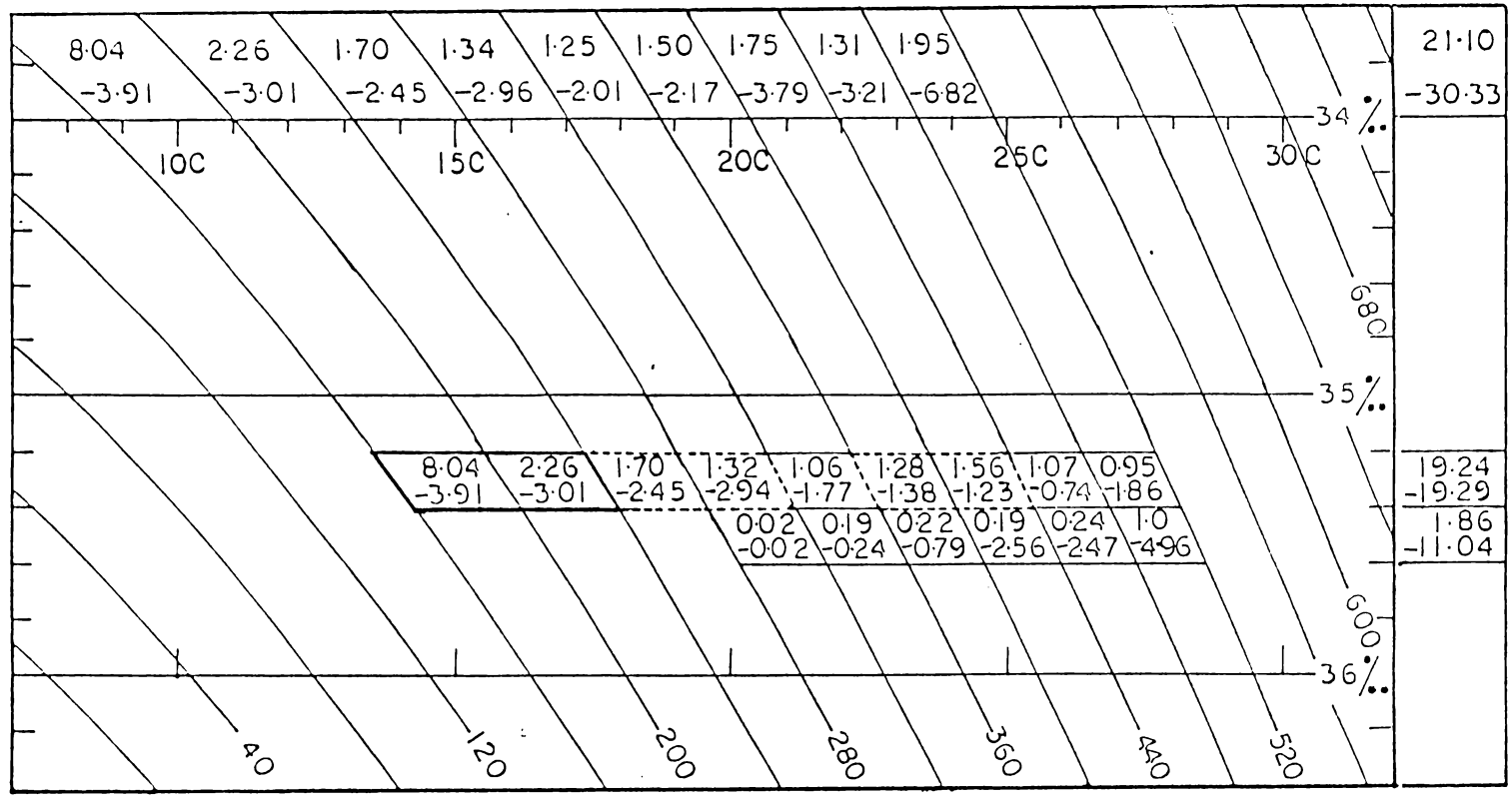

Fig. 39. The zonal flux within 2^{o}N and S at $54^{o}30'$E in July, 1975.

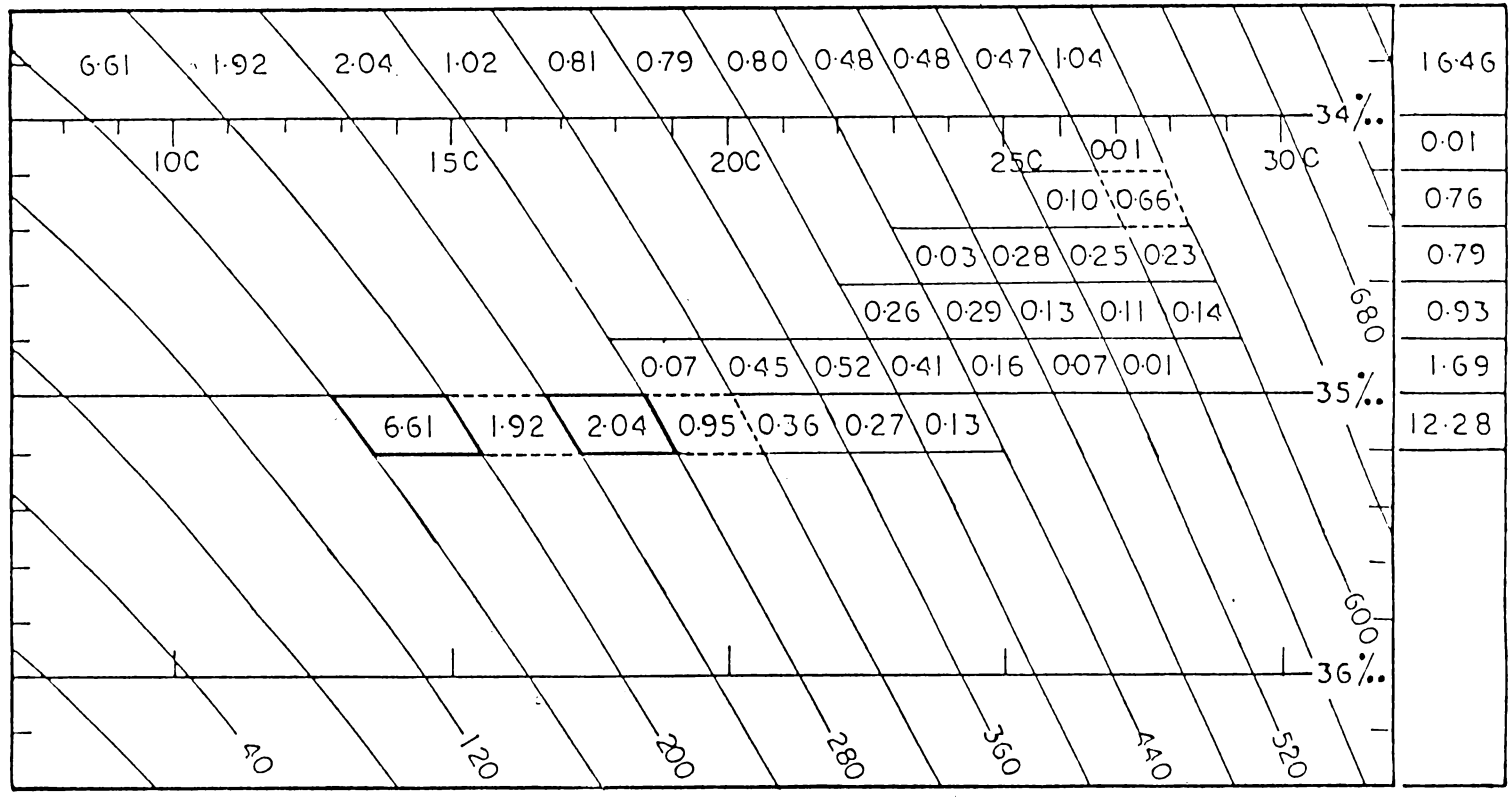

Fig. 40. The zonal flux within 2^{o}N and S (excluding westward flux) at $91^{o}30'$E in September, 1962.

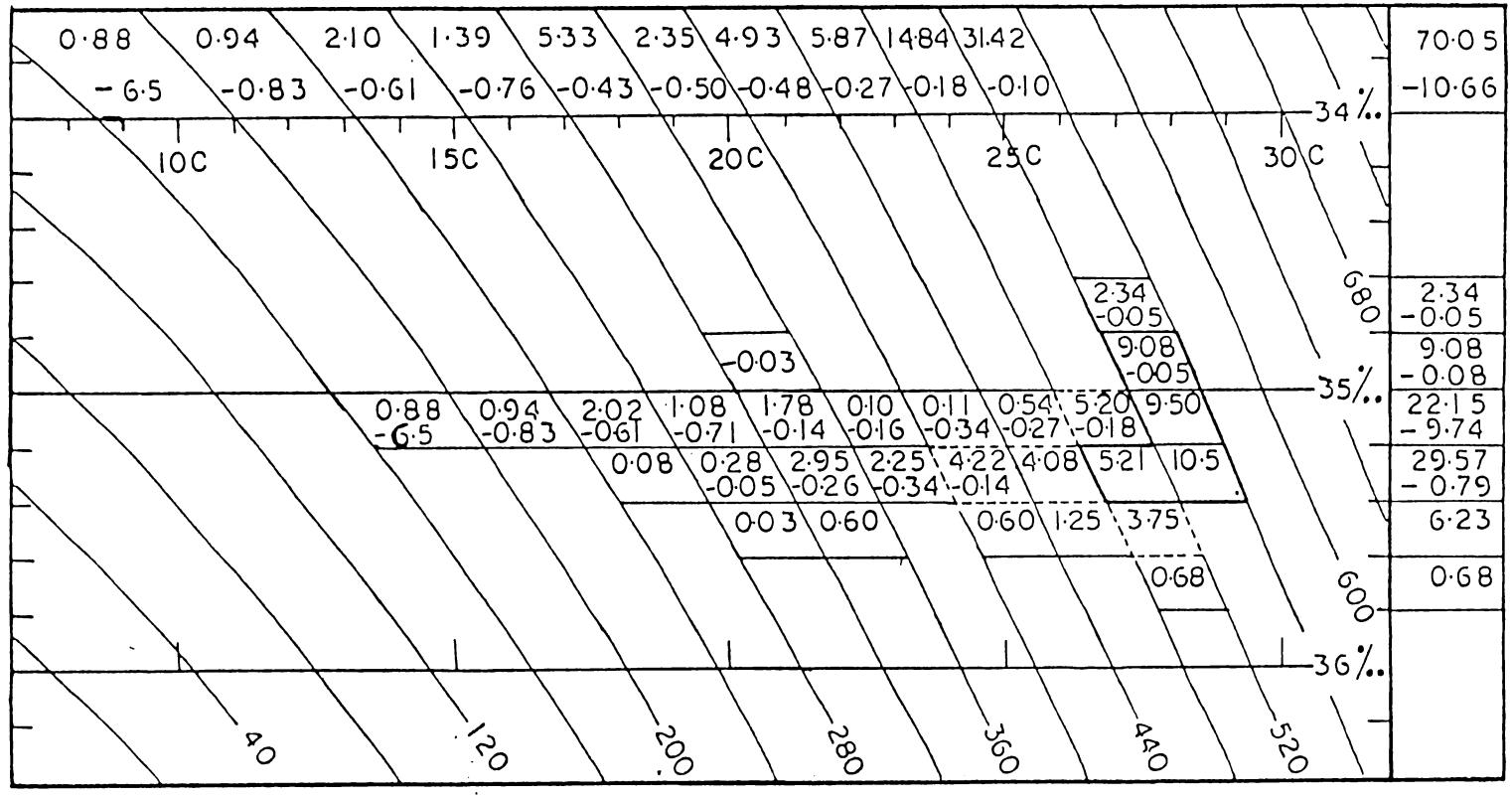

Fig. 41. The zonal flux within 3°N and S at 84°E in October, 1962.

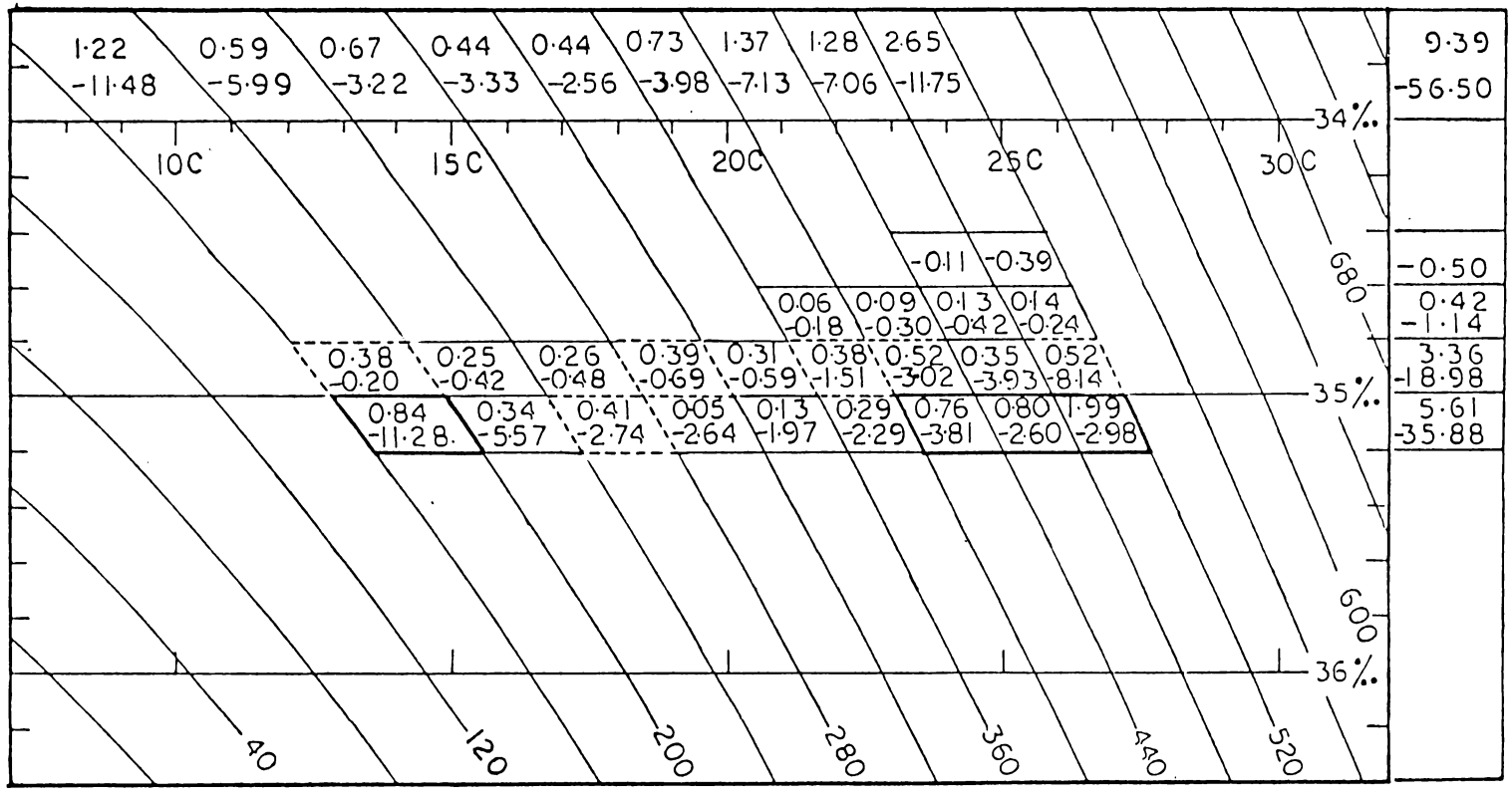

Fig. 42. The zonal flux within 3°N and S at 94°E from November to December, 1962.

G3466
COCHIN UNIVERSITY LIBRARY

the strong horizontal salinity gradient with warm water around the equator appears to be the causative factor for such a high easterly flux. Evidently, it is the Equatorial Jet that is confined to the upper levels above 480 cl/t that is responsible for the eastward flux. Of the bivariate distributions, salinity between 35.0 and 35.4‰ and thermosteric anomaly between 480 to 560 cl/t cover the major easterly flux.

The trough structure at the equator (Fig. 26) indicates the penetration of the easterly flow to the deeper levels as is evident from the distribution of easterly fluxes to an isanosteric surface of 160 cl/t. The flux, within the high salinity core, covered by the 35.4‰ isohaline constitutes nearly 10% of the total easterly flux.

3.12. The zonal flux distribution depicted in Fig. 42. covers the flow between 3^{o}N and S along 94^{o}E during late November and early December. Compared to the westward flux the eastward flux is insignificant, which may be due to the fact that the Equatorial Jet disappears at this longitude by late November. Instead, the westerly flux predominates the easterly. Nevertheless, the subsurface easterly flow starts increasing below the isanosteric surface of 280 cl/t. Of the total easterly flux of 9.39×10^{6} m^{3} s^{-1}, 5.61×10^{6} m^{3} s^{-1} covers the water in the high salinity core as shown in the

Fig. 31. Compared to the previous section, the westward flux is evidently dominating because of the ridging of the isohalines between $1^{o}N$ and S which gives rise to a strong westerly flow.

CHAPTER - IV

CHAPTER - IV

EQUATORIAL UNDERCURRENT IN THE INDIAN OCEAN

A critical review of the available information on the Equatorial Undercurrent has been carried out in the introduction of the present thesis. In that, the significance of the unique nature of the Indian Ocean from those of the other two major oceans, namely, the Pacific and Atlantic has been brought to focus. The distinction, mainly, being the contrasting atmospheric circulation that in turn reflects on the oceanic surface and subsurface currents has also been emphasised. In this chapter an attempt is being made to discuss the results of the present study on the Equatorial Undercurrent in the Indian Ocean with an objective of explaining the physical processes involved in its formation, establishment and termination, and also its deviation from the Undercurrent present in the Pacific and Atlantic.

4.1.1. From the distribution of temperature, salinity and oxyty at various transequatorial sections and the flux, it can be inferred that the Equatorial Undercurrent in the Indian Ocean is present only during January to early June with varied intensity and latitudinal shift in different

months, sometimes commencing even in December. During the rest of the period of the year, the Equatorial Undercurrent with its normal characteristic features is not identified in the Indian Ocean, although there is easterly flow observed both at the surface and subsurface levels with different structure in its magnitude as well as direction. Some of the important features associated with the presence or the absence of the Undercurrent are as follows.

4.1.2. The Equatorial Undercurrent in the Indian Ocean commences its development from the west in January or December and extends eastward with time. From the figures 1, 2 and 3, it is obvious that the Undercurrent is present slightly north of the equator along 58°E with the associated characteristic features of spreading of thermocline, high salinity core and penetration of oxyty to deeper levels, while such features are not conspicuous along 76° and 86°30'E. It can be seen that the core of the Undercurrent appears to be slightly north of the equator at 58°E which may be due to the upwind shift, resulted from the northerly winds prevailing at the equator. Such a wind shift was also reported by Leetmaa and Stommel (1980) while explaining the features of the current observations made in the western Indian Ocean in 1975 and 1976. The measurements of Duing et al. (1967) at 58°E during the end of January 1965 do not show the

evidence of an eastward flow above 100 m. Based on this observation Leetmaa and Stommel (1980) concluded that the Undercurrent either sets up extremely quick (from mid January to mid February) or 1965 was an unusual year. From the section along 76°E, a comparatively weak indication of Undercurrent is noticed, based on the salinity structure. The indication of the Undercurrent is still north of the one found along 58°E, probably, because of strong northerlies prevailing over in the western region. The surface flow at 86°30'E is easterly, penetrating to subsurface depth, as a result, the Undercurrent is not conspicuous (Fig. 3). An examination of the wind data between the east and western regions of the Indian Ocean reveal that the winds are northeasterlies in the western region and also strong while they are weakened towards the east and even reverse the direction in the easternmost region (Anonymous, 1952). It is, therefore, likely that the northeasterly winds prevailing in the western region are responsible for the development of the Undercurrent in this region, with a demarcation of the westerly flow in the surface and easterly in the subsurface layers, whereas, in the eastern region because of the westerly wind, the surface flow also is easterly and the Undercurrent is not at all conspicuous to be identified with the normal characteristics. It is further confirmed from the hydrographic properties that the sloping of the sea surface is steep between 76° and 86°30'E compared to that between 58° and 76°E. It is, perhaps,

possible that the variation in the sloping of the sea surface steepens from west to east.

4.1.3. From the distribution pattern of the hydrographic properties in February along $54^{o}30'E$, $65^{o}E$ and $85^{o}E$, the Equatorial Undercurrent is conspicuously observed along the equator in all the three sections (Figs. 4,5 and 6). It is, therefore, evident that the Undercurrent has shifted southward to the equator in the western region from January to February and also extended to the eastern region. The current measurements of Leetmaa and Stommel (1980) along $55^{o}30'E$ in February 1975 and that of Ivanov (1964) in February 1961, along $93^{o}E$, confirm the presence of the Undercurrent with velocities 80 and 63 cm s^{-1} at 75 m and 150 m respectively. But Taft and Knauss (1967) noticed an eastward current of only 15 cm s^{-1} at a depth of 135 m along $85^{o}E$. The low value reported by Taft and Knauss (1967) can be due to a deviation in the atmospheric condition in 1963 compared to the other years (Taft and Knauss, 1967; Uda and Nakamura, 1973). The present results as well as the observations of Ivanov (1964) and Leetmaa and Stommel (1980) reveal that the Undercurrent is deepened from a depth of about 75 m at $55^{o}30'E$ to a depth of 150 m at $93^{o}E$. According to Taft and Knauss (1967) also, the Undercurrent is shallower in the west (85 m at $61^{o}E$) than in the east (110 m at $92^{o}E$). Based on the zonal flux,

the Undercurrent appears to be present a steric level of 300 cl/t coinciding with the 20°C isotherm which runs slightly at a deeper level than that of the high salinity core.

4.1.4. The transequatorial distribution of hydrographic properties in March and April confirm the presence of the Undercurrent all along the width of the Indian Ocean. (Figs. 7 to 12). The distribution of the flux indicates the presence of the Undercurrent at the bottom of the thermocline between 200 and 280 cl/t in March and at 200 cl/t in April at 92°E. Both the distributions confirm the deepening of the Undercurrent towards the east. In these months the higher eastward flux is neither coinciding with the high salinity core nor is it within the thermocline but at the bottom of the thermocline. Knauss (1960), Montgomery and Stroup (1962) report that the core of the Undercurrent lies within the thermocline in the Pacific. Halpern's (1980b) observations at 152°W are also in agreement with the above results and his observations at 166°E indicate that the core of the Undercurrent is near the bottom of the thermocline. Stevenson and Taft (1971) conclude that there is no close association between the Undercurrent and the high salinity core.
Philander (1973), who made a critical review of the Equatorial Undercurrent in all the oceans remarks that

though the region of high salinity coincides with the region of strong eastward velocity, the two maxima need not coincide. Sturn and Voigt (1966) and Voigt et al. (1969) found that the maximum current to be below the salinity maximum which agrees with the present results.

The flux computed by Swallow (1964,1967) based on the direct current observation in March 1964 comes to 14×10^6 m^3 s^{-1} while the present computation at 58^oE in March, based on the bivariate distribution, gives a total flux of 13.91×10^6 m^3 s^{-1} between the isanosteric surfaces of 200 and 400 cl/t (Fig. 33). Along 65^oE the total flux in the same month between these isanosteric surfaces is 18.38×10^6 m^3 s^{-1} (Fig. 34). In April, along 92^oE, within the same isanosteric surfaces the total flux is 18.19×10^6 m^3 s^{-1} (Fig. 35). The eastward volume transport computed from the current measurement by Taft and Knauss (1967) at 92^oE within the Undercurrent came to 11×10^6 m^3 s^{-1}. The difference in the mass transport computed by Taft and Knauss (1967) and the present computation may be due to the fact that their volume transport may be within the core of the Undercurrent while the present estimate of a total volume of 18.19×10^6 m^3 s^{-1} is within the isanosteric surfaces of 200 and 400 cl/t but not within the Undercurrent. From the above flux values at different longitudes, it appears that

the maximum mass transport takes place in the central region compared to the regions on either side. From the primary mode distribution of the zonal flux it appears that the Equatorial Undercurrent in the Indian Ocean is deepening from February to May.

4.1.5. The Equatorial Undercurrent appears to be absent during May in the eastern and central regions of the Indian Ocean while it is present in the western region (Figs. 13 to 15). In the place of the Undercurrent strong westerly flow is conspicuous from the zonal flux distribution along $84^{o}E$ (Fig. 37). The mass transport at the surface is eastward and its total value is 48.15 x 10^{6} m^{3} s^{-1}, mostly confined to the upper layers. The zonal flux between 200 and 400 cl/t accounts to 29.44 x 10^{6} m^{3} s^{-1} in the westward direction. Obviously, the Equatorial Undercurrent disappears in the eastern region by May itself, whereas in the western region the eastward flux between 200 and 400 cl/t isanosteric surfaces comes to 12.44 x 10^{6} m^{3} s^{-1} (Fig. 36). It is, therefore, evident that the Undercurrent is present in the western region while it is absent in the eastern region in May. According to Swallow (1964), the Equatorial Undercurrent was still present even upto 7th June 1964 along $58^{o}E$, but some what weaker and shallower and it was distinctly assymetric about the equator with a maximum eastward speed at a depth of 50 m around $1^{o}S$. The flow is westward below 200 m, which

decreases with depth between 400 and 500 m. The measurements of Leetmaa and Stommel (1980) show a southward shift of the Equatorial Undercurrent in 1975 and 1976 along 55°30'E. But in the present investigation, while the salinity core with values greater than 35.6% is slightly north of the equator, the spreading of the thermocline is between the equator and 1°S (Fig. 13). The zonal flux indicates the primary mode between 200 and 400 cl/t surface is confined to the salinity range of 35.2 to 35.4%. . Therefore, the core of the Undercurrent may not be in coincidence with the high salinity core but probably, with the spreading of thermocline as the frequencies of the mode are within the thermocline. Hence, it can be construed that the core of the Equatorial Undercurrent is between the equator and 1°S agreeing with the observation of Leetmaa and Stommel (1980).

4.1.6. The transequatorial distribution of hydrographic properties in June at 65°E indicates the presence of the Undercurrent with the associated characteristics of spreading of thermocline, high salinity core and penetration of oxygen rich water to deeper layers (Fig. 17). While there is no Undercurrent along 88°E, it is not very clear whether the Undercurrent is present or not along 58°E because there is spreading of the thermocline between 1°S and 3°S

without any associated high salinity core. However, the observations of Swallow indicate the presence of the Undercurrent at about 50 m along 58°E and also along 60° and 67°30'E. Along 67°30'E the strength of the Undercurrent decreased to a maximum speed of 44 cm s^{-1} while it was more than 80 cm s^{-1} in April.

4.1.7. During July, August and September there are no indications of the Equatorial Undercurrent in the distribution of hydrographic properties, although they indicate easterly flow extended to the deeper levels, probably, because of the Equatorial Countercurrent merging with the Southwest Monsoon Current except in the southern region where the flow is, invariably, westerly depicting the South Equatorial Current (Figs. 19 to 24). The zonal flux distribution in July along 54°30'E confirms that the westerly flow predominates over the easterly flow with values 30.33 x 10^6 m^3 s^{-1} and 21 x 10^6 m^3 s^{-1} respectively (Fig. 39). The easterly flow is, mainly, confined to the upper layers in the northern hemisphere associated with the high salinity water. In all the sections it seems that the easterly flow penetrates to deeper layers with increasing strength. The zonal flux along 91°30'E for September has been computed between 2°N and 2°S for the eastward flow only, as the Equatorial Countercurrent

dominates that region without much westerly flow (Fig. 40). From the total eastward flux of 16.46 x 10^6 m^3 s^{-1}, it is clear that the currents are relatively weak. Of this total, 75% accounts for the easterly flow in the deeper layer alone, indicating very weak current at the surface. Taft and Knauss (1967) also noticed strong easterly flows along 79° and 89°E with values ranging from 34 to 67 cm s^{-1}, in the depth range 110 to 140 m during their observations in 1962. Although the current direction indicates an easterly, it cannot be identified as an Equatorial Undercurrent with normal characteristics. The deepening of the easterly flow was noticed by Kort (1977) and Erickson (1979).

4.1.8. The distribution of hydrographic properties do not indicate the Equatorial Undercurrent, on the contrary show very strong eastward flow particularly in the upper layers during October (Figs. 25,26). This is further confirmed with the highest eastward flux of 70.05 x 10^6 m^3 s^{-1} in October at 84°E between 3°N and 3°S (Fig. 41). There is a total westward flux of 10.66 x 10^6 m^3 s^{-1} and it is of less significance. The zonal flux between 3°N and 3°S along 94°E in late November and early December confirms, the westerly flow is predominant over the easterly with values of 56.50 and 9.39 x 10^6 m^3 s^{-1} respectively, probably, because of the local westerly flow in Equatorial Countercurrent which shows an unsteady nature in the eastern Indian Ocean as evident from Anonymous (1952).

4.1.9. The distribution of hydrographic properties along 71°E shows a clear spreading of thermocline between 2°N and 1°S (Fig. 30) indicating the possibility of commencement of an Undercurrent in this region. The commencement of Undercurrent is not associated with a high salinity core, perhaps, may be because it is in the transition of commencement only.

4.2. Comparison of Equatorial Undercurrent in the Indian Ocean with that of the other oceans

Unlike the other two major oceans, the Equatorial Undercurrent in the Indian Ocean is present only during the later period of the northeast monsoon season. For tracing the Undercurrent in Indian Ocean, the most reliable factor is the weakening of the thermal gradient as the high salinity core is not coinciding with the spreading of thermocline. In the Pacific, temperature is the main factor since the contrasting salinity structure is not observed between the western eastern Pacific Ocean. But in the Atlantic Ocean, due to very high saline water in the western region, salinity plays the major role in distinguishing the Undercurrent (Metcalf et al., 1962; Neumann and Williams, 1965; Rinkel et al., 1966).

In the present investigation, the Equatorial Undercurrent is present in the western Indian Ocean from January to May with a surface westerly flow. The core of the Undercurrent shifts from about $1^{o}N$ to the equator from January to February and remains along the equator upto April. Beyond April, it shifts to about 1 - $2^{o}S$. Such oscillation of the core of the Undercurrent is observed in the Pacific and Atlantic (Colin et al., 1971; Ivanov et al. 1976; Metcalf et al., 1962), which is explained to be due to wind shift (Charney and Spiegal, 1971).

The Equatorial Undercurrent is found to be well established all along the equator only during February, March and April. In the present study it is obvious that the thickness of the surface isothermal layer increases towards east on the contrary it is decreasing eastward in Pacific and Atlantic (Istoshine and Kalashnikov, 1965; Philander, 1973). Similarly, the observations of Neumann (1965) and Halpern (1980a) indicate shoaling of the core of the Undercurrent towards east, whereas deepening of the core is noticed from west to east in the Indian Ocean.

None of the sections in the present study indicates a double cell structure while it is a common feature in the Pacific and Atlantic, especially, in the

western region (Hisard et al., 1970; Bubnov et al., 1976).

From the flux distribution, it is obvious that a maximum transport of 18.34 x 10^6 m^3 s^{-1}, within 200 and 400 cl/t, is noticed during March in the central Indian Ocean. In the western Indian Ocean the value is much less. At 58°E in March, within 200 and 400 cl/t, the Undercurrent has a flux of 13.94 x 10^6 m^3 s^{-1}. But at 92°E in April the transport does not vary much from that in the central Indian Ocean. Obviously, it shows an increasing tendency from western to the central region in the Indian Ocean. But the observations of Hisard et al. (1969) and Wyrtki et al. (1981) show a decrease of mass transport from western to the central Pacific in July, though, it increases in January and April. According to Voit and Strekalov, 1964; Stalcup and Parker, 1965 and Neumann and Williams, 1965; the transport increases from 14 x 10^6 m^3 s^{-1} in the western Atlantic to 37.4 x 10^6 m^3 s^{-1} in the central Atlantic. Both in the Pacific and Atlantic the transport decreases from the central to the eastern region (Knauss, 1962,1966; Christensen, 1971; Khanaichenko, 1974).

CHAPTER - V

CHAPTER - V

EQUATORIAL JET IN THE INDIAN OCEAN

The Indian Ocean experiences well known seasonal fluctuations in wind speed and direction known as southwest monsoon and northeast monsoon over the Arabian Sea, Bay of Bengal and the Indian subcontinent. But along the equator, the variation is quarterly which results in the development of strong eastward flowing current called Equatorial Jet (Wyrtki, 1973) during the two transition periods of the monsoons. The surface circulation charts of Varadachari and Sharma (1967) prepared from the surface current vectors of the U.S. Navy Hydrographic Office Atlas of the Indian Ocean (1950) depict strong easterly currents along the equator during the transition periods of the two monsoons. The surface circulation maps presented by Sharma (1971) using the isogon - isovel technique from the current data of K.N.M.I. Atlas (Anonymous, 1952) gives a clearer indication of the jet - like structure located around the equator in the central Indian Ocean during April, May, October and November while Wyrtki (1973) reported the presence of the Jet during April, May, September and October.

In the present study, five sections have been utilised for establishing the presence of the Equatorial Jet and its latitudinal and longitudinal variation. Of the five,

two are along 84°E and 88°E in May and early June respectively. The remaining three section are occupied along 64°E, 77°E and 84°E in the October - November transition. The section along 84°E in May and October, and 88°E in June are selected for computing the zonal flux.

The transequatorial distribution of hydrographic properties at 84°E and 88°E in May and early June indicate the presence of Equatorial Jet in the surface layer with strong westerly underneath it (Figs. 15-18). The flux distribution also shows the presence of strong easterlies within 600 and 640 cl/t isanosteric surfaces and westward flow below it. A total eastward flux of 48.15 x 10^6 m^3 s^{-1} is observed in May between 3°N and 3°S whereas the westward flux accounts to 50.97 x 10^6 m^3 s^{-1} (Fig. 37). A slightly less easterly and westerly fluxes are noticed in June at 88°E (Fig. 38). Wyrtki (1973) observed an intense easterly flow around 80°E during May. Similar currents were also noticed at both the spring and fall monsoon transition by Knox (1976) and Reverdin et al. (1983).

The distribution of hydrographic properties along 77°E and 84°E in October indicates a strong eastward flow along the equator (Figs. 25 and 26). From both of these sections, it is evident that the presence of the easterly

flow can be interpreted even upto 200 m depth. The section along 64°E in November does indicate the presence of the Jet though it is less conspicuous than in the previous month. It may probably, be due to the fact that the Jet begins to terminate because of the meridional flux prevailing in this region. The distribution of zonal flux along 84°E in October amounts to 70.05 x 10^6 m^3 s^{-1} which is much higher than that of May (Fig. 41). Reverdin et al. (1983) got a highest value of eastward transport during November after substracting the mean yearly average. According to Sharma's (1971) charts the Equatorial Jet has higher speeds in October - November compared to April - May transition and the average value exceeds 63 cm s^{-1} in November and also extends to a wider region of the central Indian Ocean.

Wyrtki (1973) reports "The Jet is strongest between 60°E and 90°E, where the surface speeds often exceeds 30 mi/day (64 cm s^{-1}) and maximum values of 100 mi/day (215 cm s^{-1}) have been reported in Indian Ocean Oceanographic and Meteorological Data (Anonymous, 1952)". A close examination of these charts between 2°N and 2°S for April, May, October and November, revealed that the maximum value in any of these months between 60°E and 90°E is not more than 43 knots/day (89.6 cm s^{-1}).

Obviously, there must be some error in the report of Wyrtki (1973).

The transports estimated in May and October are much higher than the value estimated by Wyrtki. He made a rough calculation of the mass transport with an assumption that the Jet is 500 km wide and has an average speed of 75 cm s^{-1}, within a layer of 60 m which came about 22.5 x 10^6 m^3 s^{-1}. The weaker eastward flow on both sides of the Jet is not included in his estimation. In the present study, the flux is computed between 3^oN and 3^oS within the isanosteric surfaces of 160 and 640 cl/t. But the 75% level of the flux lies within the surface layer. Perhaps, this may be the reason of getting such a high value. Though, the present estimate of the flux is higher compared to Wyrtki's, it is well correlating with the inference of Reverdin et al. (1983) that the transport of the Jet during October - November transition is found to be twice that in April - May transition.

As per the present investigation, the Equatorial Jet shows its appearance from 64^oE to 84^oE during October - November transition while it is confined only in the eastern region during May and June. Results of Wyrtki (1973) and Reverdin et al. (1983) support the present inference. Sharma's charts (1971) also show that the main core of the

Jet is confined between 60°E and 85°E but the average maximum speeds at the surface being above 65 cm s^{-1}. Cresswell et al. (1981), using a satellite tracked drifting buoy, could trace the surface Equatorial Jet over 3000 km eastward and never beyond 2° off the equator between 6 November and 24 December 1980. Erickson (1979) could also trace the saline Arabian Sea Water from 60°E to 90°E during the northeast monsoon and concluded that the plausible mechanism for transporting the saline water from west to east is the Intermonsoonal Jet.

According to Cane (1980), with development of the westerlies in the equatorial Indian Ocean, downwelling is caused at the equator with an eastward flow penetrating to the deeper layers. Probably, because of such a condition, the Equatorial Jet penetrates to deeper layers during April - May as is evident from the eastward flux in the subsurface layers also apart from the one noticed in the surface layers. Narendran Nair (1983) observed that the zonal components of windstress along the equator are positive during the transition periods and consistently high while the meridional components are inconsistent and relatively weak. Thus he concludes that the zonal windstress is the main driving force of the Equatorial Jet.

CHAPTER - VI

CHAPTER - VI

SUMMARY AND CONCLUSIONS

This thesis is an outcome of the studies, carried out by the author on the Equatorial Undercurrent and the Equatorial Jet, an interesting and unique phenomenon discovered, recently, in the Indian Ocean (Wyrtki, 1973). The main objective of the thesis is to carry out a detailed investigation of the seasonal, latitudinal and longitudinal variation of the Equatorial Undercurrent in the Indian Ocean and also the Equatorial Jet, through mapping the vertical distribution of the oceanographic properties across the equator along various longitudes for all the months of an year, between 5^{o}N and 5^{o}S, utilising the oceanographic data collected during the International Indian Ocean Expedition and subsequently in the equatorial Indian Ocean.

As the distribution of the hydrographic properties give only a qualitative identification of the Undercurrent, a novel technique of computing the zonal flux through bivariate distribution of salinity and thermosteric anomaly, introduced by Montgomery and Stroup (1962), is adopted in order to have a quantitative variation of the Equatorial Undercurrent and the Equatorial Jet. Finally, an attempt

is made to give a plausible explanation of the features observed.

Transequatorial sections are chosen, as far as possible, in such a way that atleast one section is included in each month, in the three regions namely western, central and eastern that fall within the longitudinal limits of west of 65°E, 65° - 85°E and east of 85°E respectively so as to understand the longitudinal variation of the Undercurrent in each month. On the whole, 31 vertical sections are prepared, out of which 11 sections are selected for the computation of zonal flux. After mapping the distributions of temperature, salinity and oxyty along each vertical section, they are superimposed as a single section by presenting the isotherms, isohalines and oxypleths by different notations so as to enable an easy comparison of the distribution of one property with another.

The Equatorial Undercurrent is associated with specific characteristics of spreading of thermocline, high salinity core and the penetration of oxygen rich water to subsurface layers through vertical mixing. It is through such associated features in the distribution of hydrographic properties that the Equatorial Undercurrent in the Indian Ocean is identified monthwise and regionwise in the present study.

The details of the computation of zonal flux is presented in the materials and methods. The zonal flux, depicted on the bimodal distribution is demarcated into 50% and 75% of the total flux by thick and dashed lines in order to give an easy identification of different modes and their frequencies within the limits of 50% and 75% of the total flux. In general, higher number of frequencies indicate the heterogeneity while the lower number reveals the homogeneity. Further, when the Equatorial Undercurrent is present, it is normally represented by a primary mode of fewer frequencies either within the thermocline or associated with the high salinity core.

Unlike in the other major oceans of the world, namely the Pacific and Atlantic, where the Equatorial Undercurrent is present throughout the year, it appears only seasonally in the Indian Ocean because of the reversal of the atmospheric circulation over the North Indian Ocean, which reflects in turn in the surface and subsurface current pattern.

From the distribution of the hydrographic properties of the vertical sections along the various longitudes, it could be inferred that the Equatorial

Undercurrent is present all along the width of the Indian Ocean with the normal characteristic features of the Undercurrent, during February to April. But the commencement of the Undercurrent takes place in January in the western region, some times even in December, as the sections used for the present study shows some indications of the Undercurrent. Further, it is noticed that in the beginning it is located slightly north of the equator due to upwind shift of the northerlies prevailing in the western region. The Undercurrent is also found to be initially developed in the western region and extends to the east and shifts south to the equator with time. It is not very clear whether the commencement of the Undercurrent is permanent feature or only for the particular year of observation of the present study, as there is no indication of the Undercurrent in the eastern region in January.

During April and May, though the high salinity core is around $1^{o}N$, the weakening of the vertical thermal gradient is found around the equator. It is therefore difficult to distinguish the Undercurrent during these months in the western Indian Ocean. In the central and eastern Indian Ocean, the core is almost symmetrical about the equator, and it deepens in its course from west to east

and also from February to May in the western region. Before the termination of the Undercurrent it is found to shift southward due to the wind shift of the southwesterli that begin to blow by May at the equator.

At the peak of the southwest monsoon and subsequently, the surface flow is mainly easterly along the equator as the southwest Monsoon Current merges with the Equatorial Countercurrent, both being easterlies. During this period the South Equatorial Current which is a westerly, shifts to the northern most in an year. Although in the subsurface layers the easterly flow is, occasionally, noticed, it cannot be construed as the Equatorial Undercurrent as the characteristics are different from those associated with Undercurrent. It can, thus, be concluded that the Equatorial Undercurrent in the Indian Ocean is absent from late June to early December.

It is interesting to note that although the Equatorial Undercurrent is considered to be closely related with the spreading of the thermocline and high salinity core, in the Indian Ocean, seldom they coincide except in a few instances during February to April. Invariably, the Undercurrent appears to be identified below the high salinity core and at the bottom of the thermocline as is

evident from the zonal flux distribution also.

During May, October and November the hydrographic properties indicate the presence of strong easterly flow with intense gradients in temperature and salinity distribution. Thus, the presence of the Equatorial Jet in the central Indian Ocean is well depicted in the vertical sections, but, its intensity decreases on either side along the equator.

Flux distribution during February, March and May in the western Indian Ocean presents slightly higher value in March. In general, the transport increases from the western to the central Indian Ocean during the latter period of northeast monsoon while it remains almost unchanged in the eastern region. The transport during May and June, especially in the eastern region indicates a strong easterly flow at the surface within $3^{o}N$ and $3^{o}S$ with equally strong flow underneath it. Similar transport is observed in October with higher values indicating stronger flow in the surface layer. The transport does not indicate a westward flow during October in the subsurface layers as in the case of May.

The estimated geostrophic transport, within 200 and 400 cl/t, gives a total flux of 13.91×10^{6} m^{3} s^{-1} at $58^{o}E$

in March and it is in accordance with the value 14×10^6 m^3 s^{-1} computed by Swallow (1964) from direct current observations. But, the transport at $92^{\circ}E$ in April deviates much from the values of Taft and Knauss (1967), as their volume transport is within the core of the Undercurrent while the present estimate is within the isanosteric limits of 200 and 400 cl/t but not within the Undercurrent.

The Equatorial Undercurrent appears to be absent during May and June in the eastern region of the Indian Ocean while it is present in the western region. In the place of the Undercurrent strong westerly flow is conspicuous from the zonal flux distribution in the eastern sections. Obviously, the Equatorial Undercurrent disappears in the eastern region by these months.

The strong surface easterly flux present during the two transition periods denotes the Equatorial Jet and is symmetrical about the equator within $3^{\circ}N$ and $3^{\circ}S$. The Jet in the October transition is intense with a total zonal flux of 70.05×10^6 m^3 s^{-1}, particularly, in the upper layers and it is stronger than its counter part in May.

In general, there are certain deviations in the development and termination of the Equatorial Undercurrent

in the Indian Ocean, compared with that in the Pacific and Atlantic, while the salinity core gives a major indication in the Atlantic and thermocline spreading in the Pacific. In the Indian Ocean both features are noticed but they do not coincide.

As the development and termination of the Undercurrent could not be well established with the oceanographic data available at present, it is necessary to carry out the oceanographic measurements at closer intervals of stations along the various longitudes, particularly during December, January, May and June after which alone, the actual period and place of commencement and termination can clearly be confirmed.

REFERENCES

REFERENCES

Akamatsu, H. and T. Sawara (1969). The preliminary report of the third cruise for CSK, January to March 1969. Oceanogr. Mag., 21, 83-96.

Anonymous, (1952). Koninklijk Nederlands Meteorologisch Instituut, Indische Ocean Oceanografische en Meteorologische gegevens. 2nd Ed., Publ. No. 135, 1, Text 31 pp., and 2, 24 Charts.

Arthur, R.S. (1960). A review of the calculation of ocean currents at the equator. Deep Sea Res., 6, 287-297.

Austin, T.S. (1958). Variations with depth of oceanographic properties along the equator. Trans. Amer. Geophys. Un., 39, 1055-1063.

Austin, T.S. and M.O. Rinkel (1958). Variations in upwelling in the Equatorial Pacific. Proc. 9th Pacific Sci. Congr., Bangkok, 16, 67-71.

*Berrit, G.R. (1976). Les eaux froides c'otieres du Gabon a l Angola sont-elles dues a un upwelling d Ekman? Cah. ORSTOM Ser. Oceanogr., 14, 273-278.

Bjerknes, J. (1961). 'El Nino' study based on analysis of ocean surface temperature, 1935-1957. Bull. Inter - Amer. Trop. Tuna Comm., 5, 219-303.

*Bjerknes, V. (1900). Das dynamische Prinzip der zirkulationsbewegung in der Akmosphare Meteorol. z.

Bogdanov, C.H. and B.G. Popov (1960). Currents of the surface layer of the western Pacific. Tr. Inst. Okeanol. Akad. Nauk SSSR, 40, 135-142.

*Brosin, H.J. and D. Nehring (1968). Der Aquatoriale Unterstrom im Atlantischen Ozean auf 29°30'W im September und Dezember 1966. Beitr. Meeresk., 22, 5-17.

Bruce, J.G. (1968). Comparison of near surface dynamic topography during the two monsoons in the western Indian Ocean. Deep Sea Res., 15, 665-677.

Bruce, J.G. (1969). A further estimate of maximum transport of the Somali Current. Deep Sea Res., 16, 227-229.

Bruce, J.G. (1973). Equatorial Undercurrent in the western Indian Ocean during the south-west monsoon. J. Geophy. Res., 74, 6386-6394.

Bruce, J.G., H. Stommel and J.C. Swallow (1966). Water masses and patterns of flow in the Somali Basin during the south west monsoon of 1964. Deep Sea Res., 13, 825-860.

Bryan, K. and M.D. Cox (1968). A non-linear model of an ocean, driven by wind and differential heating. J. Atmos. Sci., 25, 945-978.

Bubnov, V.A., K.V. Moroshkin, V.D. Yegorikhin and Z.N. Matveyera (1976). Variation of currents in the equatorial Atlantic. Oceanology, 16, 228-231.

Bubnov, V.A. and V.D. Yegorikhin (1982). Meanders of the Cromwell Current. Meteorologiya Gidrol, 2, 109-111.

Bubnov, V.A., V.D. Yegorikhin and A.S. Osadehy (1982). Structure of the equatorial currents in the central and western Pacific. Okeanologiia, 22, 174-178.

*Buchanan, J.Y. (1886). On similarities in the physical geography of the great oceans. Proc. Roy. Geogr. Soc. London, 8, 753-770.

*Buchanan, J.Y. (1888). The exploration of the Gulf of Guinea. Scot. Geogr. Mag., 4, 177-200.

*Burkov, V.A. (1960). Studies in equatorial currents of the Pacific Ocean. Okeanologicheskie issledovaniya, 2, 117-126.

*Burkov, V.A. (1966). Structure and nomenclature of Pacific Ocean currents. Oceanology, 6, 3-14.

Burkov, V.A. and I.M. Ovchinnikov (1960). Investigations of equatorial currents to the north of New Guinea (in Russian). Tr. Inst. Okeanol. Akad. Nauk SSSR, 40, 121-134.

*Burkov, V.A., V.S. Arsentyev and I.M. Ovchinnikov (1960). Northern and southern tropical fronts in the ocean (in Russian). Tr. Inst. Okeanol. Akad. Nauk SSSR, 40, 108-120.

Cane, M.A. (1979). The response of an equatorial ocean to simple wind stress pattern. II. Numerical Results. J. Mar. Res., 37, 253-299.

Cane, M.A. (1980). On the dynamics of equatorial currents, with application to the Indian Ocean. Deep Sea Res., 27, 525-544.

*Case, K.M. (1960). Physics Fluids, 3, 149-154.

Charney, J.G. (1960). Non-linear theory of a wind driven homogeneous layer near the equator. Deep Sea Res., 6, 303-310.

Charney, J.G. and S.L. Spiegal (1971). The structure of wind driven equatorial currents in homogeneous oceans. J. Phys. Oceanogr., 1, 149-160;

Chekotillo, K.A. (1970). Vertical circulation in the equatorial western Pacific. Oceanology, 10, 626.

Christensen, N. (1971). Observations of the Cromwell Current near the Galapagos Islands. Deep Sea Res., 18, 27-34.

Cochrane, J.D. (1963). Equatorial Undercurrent and related currents off Brazil in March and April 1963. Science, 142, 669-671.

Cochrane, J.D. (1965). Equatorial currents of the western Atlantic, Oceanography and Meteorology of the Gulf of Mexico. Progr. Rep., 66, 6-19.

Cochrane, J.D. (1966). Currents and waters of the western equatorial Atlantic, Oceanography of the Gulf of Mexico. Progr. Rep., 66, 28-32.

Cochrane, J.D., F.J. Kelly and C.R. Olling (1979). Subthermocline Countercurrents in the western equatorial Atlantic Ocean. J. Phy. Oceanogr., 9, 724-738.

*Colin, C. and H. Rotchi (1971). Aspects geostrophiques de la circulation a l equateur. C.R.H. Acad. Sci., Ser. B., 271, 929-932.

*Colin, C., C. Henin, P. Hisard and C. Oudot (1971). Le Courant de Cromwell dans le Pacifique central en ferrier. Cah. Orstom, Ser. Oceanogr., 9, 167-186.

Crawford, W.R. and T.R. Osborn (1981). Control of Equatorial Ocean currents by turbulent dissipation. Science, 212, 539-540.

Crease, J. and A. Pogson (1964). Observations of the Equatorial Undercurrent by submarine. Deep Sea Res., 11, 391-393.

*Cresswell, G., M. Fieux and J. Gonella (1981). The Wyrtki Equatorial Jet, May/June 1980. Tropical Ocean - Atmosphere Newsletter. Unpublished Manuscript.

Cromwell, T. (1953). Circulation in a meridional plane in the central equatorial Pacific. J. Mar. Res., 12, 196-213.

Cromwell, T., R.B. Montgomery and E.D. Stroup (1954). Equatorial Undercurrent in the Pacific revealed by new methods. Science, 119, 648-649.

*Defant, A. (1935). Der Aquatoriale Gegenstrom. Sitzber Preuss Akad. Will. Phys. Math. Berlin, 28 S.

*Defant, A. (1936). Die Troposphare des Atlantischen ozeans. Schichung und Zirculation des Atlantischen Ozeans. Will. Ergebn. Dtsch. Atlant. Exped. auf. dem 'Meteor' 1925-1927. Bd. VI, T.I, S, 289-411.

*Defant, A. (1941). Die physicalische Meeresniveaus des Atlantischen Ozean. Z. Ges. Erdkunde zu Berlin, S. 145.

Defant, A. (1961). Physical Oceanography, Vol. 2, Pergamon P Press, Newyork, 556-591.

*Dietrich, G. (1957). Allgemeine Meereskunde, eine Einfuhrung in die Ozeanographic. Berlin, Gebruder Borntraeger, 492 pp.

*Dikii, L.A. (1960). Prikl. Mat. Mekh., 24, 357-369.

Donguy, J.R. and C. Henin (1980). Conditions in the eastern equatorial Pacific related to the intertropical convergence zone of the winds. Deep. Sea Res., 27, 693-714.

*Drazin, P.G. (1958). J. Fluid Mech., 4, 214-222.

Duing, W.O. (1974). Review of the Equatorial Oceanographic Experiment. Bull. Am. Met. Soc., 55, 398-404.

Duing, W.O., K. Grasshoff and G. Krause (1967). Hydrograph observations on a transequatorial section in the Indian Ocean. Meteor. Forsch. Erg., A3, 84-92.

Eckart, C. (1960). Hydrodynamics of Oceans and Atmospheres. Pergamon Press, Macmillan, Newyork, 302 pp.

*Ekman, V.W. (1905). On the influence of the earth rotation on ocean currents. Ark. Math. Astr. Och. Fys., 2, 1-53.

*Ekman, V.W. (1923). Uber die horizontal zirkulation winder zeugter Meeresstromungen. Ark. Math. Astr. Och Fys., 17, 1-74.

*Ekman, V.W. (1939). Neuere Ergebnisse und probleme zur theorie der konvenktionsstrome im Meere. Gerlands Beitr. z. Geophysik, Suppl. Bd. 4, Ergebn. d. kosmischen Physik IV, Physik d. Hydro - u Lithosphare, 74 pp.

*Eliassen, A., E. Hoiland and E. Riis (1953). Norw. Acad. Sci. and Lett. Publ., 1, 1-30.

Eriksen, C.C. (1979). An equatorial transect of the Indian Ocean. J. Mar. Res., 37, 215-232.

*Federov, K.N. (1965). Equatorial seiches. Oceanology, 5, 37 p.

Flohn, H. (1972). Investigation of equatorial upwelling and its climatic role. In Studies in Oceanography, Vol. I, 93-102.

Fofonoff, N.P. and R.B. Montgomery (1955). The Equatorial Undercurrent in the light of the vorticity equation. Tellus, 7, 518-521.

Forrester, W.D. (1964). Thermocline structure in the Equatorial Pacific. J. Mar. Res., 22, 142-151.

Fuglister, F.C. (1960). Atlantic Ocean Atlas. Vol. I, Woods Hole Oceanogr. Inst., Woods Hole, Mass., 209 pp.

Garrett, C. and W. Munk (1972). Oceanic mixing by breaking internal waves. Deep Sea Res., 19, 823-832.

Gerard, R., R. Sexton and P. Mazeika (1965). Parachute drogue measurements in the eastern Tropical Atlantic in September 1964. J. Geophys. Res., 70, 5696-5698.

Gill, A.E. (1971). The equatorial current in a homogeneous ocean. Deep Sea Res., 18, 421-431.

Gill, A.E. (1972). Models of equatorial currents. Paper presented at symposium on Numerical Models of Ocean Circulation, Nat. Acad. Sci., Durhan, N.H., 17-20.

Goldstein, S. (1931). On the stability of superposed streams of fluids of different densities. Proc. Roy. Soc. London, ser. A. 132, 524-548.

Halpern, D. (1980a). A Pacific equatorial temperature section from 172°E to 110°W during winder and spring 1979. Deep Sea Res., 27, 931-940.

Halpern, D. (1980b). A note on vertical motion at the equator in the eastern Pacific Ocean. Proceedings of the symposium on the bio-productivity of upwelling ecosystems. EOS, 61, 998.

Hasong, P. and J.R.V. Zaneveld (1973). The Cromwell Current on the east side of the Galopagos Islands. J. Geophy. Res., 78, 7845-7859.

Hasong, P. and J.R.V. Zaneveld (1974). Equatorial front in the eastern Pacific Ocean. J. Phy. Oceanogr., 4, 570-578.

*Haurwitz, B. (1931). Zur Theorie der wellen bewegung in Luft und Wasser. Veroff. Geophys. Inst. Lpz., 5, ser. 2.

Hayes, S.P. and H.B. Milburn (1980). On the vertical structure of velocity in the eastern equatorial Pacific. J. Phy. Oceanogr., 10, 633-635.

Hayes, S.P. (1981). Vertical fine structure observation in the eastern equatorial Pacific. J. Geophy. Res., 86, 10983-10999.

Hayes, S.P. (1982). A comparison of geostrophic and measured velocities in the Equatorial Undercurrent. J. Mar. Res., 40 (Suppl.), 219-229.

*Helmholtz, V.H. (1868). Monatsber. Akad. Wiss. Berlin, 23, 215-229.

*Helmholtz, V.H. (1890). Die Energie der Wogen und des Windes. S.B.K. Akad. Wiss., Berl., 853 pp.

Henin, C. and J.R. Donguy (1980). Heat content changes within the mixed layer of the equatorial Pacific Ocean. J. Mar. Res., 38, 767-780.

Hidaka, K. (1962). Non-linear theory of an equatorial flow, with special application to the Cromwell Current. J. Oceanogr. Soc. Jap., 20th Anniv. Vol., 223-241.

Hidaka, K. (1966). Non-linear computation of the Equatorial upwelling. J. Oceanogr. Soc. Jap., 22, 145-153.

Hidaka, K. (1972). Wind produced horizontal circulation in the Pacific, considered as zonal motion, in the presence of both vertical and horizontal eddy viscosity. In Biological Oceanography of the northern north Pacific Ocean, A.Y. Takenonti, Chief Editor, Idemitsu shoten, Tokyo, 83-95.

Hidaka, K. (1980). Non-linear theory of an equatorial flow. I - II. Proc. Japan Acad.,(B), 56, 1-12.

Hidaka, K. and Y. Nagata (1958). The dynamic computation of the equatorial current system of the Pacific, with special application to the Equatorial Undercurrent. Geophys. J., 1, 198-207.

*Hisard, P. and A. Morliere (1973). La terminaison due contre courant equatorial sub superficiel Atlantique (Courant de Lomonosov) dans le Golfe de Guinee. Cah. ORSTOM, ser. Oceanogr., 9, 455-464.

Hisard, P., J. Citeau and B. Voituriez (1977). Equatorial Undercurrent influences on enrichment processes of upper waters in the Atlantic Ocean. Report of the International workshop on the GATE Equatorial Experiment, Miami, 28 February to 10 March 1977.

Hisard, P. and J. Merle (1978). Equatorial Undercurrent influences on summer cooling of surface waters in the Gulf of Guinea as illustrated through GATE data. Proc. Gate symp. on Oceanogr. and Surface Layer Met., Kiel, W. Germany.

Hisard, P., J. Merle and B. Voituriez (1970). The Equatorial Undercurrent at 170°E in March and April, 1967. J. Mar. Res., 28, 281-303.

*Hisard, P. and P. Rual (1970). Courant equatorial intermediaire de l'Ocean Pacifique et contre - courants adjacents. Cah. ORSTOM, ser Oceanogr., 8, 21-45.

Hisard, P., Y. Magnier and B. Wauthy (1969). Comparison of the hydrographic structure of equatorial waters north of New Guinea and at 170°E. J. Mar. Res., 27, 191-205.

Ichiye, T. (1964). An essay on the equatorial current system. In Studies on Oceanography, ed. Kozo Yoshida, Tokyo, University of Tokyo Press, 38-46.

Ichiye, T. (1966). Vertical currents in the equatorial Pacific Ocean. J. Oceanogr. Soc. Jap., 22, 274-284.

Ingham, M.C. and R.B. Elder (1970). Oceanic conditions off north east Brazil February - March and October - November 1966. U.S. Coast Guard Oceanogr. Unit, Washington, Rep. 34, 1-25.

Iselin, C. (1959). New discovery in Physical Oceanography. "Oceanus", 6, 11-12.

Istoshin, Yu. V. and A.A. Kalashnikov (1965). The Cromwell Current in the western part of the Pacific. Oceanology, 5, 14-17.

*Istoshin, Yu. V. and G.N. Kuklin (1962). The Cromwell Current at 154°W (in Russian), Okeanologiya, 2, 262-263.

Ivanov Frantiskevich, G.N., V.G. Kort and V.B. Titov (1976) Structure of zonal currents in the western equatorial Pacific. Oceanology, 16, p. 22.

*Ivanov, Yu. A. (1964). Hydrological researches in the northern part of the Indian Ocean (in Russian), Tr. Inst. Okeanol. Akad. Nauk SSSR, 64, 22-42.

Jarrige, F. (1968). On the eastward flow of water in the western Pacific south of the equator. J. Mar. Res., 26, 286-289.

Jerlov, N.G. (1953). Studies of the equatorial currents in the Pacific. Tellus, 5, 308-314.

Jones, J.H. (1969). Surfacing of Pacific Equatorial Undercurrent. Direct observations, Science, 163, 1449-1450.

Jones, J.H. (1973). Vertical mixing in the Equatorial Undercurrent. J. Phy. Oceanogr., 3, 286-296.

Kaiser, W. and L. Postel (1979). Importance of the vertical nutrient flux for biological production in the Equatorial Undercurrent region at 30°W. Mar. Biol., 55, 23-27.

Katz, E.J. and Collaborators (1977). Zonal pressure gradient along the equatorial Atlantic. J. Mar. Res., 35, 293-307.

Katz, E.J. and G. Silvia (1982). Response of the western equatorial Atlantic Ocean to an annual wind cycle. J. Mar. Res., 40 (Suppl.), 307-327.

Katz, E.J., R.L. Molinari, D.E. Cartwright, P. Hisard, H.U. Lass and A. de Mesquita (1981). The seasonal transport of the Equatorial Undercurrent in the western Atlantic. Oceanologica Acta, 4, 445-450.

Kendall, T. (1969). Net transports in the western equatorial Pacific Ocean. J. Geophy. Res., 74, 1388-1396.

Khanaichenko, N.K. (1966). Some features of the circulation system in the troposphere of the tropical zone in the Atlantic Ocean. Tr. MGI, 34, 154-163.

Khanaichenko, N.K. (1969). Confirmation of the existence of the southern branch of the Equatorial Undercurrent in the Atlantic Ocean. DAN SSSR, 187, 1394-1396.

Khanaichenko, N.K. (1972). Characteristics of the thermocline structure of waters of the Lomonosov Current. Oceanology, 12, 485-495.

Khanaichenko, N.K. (1974). The system of Equatorial Countercurrents in the Ocean. Gidvometeoizdat Publishers, Leningrad, 158 pp.

Khanaichenko, N.K. and N.Z. Khlystov (1966). The south branch of the Equatorial Countercurrent in the Atlantic Ocean. Dokl. U.S.S.R. Acad. Sci., 166, 205-207.

Khanaichenko, N.K., N.Z. Khlystov and V.G. Zhidkov (1965). The system of Equatorial Countercurrents in the Atlantic Ocean, Oceanology, 5, 24-32.

Kindle, J.C. (1979). Equatorial Pacific Ocean variability - seasonal and El Nino time scales. Ph.D. thesis, Florida State Uty., 134 pp.

King, J.E., T.S. Austin and M.S. Doty (1957). Preliminary report on expedition EASTROPIC. Spec. Sci. Rep. U.S. Fish. Wildl. Serv., Fish. No. 201, 155 pp.

*Kitaigorodsky, S.A., Yu. Z. Miropolsky and B.N. Filyushkin (1973). On distinguishing between internal waves and turbulence in the ocean by temperature fluctuation data. Fiz. Okean. Atmosfer. Izv. Akad. Nauk SSSR, 9, 272-292.

Knauss, J.A. and J.E. King (1958). Observations of Pacific Equatorial Undercurrent, Nature, 182, 601-602

Knauss, J.A. (1960). Measurements of the Cromwell Current. Deep Sea Res., 6, 265-286.

Knauss, J.A. (1961). The structure of the Pacific Equatorial Countercurrent. J. Geophy. Res., 66, 143-145.

Knauss, J.A. (1962). On some aspects of the deep circulation of the Pacific. J. Geophys. Res., 67, 3943-3954.

Knauss, J.A. (1963). The equatorial current systems. The Sea, Vol. I, 235-252.

Knauss, J.A. (1966). Further measurements and observations on the Cromwell Current. J. Mar. Res., 24, 205-240.

Knauss, J.A. and B.A. Taft (1963). Measurements of currents along the equator in the Indian Ocean. Nature, 198, 376-377.

Knauss, J.A. and B.A. Taft (1964). Equatorial Undercurrent of the Indian Ocean, Science, 143, 354-356.

Knox, R. (1974). Reconnaissance of the Indian Ocean Equatorial Undercurrent near Adu Atoll. Deep Sea Res.,21. 123-129.

Knox, R. (1976). On a long series of measurements of Indian Ocean equatorial currents near Adu Atoll. Deep Sea Res., 23, 211-221.

Knox, R.A. and D. Halpern (1982). Long range kelvin wave propagation of transport variations in Pacific Ocean equatorial currents. J. Mar. Res., 40, 329-339.

*Kolesnikov, A.G., G.P. Ponomarenko, N.K. Khanaichenko and V.R. Shapkina (1966). Subsurface Lomonosov Current. Publ. 34, Moscow Hydrol. Inst., Ukr. Acad. Sci., Kiev, U.S.S.R., 3-23.

Kolesnikov, A.G., S.G. Boguslavskiy, G.N. Kuklin, V.A. Shirey and V.G. Kirynkhin (1971). Lomonosov Current in the Gulf of Guinea. Oceanology, 11, 311-315.

*Korotayev, G.K., E.N. Mikhaylova and N.B. Shapiro (1977). Theory of Equatorial Undercurrent in a baroclinic Ocean. Izv. Akad. Nauk SSSR, FAO, 13.

*Kort, V.G., V.A. Burkov and K.A. Chekotillo (1966). New data on equatorial currents in the western Pacific (in Russian). Dokl. Akad. Nauk SSSR, 171, 337-339.

Kort, V.G. (1977). Equatorial currents in the Indian Ocean during the north east monsoon. Oceanology, 17, 115-120.

Kosnyrev, V.K. and A.I. Felsenbaum (1973). On the theory of the Cromwell and Lomonosov Currents (English abstract). Fizika Atmosfer. Okean. Izv. Akad. Nauk SSSR, 9, 618-629.

Kozlov, V.F. (1967). On the theory of a baroclinic layer at the equator. Oceanology, 7, 448-455.

Krauss, W. (1966). Internal Waves in the sea. Oceanogr. Mar. Biol. Ann. Rev., 4, 11-32.

*Krivelevitch, L.M. (1968). A non-linear model of the flow of an inhomogeneous fluid at the equator. Izv. Acad. Sci. USSR Atmos. Oceanic Phys., 4, 105-110.

*Krivelevitch, L.M. (1969). To the theory of wind-drift currents in the equatorial region. Fizika Atmosfer. Okean. Izv. Akad. Nauk SSSR, 5, 285-292.

*Krummel, O. (1877). Die acquatorialen Meeresstromungen des Atlantischen Ozeans und das algemeine system der Meerescirculation. Leipzig.

*Krummel, O. (1911). Handbuch der Ozeanographie 2 Bd. Stuttgart.

Lass, H.U. and E. Hagen (1980). Seasonal variation of the Atlantic Equatorial Undercurrent at 30°W. Gerl. Beitr. Geophys., 89. 1-14.

Leetmaa, A. (1972). The response of the Somali Current to the southwest monsoon of 1970. Deep Sea Res., 19, 319-325.

Leetmaa, A. (1982). Observations of near equatorial flows in the eastern Pacific. J. Mar. Res., 40 (Suppl), 357-370.

Leetmaa, A. and H. Stommel (1980). Equatorial current observations in the western Indian Ocean in 1975 and 1976. J. Phy. Oceanogr., 10, 258-269.

Leetmaa, A. and P.F. Spain (1981). Results from a velocity transect along the equator from 125° to 159°W. J. Phy. Oceanogr., 11, 1030-1033.

Leishman, C. (1967). Numerical methods for solving the non-linear problem of a wind driven homogeneous Equatorial Undercurrent. M.S. Thesis, Dept. of Meteorology, Mass. Inst. Technol., Cambridge, Mass., 42 pp.

*Lemasson, L. and B. Piton (1968). Anomalie dynamique de la surface de la mer le long de l'equateur dans l ocean Pacifique. Cah. ORSTOM, ser. Oceanogr., 6, 39-46.

*Lemasson, L. and B. Piton (1969). Le Contre - courant de Cromwell et la distribution verticale de quelques proprietes physico - chimiques de eaux equatoriales. Cah. ORSTOM, ser. Oceanogr., 7, 73-81.

Long, R.R. (1972). Turbulence from breaking of internal gravity waves. Rapp. Proc. - V. Reun. Cons. int. Explor. Mer., 162, 13-18.

Lukas, R. (1981). The termination of the Equatorial Undercurrent in the eastern Pacific. Ph.D. Thesis Graduate Division, University of Hawaii, 127 pp.

Lukas, R. and E. Firing (1984). Geostrophic balance of the Pacific Equatorial Undercurrent. Deep. Sea Res., 31, 61-66.

Magnier, Y., H. Rotschi, P. Rual and C. Colin (1973). Equatorial circulation in the western Pacific. Progress in Oceanography, Vol. 6, 29-47.

*Makarov, S.O. (1894). Vityaz'i Tikhii okean. Vol. 1 and 2, S. Pb.

Mallik, D.D. (1982). The theory of the Equatorial Undercurrent - Analytical Model. Okeanologiia, 22, 12-18.

Masaaki, C. and K. Wyrtki (1981). The 20°C isotherm depth and sea level in the western equatorial Pacific. J. Oceanogr. Soc. Jap., 37, 198-200.

Masuzawa, J. (1964). Flux and water characteristics of the Pacific North Equatorial Current. Studies on Oceanography, 121-128.

Masuzawa, J. (1967). An Oceanographic section from Japan to New Guinea at 137°E in January 1967. Oceanogr. Mag., 19, 95-118.

Masuzawa, J. (1968). Second cruise for C.S.K., Ryotu Maru, January to March 1968. Oceanogr. Mag., 20, 173-185.

Masuzawa, J. (1969). The Mindanao Current. Bull. Jap. Soc. Fish. Oceanogr., (Prof. Uda's commem. Pap.), 99-104.

Masuzawa, J., T. Akiyama, Y. Kawarads, and T. Sawara (1970). Preliminary reports of the Ryofu Maru Cruise Ry 7001 in January-March 1970, Oceanogr. Mag., 22, 1-25.

Matsuno, T. (1966). Quasi geostrophic motions in the equatorial area. J. Met. Soc. Jap., 44, 25-43.

Mazeika, P.A. (1968). Mean monthly sea surface temperature and zonal anomalies of the tropical Atlantic. Serial Atlas of the Marine Environment, Amer. Geogr. Soc., Folio, 16.

Mc Creary, J. (1980). A model of the Equatorial Undercurrent, the coastal undercurrent and deep equatorial jets. Unpublished manuscript.

Mc Creary, J. (1981). A linear stratified ocean model of the Equatorial Undercurrent. Phil. Trans. Roy. Soc., Ser. (A), 298, 603-635.

Mc Kee, W.D. (1973). The wind driven equatorial circulatio in a homogeneous ocean. Deep Sea Res., 20, 889-899.

Mc Phaden, M.J. (1981). Continuously stratified models of the steady state equatorial ocean. J. Phy. Oceanogr., 11, 337-354.

Mc Phaden, M.J. (1982). Variability in the equatorial Indian Ocean, part I, Ocean dynamics. J. Mar. Res., 40, 157-176.

*Menkes, J. (1960). Jet Prop. Lab. Pasadena, Tech. Rep., No. 31-12.

Metcalf, W.G., A.D. Voorhis and M.C. Stalcup (1962a). The Atlantic Equatorial Undercurrent. J. Geophys. Res., 67, 2499-2508.

Metcalf, W.G., A.D. Voorhis and M.C. Stalcup (1962b). Observations of the Atlantic Equatorial Undercurrent. J. Geophys. Res., 67, 3580.

Metcalf, W.G. (1963). Reply to comments by E.D. Stroup and R.B. Montgomery concerning the history of the Equatorial Undercurrent. J. Geophys. Res., 68, 343.

Metcalf, W.G. and M.C. Stalcup (1967). Origin of the Atlantic Equatorial Undercurrent. J. Geophys. Res., 72, 4959-4975.

Metcalf, W.G. (1968). Shallow currents along the northeast coast of South America. J. Mar. Res., 26, 232-243.

Meyers, G. (1979). Annual variation in the slope of the 14^{o} isotherm along the equator in the Pacific Ocean. J. Phy. Oceanogr., 9, 885-891.

Miles, J.W. (1961). On the stability of heterogeneous shear flows. J. Fluid Mech., 10, 496-508.

Montgomery, R.B. (1940). The present evidence on the importance of lateral mixing processes in the oceans. Bulletin of American Met. Soc., 21, 87-94.

Montgomery, R.B. (1962). Equatorial Undercurrent observations in review. J. Oceanogr. Soc. Jap., 20th Anniv. Vol., 487-498.

Montgomery, R.B. and A.F. Spilhaus (1941). Examples and outline of certain modifications in upper air analysi J. Aeron. Sci., 8, 276-283.

Montgomery, R.B. and E. Palmen (1940). Contribution to the question of the Equatorial Countercurrent. J. Mar. Res., 3, 112-133.

Montgomery, R.B. and E.D. Stroup (1962). Equatorial waters and currents at 150°W in July-August 1952. Johns Hopkins, Oceanogr. Stud., 1, 68 pp.

Moore, D.W., P. Hisard, J. Mc Creary, J. Merle, J.J. O'Brien, J. Picaut, J. M. Verstraete and C. Wunch (1978). Equatorial adjustment in the eastern Atlantic. Geophy. Res. Lett., 5, 637-640.

Morozov, E.G. (1974). Experimental studies of internal wave breaking. Okeanologiia, 14, 25-29.

Munk, W.H. and C.J.R. Garrett (1973). Internal wave breaking and microstructure. Boundary-layer Met., 4, 37-45.

Munk, W.H. and D. Moore (1968). Is the Cromwell Current driven by equatorial rossby waves? J. Fluid Mech., 33, 241-259.

Muraleedharan, P.M., Basil Mathew and R.N.Nair (1980). Some studies on the Undercurrent and Equatorial Jet in the Indian Ocean from the hydrographic characteristics. Bull. Dept. Mar. Sci. Univ. Cochin, XI, 113-126.

Murthy, T.S. and J.D. Taylor (1969). An estimation of the intensity of upwelling in the Cromwell Current. J. Oceanogr. Soc. Japan, 25, 167-171.

Neumann, G. (1960). Evidence for an Equatorial Undercurrent in the Atlantic Ocean. Deep Sea Res., 6, 328-334.

*Neumann, G. (1965). Equatorial currents in the Atlantic Ocean with special consideration of the Gulf of Guinea during Equalant I and II. Intern. Gulf Conf. Tropical Oceanogr., Miami, Fla.

Neumann, G. and R.E. Williams (1965). Observations of the Equatorial Undercurrent in the Atlantic Ocean at 15°W during Equalant I. J. Geophy. Res., 70, 297-304.

Neumann, G. (1969). The Equatorial Undercurrent in the Atlantic Ocean. Proceedings of the symposium on Oceanography and Fisheries Resources of the Tropical Atlantic, Abidjan, 33-44.

Neyman, V.G., V.A. Bubnov and V.D. Yegorikhin (1978). Investigations of equatorial currents in the western part of the Indian Ocean. Oceanology, 18, 27-30.

*Noel, J. and J. Merle (1969). Analyse des courants superficiels et subsuperficiels equatorianx durant une periode de six jours a 170°E. Cah. Oceanogr., 21, 663-671.

O'Brien, J.J. and H.E. Hurlburt (1974). Equatorial Jet in the Indian Ocean, Theory. Science, 184, 1075-1077.

Pao Yih-Ho (1973). Measurements of internal waves and turbulence in two dimensional stratified shear flows Boundary layer Met., 5, 177-193.

Philander, S.G.H. (1971). The equatorial dynamics of a shallow homogeneous ocean. Geophys. Fluid Dyn., 2, 219-245.

Philander, S.G.H. (1972). The equatorial dynamics of a deep homogeneous ocean. Geophys. Fluid Dyn., 3, 105-123.

Philander, S.G.H. (1973). Equatorial Undercurrent. Measurements and theories. Rev. Geophys. Space Phys., 11, 513-570.

Philander, S.G.H. (1979). Non-linear coastal and equatorial jets. J. Phy. Oceanogr., 9, 739-747.

Philander, S.G.H. and R.C. Pacanowski (1980). The generation and decay of equatorial currents. J. Geophys. Res., 85, 1123-1136.

Philander, S.G.H. and R.C. Pacanowski (1981). Response of equatorial oceans to periodic forcing. J. Geophys. Res., 86, 1903-1916.

Philander, S.G.H. (1981). The response of equatorial oceans to a relaxation of the trade winds. J. Phy. Oceanogr., 11, 176-189.

Pochapsky, T.E. (1962). Measurement of current below the surface at a location in the western equatorial Atlantic. Nature, 195, 767-768.

Ponomarenko, G.P. (1963). The lomonosov deep Countercurrent on the equator in the Atlantic. Dokl. Akad. Nauk SSSR, 149, 1178-1181.

Ponomarenko, G.P. (1965). Discovery of a deep Countercurren at the equator in the Atlantic Ocean. Akad. Nauk SSSR, No.13, 77-81.

Pozdynin, V.D. (1982). Estimation of the small scale turbulence level from an empirical relation with the Richardson number. Okeanologiia, 22, 30-34.

*Puls, C. (1895). Oberflachentemperaturen und Stromungsverhaltmisse des Aquatorial-guertels des stillen ozeans. Arch, Seewarie, 18, 1.

Reid, R.O. (1948). A model of the vertical structure of mass in equatorial wind driven current of a baroclinic ocean. J. Mar. Res., 1, 304-312.

Reid, J.L. (1959). Evidence of a south Equatorial Countercurrent in the Pacific Ocean. Nature, 184, 209-210.

Reid, J.L. (1964). A transequatorial Atlantic Oceanographic Section in July 1963 compared with other Atlantic and Pacific sections. J. Geophys. Res., 69, 5205-5215.

Reid, J.L. (1965). Intermediate waters of the Pacific Ocean. Johns Hopkins Oceanogr. Stud., 2, 85 pp.

Reverdin, G., M. Fieux, J. Gonella and J. Luyten (1983). Free drifting buoy measurements in the Indian Ocean Equatorial Jet. Proceedings of the 14th International liege Colloquium on Ocean hydrodynamics, 99-120.

*Rinkel, M.O. (1963). Cruise report P - 6302 Equalant II. Institute of Marine Science, University of Miami.

*Rinkel, M.O. (1966). Cruise report P - 6503, Equalant V. Institute of Marine Science, University of Miami.

Rinkel, M.O. (1969). Some features of relation-ships between the Atlantic Equatorial Undercurrent and its associated salinity core. Proceedings Symp. Oceanography and Fisheries Resources of the Tropical Atlantic. Abidjan, C.I., Unesco, Paris, 193-212.

Rinkel, M.O., P. Sund and G. Neumann (1966). The location of the termination area of the Equatorial Undercurrent in the Gulf of Guinea during Equalant J. Geophys. Res., 71, 3893-3981.

Ripa, P. and S.P. Hayes (1981). Evidence for equatorial trapped waves at the Galapagos Islands. J. Geophys. Res., 86, 6509-6516.

Robinson, A.R. (1960). The general thermal circulation in the equatorial regions. Deep Sea Res., 6, 311-317.

Robinson, A.R. (1966). An investigation into the wind as the cause of the Equatorial Undercurrent. J. Mar. Res., 24, 179-204.

Roden, G.I. (1962). Oceanographic aspects of the eastern equatorial Pacific. Geophysica International 2, 77-92.

*Rotschi, H. and B. Wauthy (1969). Remarques sur le courant de Cromwell. Cah. ORSTOM, Ser. Oceanogr., 7, 27-43.

*Rougerie, F. (1969). Sur un noyau a forte teneur en oxygene dans la partie interieure du courant de Cromwell. Cah. ORSTOM, Ser. Oceanogr., 7, 21-28.

*Rual, P. (1969). Courants equatoriaux profonds (abstract). Deep Sea Res., 16, 387-391.

Rythe[illegible]., J.R. Hall, A.K. Pease, A. Bakun and M.M.Jones 66). Primary organic production in relation to [illegible] chemistry and hydrography of the western Indian [illegible]ean. Limnol. Oceanogr., 11, 371-380.

*Sandstrom, J.W. and B. Helland-Hansen (1903). Uber die Berechung von Meeresstromungen. Reports on Norvegian Fishery and Marine Investigations. Bd. 2, Nr. 4, 43 pp.

Schott, F. and R. Zantopp (1980). On the effect of vertical mixing on the determination of absolute currents by the beta spiral method. Deep Sea Res., 27, 173-180.

*Schott, G. (1935). Geographie des Indischen und stillen ozeans. Hamburg.

*Schott, G. (1939). Die Aquatorialen Stromungen des Westischen Stillen Ozeans. Ann. der Hydrogr. und Marit. Met., H.V.

*Schumacher, A. (1940). Monatskarten den Oberflachenstromun im Nordatlantischen Ocean (50°S bis 50°N). Ann. Hydro. Mar. Met., 109 pp.

Seitz, R.C. (1967). Thermostad, the antonym of thermocline. J. Mar. Res., 25, 203.

*Semtner, A.J. and W.R. Holland (1980). Numerical simulation of equatorial ocean circulation. Part I. A basic case in turbulent equilibrium. J. Phy. Oceanogr.

Shapiro, N.B. (1974). On a non-linear theory of wind-driven currents on the equator. Fisika Atmosf. Okean. Izv. Akad. Nauk SSSR, 10, 178-190.

Sharma, G.S. (1968). Some inferences on the Equatorial Undercurrent in the Indian Ocean based on physical properties of the waters. J. mar. biol. Ass. India, 10, 224-236.

Sharma; G.S. (1971). Studies on divergence of the surface waters in the North Indian Ocean. Ph.D. thesis, Andhra University, Waltair, 102 pp.

Sharma, G.S., R. Narendran Nair and Basil Mathew (1982). Current structure in the Intertropical Indian Ocean during the northeast monsoon. Indian J. Mar. Sci., 11, 7-14.

*Shtokman, V.B. (1945). Dokl. Akad. Nauk SSSR., Vol. 49, No.2.

Shtokman, V.B. (1946). Equations of a field of total flow induced by the wind in a nonhomogeneous Ocean. Dokl. Akad. Nauk SSSR., 54, 406-408.

*Shtokman, V.B. (1948). E'kvatorialnye protivotecheniya v okeanakh. Godrometeoizdat, Leningrad, 156 pp.

Stalcup, M.C. and C.E. Parker (1965). Drogue measurements of shallow currents on the equator in the western Atlantic Ocean. Deep Sea Res., 12, 535-536.

Stalcup, M.C. and W.G. Metcalf (1966). Direct measurements of the Atlantic Equatorial Undercurrent. J. Mar. Res., 24, 44-55.

Stevenson, M.R. and B.A. Taft (1971). New evidence of the Equatorial Undercurrent east of the Galapagos Islands. J. Mar. Res., 29, 103-115.

Stommel, H. (1960). Wind-drift near the equator. Deep Sea Res., 6, 298-302.

Stone, P.H. (1971). The symmetric baroclinic instability of an equatorial current. Geophys. Fluid Dyn., 2, 147-164.

Stroup, E.D. (1969). The thermostad of the 13-C water in the equatorial Pacific Ocean. Ph.D. thesis, John Hopkins Univ., Baltimore, Md., 202 pp.

Stroup, E.D. and F.W. Hunt (1963). Measurements of equatorial currents in the Gilbert Island area, July-August 1963. Nature, 200, 1001-1002.

Stroup, E.D. and R.B. Montgomery (1963). Comments on the history of the Equatorial Undercurrent. J. Geophys. Res., 68, 341-342.

Sturm, M. and K. Voigt (1966). Observations of the structure of the Equatorial Undercurrent in the Gulf of Guinea in 1964. J. Geophys. Res., 71, 3105-3108.

Sverdrup, H.U. (1940). Hydrology. Brit. Australian New Newzealandic Antarctic Res., Expedition 1929-1931, ser. A, 3, 88-126.

Sverdrup, H.U., M.W. Johnson and R.H. Fleming, (1942). The oceans, their physics, chemistry and general biology. Prentece - Hall, Newyork, 1087 pp.

Sverdrup, H.U. (1947). Wind-driven currents in the baroclinic ocean with application to the equatorial current of the eastern Pacific. Proc. Nat. Acad. Sci., 33, 318-326.

Swallow, J.C. (1964). Equatorial Undercurrent in the western Indian Ocean. Nature, 204, 436-437.

Swallow, J.C. (1967). The Equatorial Undercurrent in the western Indian Ocean in 1964. Studies in Tropical Oceanography, University of Miami Press, No.5, 15-36.

*Synge, J.L. (1933). Trans. R. Soc. Can., 3, 27, 1-18.

Taft, S.A. (1971). Ocean circulation in monsoon areas. Fertility of the sea, 2, J.D. Costlow, 563-579.

*Taft, B.A., B.M. Hickey, C. Wunsch and D.J. Baker (1973). The Cromwell Current at 150°W. Deep Sea Res., 20.

Taft, B.A. and J.H. Jones (1973). Measurements of the Equatorial Undercurrent in the eastern Pacific. Progr. Oceanogr., 6, 47-110.

Taft, B.A. (1967). Equatorial Undercurrent of the Indian Ocean, 1963. Studies in Tropical Oceanography, Univ. of Miami Press, No.5, 3-14.

Taft, B.A., B.M. Hickey, C. Wunsch and D.J. Baker (1974). The Equatorial Undercurrent and deeper flows in the central Pacific. Deep Sea Res., 21, 403-430.

Taft, B.A. and J.A. Knauss (1967). The Equatorial Undercurrent of the Indian Ocean as observed by the Lusiad Expedition. Bull. Scripps Inst. Oceanogr., 9, 126 pp.

Tait, J.B. (1955). Long-term trends and changes in the hydrography of the Faroe - Shetland Channel region. Deep Sea Res., 3 (Suppl.), 482-498.

Taylor, G.I. (1931). Internal waves and turbulence in a fluid of variable density. Rapp. Cons. Explor. Mer., 76, 35-43.

Timofeev, V.T. (1956). The annual water balance of the Arctic Ocean. Priroda, 7, 89-91.

Titov, V.B. (1977). Meandering of the Cromwell Current. Oceanology, 17, 271-273.

*Torade, H. (1941). Der aquatoriale gegenstrom im Atlantischen ozean und seine Entstehung, Nach neueren Arbeiten. Ann. Hydrograph. Maritimen Meteorol., 69, 201-209.

Tsuchiya, M. (1961). An oceanographic description of the equatorial current system of the western Pacific. Oceanogr. Mag., 13, 1-30.

Tsuchiya, M. (1968). Upper waters of the intertropical Pacific Ocean. Johns Hopkins, Oceanogr. Study, 4, 50 pp.

Tsuchiya, M. (1975). Subsurface Countercurrents in the eastern equatorial Pacific Ocean. J. Mar. Res., 33 (Suppl.), 145-175.

Tsuchiya, M. (1981). The origin of the Pacific equatorial 13°C water. J. Phys. Oceanogr., 11, 794-812.

Uda, M. and Y. Nakamura (1973). Hydrology in relation to tuna fisheries in the Indian Ocean. Spl. Publ. mar. biol. Ass. India, p 276.

U.S. Hydrographic Office, 1950. Atlas of surface currents: Indian Ocean, U.S.H.O. Publ. No.566.

Varadachari, V.V.R. and G.S.Sharma (1967). Circulation of the surface waters in the North Indian Ocean. J. Indian Geophys. Union, 4, 61-73.

Veronis, G. (1960). An approximate analysis of the Equatorial Undercurrent. Deep Sea Res., 6, 318-327.

*Voigt, K. (1961). Aquatoriale Unterstroming auch im Atlantic. Beitr. Meeresk., 1, 56-60.

Voigt, K., M. Sturm, F. Moeckel and E. Benkelsdorff (1969). Salinity, temperature, velocity profiles in the equatorial waters of the Gulf of Guinea areas. Proc. Symp. Oceanography and Fisheries Resources of the Trop. Atlantic, Abidjan, Unesco, Paris, 179-184.

*Voit, S.S. and S.S. Strekalov (1964). On the Lomonosov Current. Okeanologiya, 1, 809-812.

Voituriez, B. (1981). Northern and southern equatorial undercurrents and the formation of tropical thermal domes. Oceanologiica Acta, 4, 497-506.

Voituriez, B. and P. Hisard (1975). Nutrient enrichment in the equatorial upwelling - a comparison between Atlantic and Pacific oceans. Third Internat. symp. on Upwelling Ecosystems, Kiel, FRG, 25-28.

Voituriez, B. and A. Herbland (1979). The use of the salinity maximum of the Equatorial Undercurrent for estimating nutrient enrichment and primary production in the Gulf of Guinea. Deep Sea Res., 26, 77-83.

Weenink, M.P.H. and P. Groen (1952). On the computation of ocean surface current velocities in the equatorial regions from wind data. Proc. Kongl. Nederl. Akad. waters, Amsterdam, ser. B, 55, 239-246.

White, W.B. (1969). The Equatorial Undercurrent, the South Equatorial Countercurrent and their extensions in the South Pacific Ocean east of the Galapagos Islands during February-March 1967. Texas A & M Univ., College Station, Tex., Rep. 69-4-T, 74 pp.

White, W.B. (1971). A rossby wake due to an island in an eastward current. J. Phy. Oceanogr., 1, 161-165.

White, W.B. (1973). An oceanic wake in the Equatorial Undercurrent down stream from the Galapagos Archipelago. J. Phy. Oceanogr., 3, 156-161.

Williams, R.G. (1966). An investigation of the intermediate salinity maximum in equatorial Atlantic during Equalant I. Rep. G.S.L. - T.R. 66-4, Res. Div., N.Y. Univ., New York, 93 pp.

Williams, R.G. and C.H. Gibson (1974). Direct measurements of turbulence in the Pacific Equatorial Undercurrent. J. Phy. Oceanogr., 4, 104-108.

Wooster, W.S. (1960). Investigations of Equatorial Undercurrent. Deep Sea Res., 6, 263-264.

Wooster, W.H. (1961). Further evidence of a Pacific South Equatorial Countercurrent. Deep Sea Res., 8, 294-297.

Wooster, W.S. (1969). Equatorial Front between Peru and Galapagos. Deep Sea Res., 16 (Suppl.), 407-419.

Wooster, W.S. and F. Jennings (1955). Exploratory oceanographic observations in the eastern tropical Pacific, January to March 1953. Calif. Fish. Game, 41, 79-90.

Wooster, W.S. and T. Cromwell (1958). An oceanographic description of the eastern tropical Pacific. Bull. Scripps. Inst. Oceanogr., 7, 169-282.

Wunsch, C. (1977). Response of an equatorial ocean to a periodic monsoon. J. Phy. Oceanogr., 7, 497-511.

Wyrtki, K. (1956). The computation of oceanic and meteorological fields of motion with friction proportional to the velocity. Mar. Res., Indonesia, 2, 1-26.

Wyrtki, K. (1965). Surface currents of the eastern tropical Pacific Ocean. Bull. Inter. Amer. Trop. Tuna Comm., 9, 271-304.

Wyrtki, K. (1967). Circulation and water masses in the eastern equatorial Pacific. Inst. J. Oceanol. Limnol., 1, 117-147.

Wyrtki, K. (1971). Oceanographic atlas of the International Indian Ocean Expedition. Washington, D.C. National Sci. Foundation, 531 pp.

Wyrtki, K. (1973). An Equatorial Jet in the Indian Ocean. Science, 181, 262-264.

Wyrtki, K. (1974). Sea level and the seasonal fluctuations of the equatorial currents in the western Pacific Ocean. J. Phy. Oceanogr., 4, 91-103.

Wyrtki, K. (1975). El Nino - The dynamic response of the equatorial Pacific Ocean to atmospheric forcing. J. Phy. Oceanogr., 5, 572-584.

Wyrtki, K. (1981). An estimate of equatorial upwelling in the Pacific. J. Phy. Oceanogr., 11, 1205-1214.

Wyrtki, K. (1982). An attempt to monitor the Equatorial Undercurrent. J. Geophys. Res., 88, 775-777.

Wyrtki, K., E. Firing, D. Halpern, R. Knox, G.T. Mc Nally, W.C. Patzert, E.D. Stroup, B.A. Taft and R. Williams (1981). The Hawaii to Tahiti Shuttle Experiment. Science, 211, 22-28.

Wyrtki, K. and E.B. Bennet (1963). Vertical eddy viscosity in the Pacific Equatorial Undercurrent. Deep Sea Res., 10, 449-455.

Wyrtki, K. and G. Eldin (1982). Equatorial Upwelling events in the central Pacific. J. Phy. Oceanogr., 12, 984-988.

Wyrtki, K., G. Meyers, D. Mc Lain and W. Patzert (1977). Variability of the thermal structure in the central equatorial Pacific Ocean. Hawaii Inst. of Geophy., Honolulu, HI, HIG 77 - 1, 75 pp.

Wyrtki, K. and R. Kendall (1967). Transports of the Pacific Equatorial Countercurrent. J. Geophys. Res., 72, 2073-2076.

Yamanaka, H. (1958). Conditions of the oceans in relevant to fishing conditions for tunas in the eastern Indian Ocean. 1. Several informations in regard to the structure of the ocean during the period from January to March. Report of Nankai Regional Fish. Res. Lab., No.9, 117-124.

Yamanaka, H., N. Anraku and J. Morita (1965). Seasonal and long-term variations in oceanographic conditions in the western North Pacific Ocean. Nankai Reg. Fish. Res. Lab., Sanbashidori, Kochi, Japan, Rep. 22, 35-70.

Yoon, J.H. (1981). Effects of Islands on equatorial waves. J. Geophys. Res., 86, 10913-10920.

Yoshida, K. (1955). A note on dynamics near the equator in view of recent observations in the eastern equatorial Pacific. J. Oceanogr. Soc. Japan, 11, 33-37.

Yoshida, K. (1959). A theory of the Cromwell Current and of the equatorial upwelling - an interpretation in a similarity to a coastal circulation. J. Oceanogr. Soc. Japan, 15, 159-170.

Yoshida, K. (1961). Some calculations on the equatorial circulation. Rec. Oceanogr. Works Japan, 6, 101-105.

Yoshida, K. (1967). Circulation in the eastern tropical oceans with special references to upwelling and undercurrents. Japan J. Geophys., 4, 1-75.

Yoshida, K., Hamlee Mao and P.L. Horrer (1953). Circulation in the upper mixed layer of the equatorial north Pacific. J. Mar. Res., 12, 99-120.

Yosida, S., H. Nitani and N. Suzuki (1959). Report of multiple ship survey in the equatorial region (I.G.Y.) January-February 1958, Hydrogr. Bull. Tokyo, 59, 1-30.

---

*Not referred in original.